Scour around structures in tidal flows

M Escarameia
R W P May

Report SR 521
April 1999

HR Wallingford

Address and Registered Office: HR Wallingford Ltd. Howbery Park, Wallingford, OXON OX10 8BA
Tel: +44 (0) 1491 835381 Fax: +44 (0) 1491 832233

Registered in England No. 2562099. HR Wallingford is a wholly owned subsidiary of HR Wallingford Group Ltd.

Contract

This report describes work funded by the Construction Directorate of the Department of the Environment, Transport and the Regions, DETR, under research contract CI 39/5/111 for which the DETR nominated officer was Mr P B Woodhead and the HR Wallingford nominated officer was Dr S W Huntington. The HR job number was RTS 0066. The report is published on behalf of DETR, but any opinions expressed in this report are not necessarily those of the funding department. The work was carried out by M Escarameia and R W P May in the Water Management Group.

Prepared by ..... Manuela Escarameia .....

(name)

..... Senior Engineer .....

(Title)

Approved by ..... RWP. May .....

(name)

..... Principal Engineer .....

(Title)

Date 27-4-99

Summary

Scour around structures in tidal flows

M Escarameia
R W P May

Report SR 521
February 1999

Large numbers of temporary structures (e.g. cofferdams) and permanent structures (e.g. caissons and bridge piers) are built every year worldwide in estuaries and tidal river reaches. Tidal flows can produce large depths of local scour around these structures, which can jeopardise their stability or otherwise require deep sheet piling or local armouring of the bed. Considerable effort has in the past been directed towards the study of scour in unidirectional flows, but the important effects produced by tidal conditions have not previously been quantified.

This report describes a laboratory study carried out at HR Wallingford to investigate scour development around obstructions that are large in relation to the flow depth and the development of a design procedure to determining scour depths. The tests were performed to assess the influence of the following parameters: reversal of the flow direction, tidal cycle duration, water depth, shape of the obstruction and sediment size. The experimental facility used in the study was a 24m long flume by 0.6m width fitted with an axial pump that allowed reversal of the flow direction. The test section was formed by a 4m long granular mobile bed where typical structures were placed.

Preliminary tests were performed to measure scour development in unidirectional flows in order to allow later comparisons with tidal flow conditions. During the test programme the above flow parameters were varied to provide a wide range of conditions, and several typical shapes of structure were investigated: square, circular and rectangular as well as square shape with a transverse sill. The results of the tests were checked against field data for two types of complex bridge pier each consisting of a number of circular piles supporting a pier cap above bed level.

The data were analysed to determine the influence of the various factors on the equilibrium scour depths measured. A design procedure was developed that relates the time scale to the rate of scour and allows designers to predict scour depths around structures in tidal conditions. Information is also given on the plan shape of scour holes and recommendations are made on the extent of rock protection needed to prevent scour around the structures.

The work described in this report was partly funded by the Construction Directorate of the Department of the Environment, Transport and the Regions.

Notation

a	Coefficient in Equation (11)
B	Pier or structure width, i.e. dimension measured perpendicularly to the flow direction
D_p	Pile diameter
D_T	Half-cycle tidal duration
d	Nominal sediment size
d_x	Sediment size for which x% of the sample is smaller in weight
E_x	Extent of scour in plan, defined as the maximum horizontal distance from the face of the structure to the edge of the scour hole, measured normal to the face of the structure
g	Acceleration due to gravity
L	Length of rectangular structure
P	Spacing between centrelines of piles
S	Scour depth at time t
S_{DT}	Scour depth after first half tidal cycle
S_{eq}	Equilibrium scour depth for tidal conditions
S_{max}	Maximum scour depth
S_{meas}	Measured scour depth
S_{pred}	Predicted scour depth
S_{50}	Half the scour depth for unidirectional flow conditions
S_∞	Equilibrium scour depth for unidirectional flow conditions
T_i	Tidal period
T_{50}	Time factor, defined as the time taken for the scour depth to reach 50% of the equilibrium scour depth
T_c	Characteristic time
T_e	Time to reach equilibrium scour depth in unidirectional flow
t	Time
U	Mean flow velocity of the undisturbed flow field, upstream of a structure
U_c	Critical flow velocity, i.e. the threshold velocity for movement of the sediment bed
U_s	Peak velocity in a tidal cycle
$\bar{u}$	Net flow velocity in tidal waters
u_o	Velocity amplitude
u'	Non-periodic velocity residuals
y_o	Flow depth
Z	Level of the underside of a pile cap
α	Numerical coefficient
β	Numerical coefficient

Δ	Relative density of the sediment ; $\Delta = (\rho-\rho_s)/\rho$, where ρ is the density of the water and ρ_s is the density of the sediment
λ	Geometric scale

Subscripts

m	Model
p	Prototype
s	Sinusoidal

Contents

Contents continued

Tables

Figures

Contents continued

Plates

1. INTRODUCTION

Scouring of the bed is a natural phenomenon which occurs particularly in alluvial rivers, as part of their morphological adjustment. When structures are built in the flow path, they produce additional scour (usually denoted local scour), as a result of the complex three-dimensional flow patterns created by the impact of the structure on the flow. This is reflected in changes in the flow turbulence and in the sediment transport characteristics in the vicinity of the structure.

For the same flow conditions and structure shape, the larger the structure, the bigger the obstruction it will cause to the flow. Large structures (typically with widths bigger than 10 to 15m) are often built in river estuaries and tidal river reaches for a wide range of civil engineering projects. Amongst these are cofferdams, which are temporary structures used to exclude water from areas where construction work needs to be carried out. They can be built for the construction or repair of structures such as weirs, barrage gates, bridge piers, locks, sluices, intakes, outfalls, etc. Other examples of structures that are large in relation to the flow depth include caissons (permanent structures that can form parts of barrages or bridge foundations) and complex pier shapes, such as those formed by groups of piles supporting capping beams. The geometry of these structures tend to be unsatisfactory from the hydrodynamic point of view, either because they are temporary and designed for ease of construction or because their shapes are dictated by structural or constructional requirements. The shape and relatively large size of these structures can produce large scour depths in erodible material, and this can threaten their own stability or the integrity of the works they are intended to protect.

Although there has been considerable research on scour around structures in unidirectional flows, there is very little knowledge regarding the effects of tidal conditions. Uncertainties in the depth of scour to assume for the design of cofferdams and other such structures in tidal waters can have a significant impact in terms of the safety and cost of engineering schemes.

In the late 1980's a laboratory study was carried out by HR Wallingford to investigate the depth of local scour produced around large obstructions in unidirectional flows. The results are described in HR report SR240 (May & Willoughby, 1990), which also gives background information on the mechanisms of local scour and on the threshold of movement. It includes an extensive literature review of the formulae for predicting equilibrium scour depths caused by obstructions to the flow. The experiments were performed with square and circular piers and a range of flow depths. Based on the laboratory work, design equations were developed to estimate scour depths in relatively shallow water, which took account of pier size and shape, flow depth and velocity.

Eight years later, the Construction Directorate of the Department of the Environment, Transport and the Regions (DETR) commissioned the present project to complement the results of the first study and extend the range of conditions studied. The objectives were threefold:

1. to investigate in the laboratory the scour produced by tidal flows around structures such as cofferdams and caissons;

2. to produce design equations for predicting scour depths around such structures; and

3. to produce recommendations on the extent of the bed protection required.

The study was carried out between April 1996 and February 1999 and was, as mentioned above, partly funded by DETR with contributions from HR Wallingford and industrial partner Novaponte, a consortium of contractors involved in the construction of the new Tagus River crossing, the Vasco da Gama Bridge in Lisbon, Portugal.

A general overview of the existing knowledge about the mechanisms of scour, particularly in tidal waters, is given in Chapter 2, which should be complemented by referring to HR Report SR240 mentioned above. The programme of tests, the experimental set-up, the instrumentation and bed materials used, as well as the test procedure, are described in Chapter 3. Chapter 4 presents the analysis of the test results focusing on the effect on scour of various parameters, such as the shape of the structure, the tidal cycle characteristics and the water depth. Formulae for determining the extent of bed protection around structures are also given in this chapter. Chapter 5 presents an analysis leading to a method of scaling laboratory results to prototype conditions; design formulae for prediction of scour depth are also derived in this chapter. Chapter 6 gives a summary of the design procedure and includes a worked example to illustrate the application of the scour prediction method. Chapter 7 describes tests that were carried out to simulate complex pier structures for which prototype data were also available. The conclusions from the study are given in Chapter 8.

2. EXISTING KNOWLEDGE

2.1 Characteristics of local scour

Local scour is one of the categories into which scour is usually divided, the others being general and constriction scour:

- General scour is essentially a natural process (although in some cases triggered by human intervention) that occurs in rivers due to an increased capacity to transport sediment;
- Constriction scour results from the increase in mean flow velocity due to a reduction in the width of the waterway;
- Local scour is the direct consequence of localised increases in flow velocity and turbulence caused by the presence of an obstruction in the flow.

Structures placed in flowing water can produce two types of scour: by reducing the width available to the flow, the blockage caused by structures such as cofferdams or piers can induce constriction scour; by changing the direction of the flow streamlines, by increasing turbulence and by setting up complex vortex motions in the flow, structures can generate local scour. Analysis by Breusers et al (1977) of experimental research on local scour at obstructions revealed that local scour begins when the undisturbed upstream flow velocity is equal to about half the value corresponding to the threshold of movement of the sediment bed.

A summary of the mechanisms of local scour is given next but more comprehensive descriptions can be found, for example, in Breusers & Raudkivi (1991) and in May & Willoughby (1990). The scouring process and the resulting geometry of the scour hole are very much dependent on the shape of the structure and on the angle of repose of the bed material. However, there are a number of common features that have been observed by researchers for non-cohesive sediment beds and identified as important in the development of local scour. These features (except for the wake vortices) are shown diagrammatically in Figure 1 for the flow around a vertical cylinder, and are briefly described next:

- *Downflow at the upstream face of the structure*
  This feature results from stagnation pressures on the upstream face of the structure which are greater at the surface than at the bed due to the vertical variation of flow velocity. The differences in pressure create a downward flow towards the bed and cause a notch to be scoured at the base of the structure.

- *Re-circulating upstream surface vortex*
  This surface vortex is another direct consequence of the sudden slowing down of the flow at the face of the obstruction. Because it is generated at the surface, it only affects the development of scour in cases where the flow depth is relatively shallow compared with the size of the obstruction.

- *Horseshoe vortices*
  As the upstream notch increases in size, a larger scour hole gradually develops around the upstream face of the obstruction. Flow separating from the bed upstream of this hole produces vortices that are U-shaped in plan; these pick up and transport sediment away from the hole, thereby enlarging it.

- *Wake vortices*
  As the flow separates from the sides of the structure, a wake is created downstream. At the interface between the separation zone and the external flow, the velocity discontinuity produces vortices which have vertical axes and which are usually shed periodically from either side of the structure. The combination of low pressure at the vortex core and the interaction with the horseshoe vortices near the bed lifts sediment and transports it downstream.

Detailed measurements of the flow pattern around cylindrical bridge piers have been carried out by Ahmed and Rajaratnam (1998) using a large experimental facility. The laboratory work concentrated on the study of the effect of bed roughness on the deflection of the flow and the development of scour holes. Tests were performed both with a fixed bed (smooth and with varying degrees of roughness) and with a mobile bed formed by sediment with a mean size of d_{50} =1.84mm. The study confirmed the importance of the downflow in front of the pier, which reached 75% of the velocity of the undisturbed flow field. Once developed, the scour hole was found to play an important role in determining the flow pattern around the structure: it significantly increased the magnitude of the downflow (when compared with the flat-bed case), and also reduced the flow acceleration at the sides of the pier by increasing the local cross-sectional area of the flow.

As mentioned before, the above mechanism and flow features have been observed in laboratory conditions for beds formed by non-cohesive granular materials. The development of the scour hole and its equilibrium shape are likely to be affected if the bed sediment is cohesive and/or subject to stratification in terms of its physical properties. Erosion of muddy sediments is usually dominated by the cohesive forces resulting from electro-chemical and biological sources and depends on the degree of consolidation of the cohesive deposit. Although some studies have been carried out to investigate this phenomenon (see, for example, Mitchener et al, 1996), the effects of cohesion and stratification are not sufficiently known and will not be taken into account in the present study.

It has been found that in unidirectional flows, the equilibrium depth of scour produced around a structure is dependent on the conditions of transport of the sediment bed. Two different states can be distinguished:

- Clear-water scour when the shear stresses at the bed upstream of the structure are at or below the threshold (or critical) conditions for initiation of bed movement. The acceleration of flow in the vicinity of the structure increases the local shear stress to a level that exceeds the threshold of movement. This initiates the process of removal of sediment from around the base of the structure and, with time, a scour hole is formed.

- Live-bed scour when there is general sediment transport over the bed upstream of the structure due to bed shear stresses being above the critical value for sediment transport.

For uniformly graded sediments, maximum scour depths have been observed to occur when the upstream flow velocity corresponds to the critical velocity for the sediment bed, U_c. Increasing the velocity value above U_c, will first produce a sharp decrease in scour depth (due to the movement of large dunes into the scour hole) followed by an increase (when the dunes become flatter), although never reaching the maximum observed at U_c. In view of this behaviour, and with engineering applications in mind, it was decided to investigate scour at the critical velocity, U_c, since this will represent the most severe design case.

2.2 Previous studies

A large number of researchers have studied the development of scour around single structures placed in unidirectional flows such as those occurring in non-tidal river reaches (for a comprehensive account of these studies refer, for example, to Breusers & Raudkivi, 1991). Most of these studies have involved laboratory investigations of the scour produced by slender bridge piers of simple geometry.

The importance of relative flow depth as a significant factor affecting the depth of scour around large structures was identified by May & Willoughby (1990). These authors carried out a systematic experimental study of square and circular piers and investigated the effect on scour depth of the size and shape of the pier, the flow depth and the flow velocity. The results showed that scour depths around structures in relatively shallow water were considerably smaller than the values predicted by formulae that had been derived mainly from data for slender structures in deep water. In the design equations developed by May & Willoughby, the non-dimensional scour depth was expressed as a function of the following parameters:

$$\frac{S_\infty}{B} = f_1 \text{ (pier shape)} \times f_2 \text{ (relative water depth)} \times f_3 \text{ (relative flow velocity)} \times f_4 \text{(angle of incidence)} \qquad (1)$$

where S_∞ is the final equilibrium scour depth below bed level in unidirectional flow, B is the width of the pier normal to the flow, and $f_x(\,)$ means "function" of the factor in the brackets .

- For circular piers with sediment of uniform size, Equation (1) has the form:

$$\frac{S_\infty}{B} = 2.4 \times \left[0.55 \left(\frac{y_o}{B} \right)^{0.60} \right] \times \left[1 - 3.66 \left(1 - \frac{U}{U_c} \right)^{1.76} \right] \qquad (2)$$

for the following ranges of water depth and flow velocity:

$$y_o/B \leq 2.71 \qquad (3)$$

$$0.522 \leq U/U_c \leq 1.0 \qquad (4)$$

In the above expressions, y_o is the water depth upstream of the pier, U is the upstream depth-averaged flow velocity, and U_c is the value of U at the threshold of sediment movement (i.e. the critical flow velocity). For circular piers the angle of incidence of the flow is not relevant so f_4 in Equation (1) is defined as having a value of 1.0.

If $y_o/B > 2.71$, the first bracketed [ ] term in Equation (2) is replaced by a constant value of 1.0.

At the critical flow velocity and for relative water depths of $y_o/B \leq 2.71$, Equation (2) becomes:

$$\frac{S_\infty}{B} = 1.32 \left(\frac{y_o}{B} \right)^{0.60} \qquad (5)$$

- For square piers at zero angle of incidence to the flow (so that $f_4 = 1.0$) and with sediment of uniform size, Equation (1) has the form:

$$\frac{S_\infty}{B} = 3.2 \times \left[0.55 \left(\frac{y_o}{B} \right)^{0.60} \right] \times \left[0.6 \left(\frac{2.67\,U}{U_c} - 1 \right) \right] \qquad (6)$$

for the following ranges of water depth and flow velocity:

$$y_o/B \leq 2.71 \tag{7}$$

$$0.375 \leq U/U_c \leq 1.0 \tag{8}$$

If $y_o/B > 2.71$, the first bracketed [ ] term in Equation (6) is replaced by a constant value of 1.0. The symbols have the same meaning as for Equation (2).

At the critical flow velocity and for relative water depths of $y_o/B \leq 2.71$, Equation (6) becomes:

$$\frac{S_\infty}{B} = 1.76\left(\frac{y_o}{B}\right)^{0.6} \tag{9}$$

The above equations show that the maximum depth of scour around a square pier is likely to be about 1.33 times greater than around a circular pier having the same width, B, normal to the flow. As can be seen, the sediment size is not a parameter in the above equations. The effect of sediment size was not investigated because previous studies had shown that it did not have a significant effect on the maximum equilibrium scour depth unless the particle size was greater than about B/25. Since large structures typically have widths of 10m or more, the above limit would only be significant if the bed consisted of stones and boulders larger than about 0.4m in size, which is not the case for most rivers and estuaries in which such structures are likely to be built.

Systematic studies on the development of scour around large obstructions in tidal flows do not appear to have been carried out. In such flows the velocity varies with depth throughout the tidal cycle, as illustrated in Figure 2 (obtained from Graham & Mehta, 1981). For purposes of analysis the tidal velocity can be considered as the sum of a number of contributions:

$$u(t) = \bar{u} + \sum_{i=1}^{i=n}\left[u_{oi}\sin\left(2\pi\frac{t}{T_i} + \phi_i\right)\right] + u'(t) \tag{10}$$

where: $\bar{u}$ is the net flow velocity during a tidal cycle, u_{oi}, T_i and ϕ_i are respectively the ith velocity amplitude, period and phase angle of the n harmonic components of the flow, and $u'(t)$ corresponds to any non-periodic residuals. Since the various components usually have a low probability of acting at the same time, it is unlikely that maximising all the velocity components would give a realistic design velocity. Graham & Mehta therefore recommended that design flows be determined from statistical analyses of existing velocity records, and that the importance of each of the terms in Equation (10) should be assessed in specific cases.

However, in spite of the lack of knowledge, it seems likely that the reversal of flow during a tidal cycle will result in smaller maximum scour depths than those produced by a steady unidirectional flow: the scour hole formed around a structure during the first half-cycle of the tide will be partly filled in again by sediment transported by the flow when it reverses direction. As the flow changes direction, it will also encounter changes in the state of the bed, which will become disturbed both upstream and downstream of the structure. The maximum scour depths occurring during consecutive tides will initially increase until a quasi-equilibrium condition is reached when the quantities of sediment transported by the flow in each half-cycle become equal. The present study was designed to check this hypothesis and quantify the reduction in equilibrium scour depth compared with equivalent unidirectional flows.

Current knowledge is also very limited on the scour produced around structures that have complex geometries. Although cofferdams and caissons usually have fairly regular shapes (such as square, rectangular or circular), other types of large structure can have rather complicated geometries. Examples of these include old bridges with wide masonry piers and various forms of nose protection, and more modern bridges with main piers that are supported below the water surface by pile caps that, in turn, are supported by groups of circular piles projecting above the bed. The latter type of construction is favoured in areas of deep water where it is possible to carry out work on the pile caps at low tide or during times of year when water levels in fluvial rivers are low. Although the water may be considered as deep in absolute terms, it may still be relatively shallow when compared with the dimensions of the pier structure.

Whitehouse (1997) reports on scour observed in deep-sea conditions around offshore exploration rigs. The legs of these structures are usually formed by large diameter cylindrical piles with additional supports and cross-bracing. Although the rigs are not usually installed in shallow water and are subjected to wave action as well as currents, the scour patterns around them are likely to have some resemblance to those that would be produced in tidal estuaries. When these structures are placed in sandy beds, two types of scour have been observed:

1. local scour holes around individual piers with the shape of inverted, truncated cones. These isolated holes coalesce in some cases to form a much larger depression, which may involve the whole plan area occupied by the group of piles.

2. "dishpan" or global scour, with the shape of an elliptical bowl around the area of the structure. The major axis of the ellipse has been found to be perpendicular to the main flow direction. The causes of this type of scour are not clear, but it appears that it is not due simply to the coalescence of the local scour holes. The complex interaction of the wave and current field with the whole structure is more likely to produce such extended scour than interactions with individual piers.

3. EXPERIMENTAL STUDY

3.1 Test programme

The HR laboratory study was designed to obtain, within the overall project constraints, the maximum amount of information on scour depths around large obstructions in tidal conditions. As the literature currently offers very little information on the subject, the first objective was to identify the variables that primarily influence the development of scour in tidal conditions. Although the various parameters occur in combination under prototype conditions, separate series of tests were carried out to determine the effect of each variable in isolation. The main parameters investigated were:

Flow direction: Tidal currents exert a frictional shear stress on the bed that varies in direction as well as in amplitude. In the present tests the effect of the tidal variation was assessed by comparing tests where the direction of the flow was reversed every half-tidal cycle with results from equivalent tests with unidirectional flows.

Flow velocity and water depth: The flow velocity and the ratio of the water depth to the width of the obstruction transverse to the flow have been identified as important parameters in unidirectional flow conditions (see May & Willoughby, 1990).

Tidal cycle duration: The scaling of time in scouring processes cannot be assumed to follow the usual Froudian scaling laws that are suitable for open channel flows, such as the flow in rivers because the process is dominated by the rate of sediment erosion and only indirectly by the speed of water. Therefore, it was decided to investigate a range of tidal durations in order to establish a suitable method of scaling. The test programme included a series of tests where the duration of the tidal cycle was changed (between 0.5 and 4 hours) but all the other parameters were kept the same. The tidal cycle duration was one of the variables more closely investigated, since it was expected that it would have a strong influence on

temporary scour depths (i.e. depths at the end of each half-cycle) and equilibrium scour depths (i.e. those depths reached but not exceeded after a sufficient number of tidal cycles).

Shape and size of obstruction: The scour pattern around an obstruction is primarily dependent on the shape of the object and its size relative to the flow depth. This dependency arises from the local increase in flow velocity at points around the structure and from the type and strength of the scouring vortices that are formed. Four regular shapes were tested in the present study: square, circular and rectangular piers and a square pier with a transverse sill (see Figure 3). The last shape simulated the conditions that can apply at gated structures in which the piers are connected by a continuous sill across the channel. Two complex pier shapes, each formed by a number of piles and a large capping beam, were also investigated as part of the simulation of prototype structures (see Chapter 7).

Sediment size: Previous research has shown that the size of the sediment, provided it is not very small, does not play a significant role in determining the maximum possible depth of scour under unidirectional flow conditions. Since the mechanisms of scour development in tidal flows are essentially the same as in unidirectional flows, it appears unlikely that a strong dependence on sediment size should be found. Nevertheless, tests were carried out with two sediments sizes to check if there was an effect.

The test programme was divided into the following stages:

- Preliminary tests to determine the suitability of the existing test facility. These tests reproduced conditions studied in a previous research study (May & Willoughby, 1990) and involved only uni-directional flow.

- Tests to determine the influence of the above parameters on the formation of scour.

- Tests to investigate the extent of bed protection required around structures in tidal conditions.

- Simulation in the test facility of prototype conditions applying to a new bridge crossing over the river Tagus in Lisbon, Portugal. The tests allowed a comparison to be made between scour depths measured in the laboratory and those surveyed in the field.

3.2 Experimental facility and instrumentation

Two different test facilities at HR were considered for the present laboratory tests: (1) a large high-discharge flume used for the previous HR study with unidirectional flows (see May & Willoughby, 1990); (2) a flume specifically designed for the study of tidal flows (the Water Reversing Flume). Although the second flume was narrower than the first, its use was favoured because the preliminary tests showed that it gave comparable results to the high-discharge flume while not requiring modifications to simulate reversing flows. It was also considered that the large flow capacity of the first flume was not required for the tests.

The Water Reversing Flume is a 24m long test rig with a rectangular cross-section measuring 0.605m wide by 0.440m deep (see Figure 4). The test section was placed at the mid-length of the flume and consisted of a 4m long mobile bed. The transitions between the flume and the test section were achieved by two ramps with slopes of 1V:3H, followed by short fixed sections of bed. In order to determine the required depth for the mobile bed, calculations were carried out to estimate the maximum scour depth likely to occur during the test programme; these indicated that the bed thickness should be around 150mm.

The test facility is a closed system in which the flow is re-circulated by means of an axial pump. This pump is capable of delivering more than 60l/s and is fitted with a controller for reversing the direction of the flow. In order to ensure correct mechanical operation of this pump, a priming pump was also installed in the flume. Its function was to provide continuous lubrication to the bearings of the main pump and was therefore switched on for the whole duration of the tests. The priming pump lifted water to a high level

tank and the water was then conveyed back to a lower level and used to keep the pipework of the axial pump permanently filled. As can be seen in Figure 4 (plan view), vanes were installed at the bends of the flume at either end of the open section in order to straighten the flow and generate uniform flow conditions at the approach to the test section.

Two miniature propeller meters were used to measure the mean flow velocity and enable the speed of the pump to be adjusted to produce required flow conditions. The meters were positioned at points on either side of the test section to permit measurement of the flow velocity approaching from either direction. The water depth at these points was greater than in the test section, which had a raised sediment bed. Allowance for this difference was made when determining the values of velocity that the propeller meters needed to measure in order for the flow conditions in the test section to be set correctly.

The flow velocity was set manually by turning a dial on an electronic control mounted adjacent to the flume. By changing the direction of movement of the dial, the flow direction could also be reversed. In the initial stages of the test programme, a non-intrusive flow meter was installed on the walls of the pipework that supplied the flow to the flume. This was done to check the readings of the propeller meters and showed a satisfactory level of agreement.

Water and scour depths were measured by using an electronic point gauge with a repeatable accuracy of ±0.2mm, which was mounted on a movable carriage. In certain positions, for example very close to the modelled structures, it was impossible to use the point gauge accurately and therefore the measurements were made by means of a manual scale with a pointed end.

3.3 Choice of sediment sizes

The choice of sediment size depended on several factors which are explained next. It was decided to carry out the tests under clear-water scour conditions, i.e. with no transport of sediment into the scour hole, and to try to achieve the conditions most likely to cause the biggest scour depths. For unidirectional flows, these conditions correspond to flow velocities at the threshold of sediment transport, at critical velocity U_c. Such values of velocity were calculated for a range of sediment sizes using the following formula due to Hanco (1971), which had proved accurate in previous experimental studies carried out by HR:

$$U_c = a[g \Delta d]^{0.5} \left(\frac{y_o}{d} \right)^{0.2} \qquad (11)$$

where:

g is the acceleration due to gravity;
Δ is the relative density of the sediment defined by $\Delta = (\rho_s - \rho)/\rho$, where ρ is the water density and ρ_s is the density of the sediment;
d is the d_{50} size of the sediment, i.e. the size of particle for which 50% of the sample in weight is smaller;
y_o is the flow depth;
a is a coefficient such that : a = 1.0 for d_{90} >0.7mm and a = 1.2 to 1.4 for d_{90} < 0.7mm.

These critical velocities were compared with the range of flow velocities achievable in the flume and with flow depths that would allow accurate measurements to be taken.

Another criterion for selecting the bed material was the need to avoid rippling of the bed at critical flow velocities since rippling has previously been found to reduce the scour depth to about 70% (May & Willoughby, 1990). It has been observed that ripples tend to start forming before the critical velocity is reached for uniform sediments with d_{50} smaller than about 0.5 to 0.7mm.

Based on these considerations it was decided to use a fairly uniform sediment with d_{50} = 0.75mm, which is above the size for which rippling can occur. Most of the tests that were designed to determine the influence on scour of the various flow and structure-related parameters were carried out with this sediment size. However, in order to check the influence of sediment size on scour depths, it was also decided to carry out tests with a sand of size d_{50} = 0.44mm. The grading curves of the two sediments are presented in Figure 5; the densities of the sediment particles were ρ_s = 2.62kg/m^3 for the 0.75mm sand and ρ_s = 2.65kg/m^3 for the 0.44mm sand.

3.4 Test procedure

Apart from minor differences between tests, the test procedure for reproducing tidal flow conditions was basically as follows. Having installed the structure in the centre of the test section and laid the sand bed absolutely flat, the flume was slowly filled to the required water level and depth. The priming pump, and afterwards the main pump, were then switched on and the velocity control was adjusted to produce the required velocity and direction of the flow. At the end of each half-tidal cycle, the velocity was reduced to zero and the pumps were switched off to stop the flow so that measurement of bed level around the structure would not cause additional scour. These measurements were taken at various locations and included the points of maximum depth. The values were plotted in a graph to help indicate how the maximum depth of scour was evolving with time. The pumps were then switched on again and the flow direction was reversed by turning the dial of the controller in the opposite direction. The flow depth was checked regularly during the test and adjusted if necessary by introducing small amounts of water at one of the ends of the flume.

This procedure was repeated until the plotted values of maximum scour depth showed that these had remained constant for the last few half-cycles and further cycles would not cause an increase in the values. The average of these almost identical final values was taken as the equilibrium scour depth.

A survey of the bed was carried out at the end of each test using the electronic point gauge to define the scour patterns. In some tests this survey included the whole area of disturbed bed, whereas in others the measurements were taken only along the centreline of the flume and along the two longitudinal lines coinciding with the outside edges of the structure. Plan drawings and profiles of the bed were then made before the mobile material was carefully levelled again for the next test.

Most of the tests were carried out at the critical flow velocity, which was estimated prior to the test runs for each set of flow conditions and sediment sizes. Hanco's Equation (11) was used to provide a first estimate of this velocity. The value that actually corresponded to the threshold conditions was determined by setting the flow velocity to the value suggested by Hanco's equation, and checking whether some movement of the sediment was observed. For most test conditions, the equation proved very accurate, but some adjustments were necessary particularly for the tests with the finer sediment.

4. TEST RESULTS AND ANALYSIS

The following table describes briefly the series of tests carried out using structures of regular shape (tests with complex pier shapes are described in Section 7) and for a more detailed description refer to Sections 4.1 to 4.3. Note that in the table, n is a code number referring to the tidal cycle duration – see also Table 1):

Test Series	Description
Square structure; sediment size d_{50} = 0.75mm	
UD	Unidirectional test
C	Tidal tests: tidal half cycle simulated by constant flow velocity equal to critical velocity and water depth equal to 0.075m
VnA	Tidal tests: tidal half cycle simulated by a sinusoidal variation of velocity where the peak velocity exceeded the critical velocity; water depth equal to 0.075m.
VnB	Tidal tests: tidal half cycle simulated by sinusoidal variation of velocity where the peak velocity was equal to the critical velocity; water depth equal to 0.075m.
CnM	Tidal tests: tidal half cycle simulated by constant velocity equal to the peak velocity in Series VnA; water depth equal to 0.075m.
CnA	Tidal tests: tidal half cycle simulated by constant flow velocity equal to critical velocity and water depth equal to 0.056m.
CnB	Tidal tests: tidal half cycle simulated by constant flow velocity equal to critical velocity and water depth equal to 0.0375m.
Square structure; sediment size d_{50} = 0.44mm	
FUD	Unidirectional test
FC	Tidal tests: tidal half cycle simulated by constant flow velocity equal to critical velocity and water depth equal to 0.075m
Circular structure; sediment size d_{50} = 0.75mm	
CC	Tidal tests: tidal half cycle simulated by constant flow velocity equal to critical velocity and water depth equal to 0.075m
Rectangular structure; sediment size d_{50} = 0.75mm	
RC	Tidal tests: tidal half cycle simulated by constant flow velocity equal to critical velocity and water depth equal to 0.075m
Square structure with sill; sediment size d_{50} = 0.75mm	
SC	Tidal tests: tidal half cycle simulated by constant flow velocity equal to critical velocity and water depth equal to 0.075m

The flow conditions and results of the tests involving the structures of regular shape are summarised in Tables 1 to 5. As well as the type of flow (i.e. unidirectional or tidal), water depth and flow velocity, the tables also give the measured values of the maximum and equilibrium scour depths. The maximum scour depth, S_{max}, is defined as the largest scour depth recorded during a test. In a unidirectional test, since the scour hole tends to increase with time until an equilibrium level is reached, the maximum depth is equal to the equilibrium value. In a tidal test, the maximum scour depth may or may not coincide with the equilibrium depth, S_{eq}, as it may occur as a result of one of the earlier half-tidal cycles. It was observed in the tests that the time and conditions for occurrence of the maximum scour depth in tidal flows were quite unpredictable.

The above tables include tests in which different types of tidal cycle were simulated. A description of these tests is presented in Section 4.2.

4.1 Effect of flow direction

One of the major objectives of the study was to answer the following question: is the scour produced under unidirectional flow conditions substantially different from that produced in tidal rivers and estuaries where the flow direction is reversed every few hours? In order to answer this question, the main parameters that needed to be measured were: (1) the scour depth and (2) the extent and shape of the scour hole around the structure.

Figures 6 and 7 show two plots of equilibrium scour depth against time in order to illustrate the differences between unidirectional and tidal flows. The tests represented in these figures were all carried out with a square structure and with similar water depths and sizes of bed sediment. Test UD was the unidirectional test used in this comparison, and tests C0, C1, C2 and C3 were tidal tests with half-tidal cycles of 0.25, 0.5, 1 and 2 hours, respectively.

It can be observed in Figure 6 that the equilibrium scour depths measured in the tidal tests are always well below the equilibrium depth for equivalent unidirectional conditions. Closer observation of the results (see Figure 7) shows that in the tidal tests the equilibrium scour depths (reached after a sufficient number of tidal cycles) are somewhat greater than the scour depths occurring with unidirectional flow after a time equal to one half-cycle. In other words, this reflects what was observed during the tidal tests: that the scour depth continued to increase beyond the value reached after the first half-cycle and finally stabilised (typically after about 4 to 5 half-cycles) at an equilibrium value that was significantly less than the equilibrium depth produced by an equivalent unidirectional flow.

With regard to the plan dimensions of the scour holes, unidirectional conditions produced deeper and more extensive scour holes than the tidal flows. Values of the ratio between the horizontal extent of the scour hole and its depth were therefore found to be quite comparable for the two types of flow, as were the average slopes of the scour holes (around 35° to the horizontal). In the tidal tests the reversal of flow produced scour holes at both ends of the structure, whereas in the unidirectional test the scour hole occurred only around the upstream face of the structure. As can be seen from Plate 1 (Test UD) and Plate 2 (Test C2), the scour hole formed in Test UD extended all the way around the structure, whereas in Test C2 it was confined to the ends and corners of the structure (note that the direction of the last half-cycle was from left to right in the photograph). The tests also showed that, for short half-cycle durations (of about 30 minutes or less), the maximum scour depths occurred at the corners of the structure. As the duration of the tidal cycle increased, the points of maximum scour at either end of the structure were found to move inwards towards the centreline.

Figure 8 illustrates the flow features that were observed during the tidal tests around a square structure. Compared to the general flow patterns described by researchers of unidirectional flows (and depicted in Figure 1, for a circular pier), the similarities are apparent: both show a strong downward flow at the upstream side of the pier and the localised erosion at the base of the pier. The strong, continuous horseshoe vortex depicted around the pier for unidirectional flow conditions was, however, not so clearly observed in the present tests. One of the reasons for this difference is likely to be the shape of the pier rather than the effect of flow reversal: in a square pier the edges create marked separation zones and vertical vortices, whereas the flow patterns are generally smoother around circular shapes. Differences were also observed, as expected, at the scoured bed on the downstream side of the structure, due to the flow reversal for tidal conditions.

4.2 Effects of variations in tidal shape and flow velocity

The effect of variations in the duration of the tidal cycle on scour depth was partly discussed in the previous Section and is illustrated by Figures 6 and 7. It is apparent from these Figures that, as the tidal cycle increased in duration, so did the equilibrium scour depth.

One of the aspects considered carefully in the study was how best to simulate tidal cycles in the laboratory tests. Typically the water level during a tide varies approximately sinusoidally with time and there is a

similar type of variation in the flow velocity (see Section 2.2). In the test facility it was possible to carry out tests at different constant water levels and with the flow velocity varying with time, but not with changes in both quantities simultaneously. It was therefore decided to study both factors separately in order to be able to determine their individual effects on the maximum depth of scour.

As a result, in addition to the tests in which the flow velocity was kept constant in each direction and equal to the critical value for sediment movement, the following other types of test were carried out in which the flow velocity was varied with time in each direction:

1. A series of tests where the peak velocities in the sinusoidal cycles exceeded the critical velocity value, U_c, and had half-cycle tidal durations similar to those of the constant velocity tests. This series was denoted by the code VnA, where n is a code number referring to the tidal cycle duration (see Table 1).

2. A series of tests with sinusoidal velocity variation where the peak velocities were equal to the critical value, U_c, but with adjustment of the half-cycle durations so that the total volume of water flowing past the structure in each direction remained equal to that in the constant velocity tests. This series was denoted by the code VnB (see Table 1).

3. The effect of varying the magnitude of the flow velocity was further investigated by another series of tests in which the velocity in each direction was kept constant but above the value of U_c. The velocity used was the peak velocity in the series described in item 1 above. These tests were denoted CnM, as shown in Table 1.

A comparison between the different test series is illustrated by the graph of Figure 9; the equilibrium scour depth for unidirectional flow at the critical velocity U_c is indicated by the straight solid line and the predicted scour depth using the design equation (Equation (6)) is shown as a dashed line. It can be seen that tidal flows with $U_{max} = U_c$ (Series C and VnB) produce scour depths that are considerably smaller than the equilibrium value for unidirectional flow, which can be taken as an upper limit. However, contrary to what has been observed with unidirectional flows, there are indications in tidal conditions that increasing the flow velocity above the critical value causes the equilibrium scour depth to continue to increase. The tests carried out with $U_{max} > U_c$ (Series CnM and VnA) produced scour depths which were very close to the unidirectional equilibrium value (but below the limiting design value shown by the dashed line). In view of the limited data, it is difficult to draw general conclusions or give a full explanation for this finding. It seems plausible, however, that the alternation of flow direction and the subsequent generation of bed forms create conditions which are significantly different from those applying to unidirectional flows. In laboratory studies of unidirectional flow, the sediment bed around the structure is usually made as level as possible prior to the start of a test; provided the flow velocity does not exceed the critical value, the upstream part of the bed should remain level throughout a test. In a tidal test, after the first tidal cycle has been carried out, the sediment bed at both ends of the structure will have been disturbed by the development of scour holes; as a result, in subsequent cycles the flow no longer approaches the obstruction over a flat bed. The presence of scour holes and associated dunes will produce different local velocities and flow patterns from those occurring with a unidirectional flow. It was not possible to investigate fully the effect of velocities above critical in the present study, but this is an area that requires further research.

Figure 9 also shows that the equilibrium scour depths obtained with sinusoidal tidal simulation are similar (although on average 12% smaller) to those obtained with constant, critical velocity. This small discrepancy is likely to be due to the lower scouring power of the flow during the sinusoidal variation of velocity. Although both types of simulation corresponded to the same flow volume, in the sinusoidal simulation the flow velocity was below the scour threshold value for much of the time, thus not contributing to the scouring process.

4.3 Effect of flow depth

The tests to investigate the effect of flow depth on scour in tidal conditions were all carried out using a square structure and constant (but reversing) flow velocity. These tests were: C0 to C3 (water depth of 0.075m in the flume), C0A to C3A (water depth of 0.056m), and C0B to C3B (water depth of 0.0375m). The corresponding values of relative flow depth, y_o /B, in the three sets of tests were 1.0, 0.75 and 0.50, respectively. Data from the tests is given in Table 1.

Equilibrium scour depths are plotted against tidal cycle duration in Figure 10, whereas Figure 11 shows a similar graph for the maximum scour depths recorded during the tests. It is apparent in these figures that the flow depth has a marked effect on both the equilibrium and maximum scour depths. For the same tidal cycle duration and taking the results for $y_o/B = 1.0$ as datum, the scour depth decreases with the relative flow depth as shown in the following table:

Decrease in relative flow depth	**Average decrease in equilibrium scour depth**
25%	20%
50%	83%

Similar conclusions are generally valid for the maximum scour depths but the trend is less clear.

4.4 Effect of structure shape

The investigation of the effect of shape on local scour involved the testing of structures with four different regular shapes under tidal flow conditions: square, circular, rectangular and square with a transverse sill (see Figure 3). As can be seen in the Figure, all the structures had an equal width normal to the flow (B = 0.075m). In the fourth structure, the length of the sill in the direction of flow was the same as that of the pier (i.e. 0.075m) and its top surface was level with the bed. As well as these regular shapes, the study also investigated local scour around two complex bridge piers consisting of a number of piles linked by large pier caps (refer to Chapter 7 for the description of these tests).

The comparison between the various shapes was carried out by considering tests with equivalent flow conditions: tests C0 to C3 (for the square shape), CC0 to CC3 (for the circular shape), RC0 to RC3 (for the rectangular shape) and SC1 and SC3 (for square shape with sill). All of the above tests are summarised in Tables 1 to 4, which were presented at the beginning of this chapter, and corresponded to constant velocity conditions during each half-tidal cycle. The values of equilibrium scour depth for the four shapes are plotted in Figure 12 against the duration of the tidal cycle. Several conclusions can be drawn from this graph:

1. As the tidal cycle duration increased (i.e. the length of time the structure was exposed to flow in each direction), the differences in the equilibrium scour depths between the various shapes also increased;

2. The square shape generally produced the largest equilibrium scour depths;

3. The square pier with a transverse sill and the rectangular structure produced the lowest equilibrium scour depths;

4. For tidal cycle durations of less than about two hours (in the laboratory), the square and circular shapes produced similar values of equilibrium scour depths but the circular shape became more "efficient" than the square shape for longer cycle durations (i.e. it produced less scour).

Apart from minor differences, the above conclusions apply also to the maximum scour measured during the tests, as can be seen in Figure 13. Previous experiments by May & Willoughby (1990) with

unidirectional flows showed that, for a relative flow depth of $y_o/B = 1.0$, the ratio between the maximum scour depths for square and circular piers was 1.20. This value compares well with the following ratios obtained in the present study for half-cycle durations of 2 hours: 1.10 (for the equilibrium tidal scour) and 1.20 (for the maximum scour depths reached during tidal tests).

Plate 3 shows the final scour pattern around the square structure after a test with a 0.5 hour half-cycle duration, and can be compared with Plates 4 and 5 which show equivalent results for the same structure with an additional transverse sill. In the plan view of Plate 3 it can be seen that the sediment bed was considerably disturbed by the sequence of reversing flows. It is also apparent that a well-defined scour hole had developed at the upstream face (i.e. relative to the direction of the flow in the last half-cycle of the test) and at the corners of the structure. Plates 4 and 5 show that the shape of the scour hole was significantly affected by the presence of the sill. As can be seen, the lateral extent of the scour was greater on the upstream side of the sill that had been facing the flow during the last half-cycle of the test. The extent of the scour was also considerably greater than it was for the case of the square structure without the sill; this was because the sill prevented the development of the scour hole in the downstream direction and directed flow more strongly sideways.

The equilibrium scour depths measured for rectangular structures (see Plates 6 and 7) were found to be between 10% and 14% smaller than those measured for square structures in similar flow conditions. This behaviour appears to be logical for structures having length/width ratios greater than 1.0 because the scour holes that form at the corners of the structure in successive half-cycles of the tide are farther apart and therefore cannot merge so easily to produce a larger single scour hole. As the half-cycle duration is increased, it would be expected that the equilibrium scour depth at a rectangular structure would increase towards the value for a square structure of the same width.

4.5 Effect of sediment size

As mentioned in Section 3.1, previous research studies with unidirectional flows showed that the influence of the sediment size on the maximum depth of local scour was normally small enough to be neglected. This assumption was checked in the present study by running a series of tests with a sediment finer than the one used in the majority of tests. This series was carried out with a sand of $d_{50} = 0.44$mm and the results were compared to those obtained with sediment size $d_{50} = 0.75$mm.

The test procedure was similar to that described in Section 3.4, and the flow velocity was estimated using Hanco's equation (Equation (11)). However, a correction to this estimated velocity was necessary since preliminary tests showed that threshold conditions for sediment movement were achieved at a flow velocity of $U_c = 0.253$m/s which was slightly lower than the value of U_c=0.283m/s predicted by Equation (11).

All the tests in this series were carried out with a square structure measuring 0.75mm x 0.75mm in plan and a water depth in the flume of 0.075m. Table 5 summarises the flow conditions and the results of the tests: one unidirectional test (FUD – see Plate 8), and three tidal tests at constant flow velocity with tidal half-cycle durations of 0.25, 1 and 2 hours (FC0, FC2 and FC3, respectively).

During the unidirectional test, the maximum scour depths around the structure were measured at frequent intervals until equilibrium was reached. The resulting scour hole (see Plates 9 and 10) was surveyed at the end of the test and is depicted in Figure 14 as a longitudinal profile along the centreline of the flume and as a plan view. The recorded maximum scour depths are plotted in Figure 15 together with the results of the corresponding unidirectional test using the coarser sediment size. This comparison indicates that, for the type and sizes of sediment tested, the bed sediment size has a negligible effect on the development of the scour hole and on the equilibrium scour depths reached.

A similar comparison was made for the tidal tests, as shown in Figure 16, where the equilibrium scour depths (reached at the end of a number of tidal cycles) were plotted against time. This graph also suggests that the final scour depths at an obstruction are not appreciably dependent on the size of the bed sediment.

4.6 Extent of scour around structures

In the present study the extent of scour around a structure is defined as the maximum horizontal distance from the structure to the edge of the scour hole, measured normal to the face of the structure. The extent of the scour hole around a structure is likely to be dependent on the geometric characteristics of the structure, the flow conditions (such as the water depth, the tidal cycle and the flow velocity) and the properties of the bed sediment, particularly the angle of repose (and the cohesiveness or lack of it). The present study could not investigate the influence of all these potential parameters but, as can be seen below, useful and simple relationships were found for design.

Amongst the data collected during the test programme was the extent in plan of the scour hole around each structure. This was obtained by surveying the bed at the end of each test. Longitudinal surveys were carried out along the centreline of the structure and along its left and right corners or sides (when viewing downstream) - this information was plotted for each test. Full surveys of the bed were also carried out for a number of tests from which scour maps were later drawn. Due to time constraints and the limited additional information this lengthy exercise produced, this procedure was not carried out for all the tests.

The maximum length of the scour hole on either side of the structure was obtained from the survey plots. This length, the maximum extent of scour E_x, is tabulated in Table 6 together with values of the equilibrium and maximum scour depths (S_{eq} and S_{max}, respectively), the width of the structure and the depth of the flow. Ratios of the extent of scour to the two different scour depths and to the water depth are also listed in the Table.

It is apparent that, apart from the case of the square structure with a transverse sill, the ratios of the extent of scour to the equilibrium scour depth are very similar for all the various structures and flow conditions. The values of the extent of scour are plotted in Figure 17 against the values of the equilibrium scour depth. A regression analysis of the data for all the structures except the square pier with a sill revealed the following relationship (with a correlation coefficient of 0.79), which is plotted as a continuous line in Figure 17:

$$E_x = 2.58\, S_{eq} \qquad (12)$$

For design purposes, the extent of scour in plan for isolated structures can be taken as 3.5 times the estimated scour depth, which corresponds to the upper envelope shown as a dashed line in Figure 17:

$$E_x = 3.5\, S_{eq} \qquad (13)$$

where S_{eq} is the equilibrium scour depth.

When using this value in design, it should be borne in mind that it applies to an area surrounding the structure. For example, for a square cofferdam measuring 10m x 10m in plan and with an estimated equilibrium scour depth of 7m, the extent of scour to be considered in design should be 25m upstream of the upstream face of the cofferdam, 25m downstream of the downstream face and 25m from the sides. This therefore would correspond to a 3500m^2 area of bed around the cofferdam that could be subject to local scour.

The experimental data obtained for the square structure with a transverse sill was not sufficient to draw accurate conclusions but it indicated that, for the same shape and width of structure, larger extents of scour will be produced when compared with isolated structures. This is an expected finding since the sill causes

a substantial obstruction to the flow around the structure, where the bed is not "allowed" to scour. Therefore the scouring potential of the flow is transferred farther away from the structure.

A similar analysis was carried out to investigate the relationship between the water depth and the extent of scour, which would in principle be easier to apply in design. Figure 18 (which includes only data for the square structure since tests were not carried out with variation of the water depth for other shapes), indicates the following linear relationship, with a correlation coefficient of 0.72:

$$E_x = 2.33\ y_o \qquad (14)$$

For design purposes it is recommended to use the following relationship, which corresponds to the envelope line shown dashed in Figure 18:

$$E_x = 3.7\ y_o \qquad (15)$$

where y_o is the mean flow depth. Equations (14) and (15) are valid only for square structures and for relative water depths of y_o/B between 0.5 and 1.0.

As a method of estimating the extent of scour, Equation (13) is more general than Equation (15) and is preferable in form because the scour depth is the fundamental factor determining the plan dimensions of scour holes. However, Equation (15) provides a convenient means of making a quick estimate of the likely extent for the case of square structures.

If the depth and extent of scour have been estimated, it is possible to calculate the approximate total volume of sediment that might be excavated from the scour hole. A proportion of this volume will probably be deposited around the structure in the form of bars, which can locally reduce the water depth available in the river/estuary. If these bars are formed in navigable areas of the watercourse, they may constitute a hazard for boat traffic.

4.7 Extent of protection around structures

Knowing the likely depth and extent of scour expected around a structure, the designer may decide to provide some bed protection to prevent undermining of the structure and its foundations or to prevent unwanted sediment deposition in navigable areas. Protection of the bed can be carried out effectively in a number of ways, from placing of riprap (i.e. loose dumped stone) to the use of proprietary mattress systems such as open stone asphalt or cabled concrete blocks. Once a protection system is installed on the bed, the depth and extent of scour will be greatly reduced when compared with the unprotected situation (provided a suitable system is chosen and correct installation procedures were adopted).

A series of tests was carried out in order to determine the extent of protection actually needed around structures in the case where the bed is protected by loose stone. The conclusions are valid also for other revetment systems as long as they are stable under the same flow conditions. The minimum size of gravel that would not be eroded by flow conditions around the structures during the tests was determined, and as a result it was decided to use a fairly uniform gravel with d_{50} = 8mm.

Most of the tests in this series on scour protection were carried out with the 75mm x 75mm square structure. The flow conditions were tidal (half-tidal cycle of 30minutes), with a water depth of 75mm and the flow velocity equal to the critical value for the sand bed. The thickness of the protective layer placed around the structure was equal to about three times the d_{50} size of the stone, in line with normal recommendations on the use of riprap. The lateral extent of the protection from the sides of the structure was varied during the tests to determine the minimum that would be needed to prevent scour developing.

In the first test the square stone blanket extended 150mm from the sides of the structure in the streamwise and transverse directions. The test was conducted for six tidal cycles and the bed was visually observed at the end of the test to detect any movement of the stone protection. A view of the structure from above is shown in Figure 11 and it can be seen that the stone mattress had remained intact. There was some movement of sand onto the blanket but the stone was still in place beneath the sand. It was concluded that this area of protection was probably more than sufficient and that tests should be carried out with less extensive protection to determine the minimum limits. The test was therefore repeated with the extent of protection reduced to 100mm and this gave similar results to the first test. The protection was then reduced to 50mm. It was observed that, although near the structure there were no signs of instability of the bed, some stones had fallen into a scour hole that had formed at the perimeter of the mattress (see Plate 12).

An equivalent test (with the same flow conditions and a 50mm extent of stone protection) was then carried out for a circular structure. The results were found to be quite comparable to those with the square structure, i.e. some stones were dislodged but in the proximity of the structure (within a distance of 25mm from the sides) the protection remained undisturbed.

These two cases indicated that the protective mattress needed to extend somewhat further than 50mm from the sides of the structure in order to prevent the presence of the structure producing any additional disturbance of the bed. An extent of protection equal to at least the width or diameter of the structure (75mm in the case of the present tests) is therefore suggested. This conclusion was checked for the case of a square pier with a transverse sill; the results confirmed that minimal disturbance to the stone mattress occurred when the extent of the mattress was equal to (or greater than) the width of the pier (see Plate 13).

The conclusions from the above tests regarding the minimum recommended extent of protection around different types of structure are presented in Table 7 and summarised in Figure 19. These results are applicable to relative water depths of $y_o/B = 1.0$ or less.

5. DEVELOPMENT OF PREDICTION METHOD FOR TIDAL SCOUR

5.1 General approach

The HR experiments described in Chapters 3 and 4 were not intended to reproduce particular prototype situations at a given scale but were designed to investigate in a systematic way the various factors that influence the depth of local scour around structures subject to tidal flows. In this report, the word "tide" is used to describe any flow in which the flow conditions reverse direction as part of a regular periodic cycle; it includes but is not restricted to astronomic tides in estuaries and the sea having a full-cycle duration of 12.3 hours.

In the case of structures in rivers subject to unidirectional flows, the key requirement is usually to determine the maximum depth of scour which would occur if the worst possible combination of flow velocity and water depth were to continue long enough for equilibrium conditions to be reached. In practice, river flows do not normally remain constant for long periods but the value of maximum possible scour depth should provide a safe estimate for design purposes and allow some margin for inaccuracies in field data or predictions of extreme flow events. The maximum scour depth in unidirectional flow can be determined relatively easily in laboratory tests by keeping the flow conditions constant until the equilibrium state is reached (or approached so closely that the rate of change in scour depth is small enough to be neglected). With these types of test the time factor need not be considered in the analysis of the results. Data from many laboratory studies has shown that equilibrium scour depths obtained with different sizes of laboratory model can be scaled geometrically provided factors such as the relative flow depth and velocity are also correctly scaled (see Section 2.2). There is also good evidence that laboratory results can be scaled to much larger sizes of structure because the predictions match well with the upper envelope of scour depths measured in the field (see for example Melville and Sutherland (1988)).

In the case of tidal flows, the time factor cannot be ignored because the equilibrium scour depth that is reached after a sufficient number of cycles is determined by the amount of sediment that is eroded or deposited by the flow in each direction during successive half-cycles of the tide. It cannot be assumed that the time factor will necessarily scale between model and prototype according to the Froudian law (ie time scale = $\sqrt{\lambda}$, where λ is the geometric scale). This is because the time factor for the scouring process is determined by the rate of sediment erosion and is only indirectly related to the speed of the water. Therefore, the HR experiments were planned so as to cover a variety of tidal shapes, velocities and durations without attempting to model prototype astronomic tides having a period of 12.3 hours. Only after the influence of the various factors had been analysed was it possible to identify an appropriate "characteristic time" for the scouring process. Based on this characteristic time, a suitable procedure could then be developed for scaling model results to prototype conditions.

As a matter of general principle, it was decided to aim for a prediction method for tidal conditions that would be consistent with the large amount of information already existing about local scour in unidirectional flows. Put another way, the resulting method should be such that the unidirectional condition can be included as the limiting case of a tide with a very long duration.

Dimensional analysis indicates that the tidal scouring process should depend on suitable non-dimensional ratios of the key variables. The half-cycle period, D_T, of the tide is obviously an important factor, and the physics of the problem suggests that it should be compared with a characteristic time related to the rate of development of the scour hole for the flow conditions being considered. As will be explained in Sections 5.2 and 5.3, data on the variation of scour depth with time obtained from previous HR tests with unidirectional flows was used to define this characteristic time.

5.2 Rate of development of scour holes

As part of the previous HR study on scour around large obstructions in unidirectional flows, May & Willoughby (1990) measured the variation of scour depth with time in a total of 21 tests with different sizes of square and circular structures. Each test was continued until it was believed that the scour depth had effectively reached its final equilibrium value; the durations of the tests ranged between 44 hours and 76 hours depending on the flow conditions. The flow velocities used in the tests were either below or equal to the critical value for general movement of the sediment bed upstream of the structure. Full details of the measurements are given in the reference mentioned above.

Analysis of this data was carried out with the aim of producing a general method for predicting the time development of scour in unidirectional flows. Previous HR studies on marine scour have suggested that a suitable type of equation for describing the time variation is:

$$\frac{S}{S_\infty} = 1 - \exp\left[-\left(\frac{t}{T_c}\right)^p\right] \qquad (16)$$

where: S is the scour depth at time t from the start of erosion; S_∞ is the final equilibrium scour depth reached as the time $t \rightarrow \infty$; T_c is a characteristic time for the scouring process; and p is a coefficient. In the present study, the data for an individual test was analysed by assuming a value of S_∞ and using linear regression techniques to find the best-fit values of p and T_c. The procedure was repeated with a new value of S_∞ until the combination of S_∞, p and T_c was found that gave the highest value of correlation coefficient. Although this principle seems reasonable from a mathematical point-of-view, the three independent parameters were found to respond in an unstable way to small discontinuities in the test data (e.g. steps in the erosion process), gave unrealistic estimates of S_∞ and widely varying values of the characteristic time, T_c .

For this reason, it was decided to try a simpler approach by assuming that the time variation of scour depth could be described by an equation of the form:

$$\frac{S}{S_\infty} = \left(\frac{t}{T_e}\right)^\alpha \qquad \text{for } 0 \le t \le T_e \tag{17}$$

where, as before , S_∞ is the final equilibrium scour depth but now assumed to be reached after a finite time T_e. Using the actual values of S_∞ and T_e from the HR tests, consistent results were obtained for the best-fit values of the coefficient α. The twelve tests on square piers gave values between $\alpha = 0.10$ and 0.18, with an overall average of $\alpha = 0.165$. In the case of circular piers, the nine tests gave values in the range $\alpha =$ 0.21 to 0.41, with an overall average of $\alpha = 0.327$. The difference in the values of α for the two types of structure reflects the fact that the initial rate of scour development at the square piers was greater than at the circular piers. This was probably due to the sharper flow separation at the corners of the square piers which would have increased the amount of turbulence and the initial rate of sediment transport out of the scour holes.

Having established the suitability of Equation (17) for estimating scour depths at intermediate times during the erosion process, it can be used to define a new characteristic time, T_{50}, which is defined as the time taken for the scour depth to reach 50% of the final equilibrium scour value. From Equation (17) it follows that:

$$\frac{2S}{S_\infty} = \left(\frac{t}{T_{50}}\right)^\alpha \tag{18}$$

where it can be assumed that $\alpha = 0.165$ for square structures and $\alpha = 0.327$ for circular structures.

T_{50} can be considered as being somewhat similar to the "half-life" governing the decay rate of radioactive substances. The major advantage of using T_{50} as the characteristic time factor for the erosion process is that it can be found quite precisely from data on the rate of scour development, whereas the time T_e to final equilibrium can be much more difficult to determine accurately. Also, T_{50} is more relevant to practical problems of tidal scour because the half-cycle duration of the tide will usually be much closer to T_{50} than to T_e.

5.3 Factors determining T_{50}

The characteristic time, T_{50} , for the scouring process might be expected to depend on the following main factors :

- The depth-averaged velocity, U, of the flow upstream of the structure.
- The depth of flow, y_o.
- The shape of the structure (eg, square or circular).
- A characteristic length related to the scouring process (eg, the width, B, of the structure, or the final equilibrium scour depth, S_∞, for unidirectional flow).
- The particle size of the bed sediment (eg, d_{50}) and/or the critical velocity, U_c, for initiation of sediment movement.

Various types of correlation between these factors and T_{50} were investigated using the data from the HR tests carried out earlier by May & Willoughby (1990). Figure 20 shows plots of the non-dimensional quantities X and Y versus the relative flow depth y_o/B, where these quantities are defined as:

$$X = \frac{(\beta U - U_c)T_{50}}{B} \tag{19}$$

$$Y = \frac{(\beta U - U_c)T_{50}}{S_\infty} \tag{20}$$

The coefficient β is the local velocity intensification factor due to the presence of the structure. Thus βU is the effective flow velocity occurring at the structure when the upstream flow velocity is U. Values of β can be determined by assuming that local scouring of the bed will start to occur if $\beta U = U_c$. For circular structures, it follows from Equations (2) and 4 that $\beta = 1/0.522 = 1.92$; for square (and rectangular) structures in line with the flow, it can be seen from Equation (6) that $\beta = 2.67$.

From Figure 20 it can be seen that the variations in the value of the non-dimensional parameter X were reasonably small (given the complexities of the scouring process and sediment-transport problems in general) and showed no overall dependence on the relative flow depth y_o/B. By contrast, the variations in the parameter Y were very much larger and were not correlated with variations in the value of the ratio y_o/B. It was therefore decided to adopt the parameter X as the basis of a method for predicting the characteristic time, T_{50}. Using the data in Figure 20, the average value of the parameter was found to be X = 5500. Therefore, it follows from Equation (19) that T_{50} can be estimated from:

$$T_{50} = \frac{5500B}{(\beta U - U_c)} \tag{21}$$

where consistent units must be used (eg, B in m, U and U_c in m/s, and T_{50} in s). It should be noted that the analysis described so far in Sections 5.2 and 5.3 was based on the results of the earlier HR study on scour around structures in unidirectional flows.

As part of the present investigation, measurements of the scour depths were made at various times during the tests including after the very first half-cycle of each tidal sequence. Until the end of the first half-cycle the conditions were equivalent to those in a test with unidirectional flow. The data from the present study was therefore used as an independent check of the equations developed above. The value of the scour depth S_{DT} after the end of the first half-cycle (after time $t = D_T$) was estimated from Equation (18) written in the form:

$$S_{DT} = \frac{S_\infty}{2}\left(\frac{D_T}{T_{50}}\right)^\alpha \tag{22}$$

where T_{50} was predicted from Equation (21), with appropriate values of the coefficients α and β depending on whether the structure was circular or square. The equilibrium scour depth, S_∞, for unidirectional flow was predicted from Equation (2) or (6). Figure 21 shows the ratio of the predicted and measured values of S_{DT} as a function of the relative time ratio D_T/T_{50} for tests with a constant flow velocity of $U = U_c$ in each half-cycle. It can be seen that the predicted values of S_{DT} were generally close to the measured values (with an average ratio of $S_{pred}/S_{meas} = 1.03$) and did not depend significantly on the time factor D_T/T_{50}. In the tests carried out by May & Willoughby (1990), the pier sizes varied from B = 0.10m to 0.40m and the sediment size was $d_{50} = 0.145$mm; in the present study, the corresponding values were B = 0.075m and either d_{50} = 0.75mm or 0.44mm. The data in Figure 21 therefore evaluates the prediction method outside the range from which the various equations were originally developed.

The good results achieved in this independent check of Equations (21) and (22) indicate that the proposed method of determining the characteristic time T_{50} has a reasonable basis for the types of condition

investigated, ie clear-water scour with $U \leq U_c$. The use of U_c in Equation (21) accounts satisfactorily for the effect of sediment size and no separate allowance for d_{50} appears necessary. The non-dimensional form of the equations suggests that they ought to scale reasonably to prototype conditions since similar types of scaling have been found to be valid for local scour problems in general.

5.4 Equilibrium scour depths in tidal flows

As explained in Chapter 4, the test data for the case of clear-water scour shows that the equilibrium scour depth, S_{eq}, occurring after a sequence of tides will lie between S_{DT} (ie the scour depth reached after the very first half-cycle of the tide at time $t = D_T$) and S_∞ (the final equilibrium scour depth that would be reached if the flow were unidirectional or if the tidal duration $D_T \rightarrow \infty$). The relative increase in scour depth from S_{DT} to the equilibrium value S_{eq} can be expected to depend on the magnitude of the half-cycle tidal duration, D_T, compared with the characteristic time, T_{50}, for the scouring process.

Figure 22 shows values of the ratio S_{eq}/S_{DT} plotted as a function of the ratio D_T/T_{50} for the tests with square and circular structures having a constant flow velocity of $U = U_c$ in each half-cycle of the tide. The values of S_{DT} used in the plot were those measured in the tests; however, as shown by Figure 21, there would have been little difference if the values of S_{DT} predicted by the method in Section 5.3 had been used instead. As would be expected, Figure 22 indicates that repeated tides of short duration produce a relatively bigger increase in scour depth relative to S_{DT} than tides with longer durations. The following best-fit equations were fitted to the data (excluding one bracketed point for the fine sediment) and are shown as dashed lines in Figure 22:

$$\frac{S_{eq}}{S_{DT}} = 1.548 - 0.2384\left(\frac{D_T}{T_{50}}\right) \qquad \text{for } 0.55 \leq D_T/T_{50} \leq 2.0 \tag{23a}$$

and

$$\frac{S_{eq}}{S_{DT}} = 1.07 \qquad \text{for } D_T/T_{50} > 2.0 \tag{23b}$$

For design purposes, it is recommended to use the following equations which provide an upper envelope to the experimental data, shown as solid lines in Figure 22:

$$\frac{S_{eq}}{S_{DT}} = 1.80 - 0.24\left(\frac{D_T}{T_{50}}\right) \qquad \text{for } 0.55 \leq D_T/T_{50} \leq 2.5 \tag{24a}$$

and

$$\frac{S_{eq}}{S_{DT}} = 1.2 \qquad \text{for } D_T/T_{50} > 2.5 \tag{24b}$$

These last two equations therefore enable the equilibrium scour depth for clear-water scour under tidal conditions to be predicted using the values of S_{DT} and T_{50} obtained from Equations (22) and (21) respectively.

5.5 Effect of tidal shape

The results described in Sections 5.3 and 5.4 were obtained with data from the tests in which the flow velocity was kept constant with time during each half-cycle of the tide. As explained in Section 4.2, some tests were also made with the velocity varying sinusoidally with time in order to represent conditions

occurring in prototype astronomic tides. The tests were carried out in such a way as to be equivalent to some of the previous tests in terms of the volume of tidal discharge occurring in each half-cycle. Thus, for previous tests with a constant velocity of $U = U_c$ and a half-cycle duration of D_T, the equivalent tests with a sinusoidal variation were carried out so that the peak velocity U_s and the half-cycle duration D_{Ts} satisfied the following relation:

$$U_c D_T = \int_0^{D_{Ts}} U_s \sin\left(\frac{\pi t}{D_{Ts}}\right) dt = \frac{2}{\pi} U_s D_{Ts} \qquad (25)$$

One option studied was to set $U_s = U_c$, which thus required the equivalent sinusoidal test to have a duration of $D_{Ts} = \pi D_T/2$. A second option studied was to set $D_{Ts} = D_T$, which required the peak velocity to be $U_s = \pi U_c/2$. Data from the two types of tests are shown in Figure 9.

For the case of clear-water scour, it was found that sinusoidal tests with a peak velocity of $U_s = U_c$ and a half-cycle duration of D_{Ts} produced equilibrium scour depths that were between 86% and 89% of the values occurring in a constant velocity test with $U = U_c$ and a half-cycle duration of $D_T = (2D_{Ts})/\pi$. Safe design should be achieved if the ratio of scour depths between equivalent sinusoidal and constant velocity tests is assumed to be 90%. This allowance for the effect of tidal shape has been incorporated into the overall prediction method described in Chapter 6.

5.6 Summary of analysis

The prediction method developed from the analysis of the experimental data from this study and from an earlier HR study by May & Willoughby (1990) enables the equilibrium scour depth in tidal conditions to be estimated subject to the following limitations:

- Circular structures and square structures (and by inference rectangular) in-line with the flow.
- Tidal flows, with an alternating constant velocity or with a sinusoidal variation, corresponding to clear-water scouring conditions (ie, peak depth-averaged velocity, U or U_s not exceeding the critical velocity U_c).

A limited number of tests were carried out with live-bed scouring conditions (i.e. U or U_s exceeding U_c) but more data is needed to check whether the prediction method can be extended to this case.

The tests did not simulate the variation in water level that also occurs in tidal flows. This aspect requires further study, but for the present it is suggested that the prediction method should be applied using the water depth corresponding to the mean tide level since the peak velocities occurring in a prototype astronomic tide will normally occur close to this level. Estimates of scour depth based on this assumption are likely to err on the conservative side.

A full description of the recommended prediction method is given in Chapter 6.

6. SUMMARY OF DESIGN PROCEDURE

6.1 Design equations

The equations developed in the previous section can be summarised to provide engineers with a simple design procedure for the hydraulic design of cofferdams and caissons in tidal conditions. The procedure is applicable to structures that are large in relation to the flow depth, i.e. to ratios of water depth to width of structure of 0.5 to 1.0. The procedure was developed for two structure shapes (square and circular) for

which complete data was available. However, important information was collected from tests with rectangular structures and with square shape with transverse sill in tidal conditions. Recommendations are therefore also given at the end of the design procedure on how to deal with these different shapes.

Design procedure for determining the equilibrium scour depth in tidal conditions

The procedure applies to:

- Circular structures and square structures (and by inference rectangular) in-line with the flow.
- Tidal flows, with an alternating constant velocity or with a sinusoidal variation, corresponding to clear-water scouring conditions (i.e. peak depth-averaged velocity, U or U_s not exceeding the critical velocity U_c).

Consistent units should be used throughout (e.g. m/s, m, s).

(1) Calculate Time Factor

$$T_{50} = \frac{5500B}{(\beta U - U_c)} \tag{21}$$

where:

B is the width of the structure transverse to the flow direction.

β is a coefficient that takes the following values:
$\beta = 2.67$ for square structures;
$\beta = 1.92$ for circular structures;
For rectangular structures and square structures with transverse sill (as illustrated in Figure 3), use $\beta = 2.67$, as for the square shape; for shapes intermediate between square and circular, take a value between 1.92 and 2.67.

U is the undisturbed mean flow velocity upstream of the structure, corresponding to the mean tide level.

U_c is the critical flow velocity, i.e. the threshold velocity for movement of the sediment bed; U_c can be calculated with Equation (11), for example.

(2) Calculate the equilibrium scour depth in equivalent unidirectional flow conditions, S_∞

For square structures

$$S_\infty = 1.76\, B \left(\frac{y_o}{B}\right)^{0.6} \left(\frac{1.6U}{U_c} - 0.6\right) \tag{26}$$

For circular structures

$$S_\infty = 1.32\, B \left(\frac{y_o}{B}\right)^{0.6} \left[1 - 3.66\left(1 - \frac{U}{U_c}\right)^{1.76}\right] \tag{27}$$

For rectangular structures and square structures with a transverse sill (as illustrated in Figure 3), use the equation recommended for square structures.

(3) Calculate D_T for an equivalent tide having constant velocity equal to the maximum velocity that occurs during the tide

$$D_T = \left(\frac{2}{\pi}\right) \text{x (duration of half tidal cycle)} \tag{28}$$

(4) Calculate the ratio D_T / T_{50}, where D_T is the "modified" half-cycle tidal duration calculated using Equation (28)

(5) Calculate the value of half the equilibrium scour depth for unidirectional flow conditions

$$S_{50} = \frac{1}{2} S_\infty \tag{29}$$

(6) Calculate the scour depth after one half-cycle, S_{DT}

$$S_{DT} = S_{50} \left(\frac{D_T}{T_{50}}\right)^\alpha \tag{22}$$

where:

α is a coefficient that takes the following values:
$\alpha = 0.165$ for square structure
$\alpha = 0.327$ for circular structure
For rectangular structures and square structures with a transverse sill (as illustrated in Figure 3), use $\alpha = 0.165$, as for a square shape; for shapes intermediate between square and circular, take a value between $\alpha = 0.165$ and 0.327.

(7) Calculate the equilibrium scour depth in tidal conditions

For both square and circular structures

$$S_{eq} = [1.80 - 0.24 \frac{D_T}{T_{50}}] S_{DT} \qquad \text{for } 0.55 \le \frac{D_T}{T_{50}} \le 2.5 \tag{24a}$$

$$S_{eq} = 1.2 S_{DT} \qquad \text{for } \frac{D_T}{T_{50}} > 2.5 \tag{24b}$$

(8) Calculate the equilibrium scour depth taking into account tidal sinusoidal variation

For rectangular structures and square structures with a transverse sill, apply a reduction factor to Equation (24) of 0.9.

(9) Safety factor

For design purposes it is recommended to apply a safety factor to allow for the complexity of the scouring processes. The value of the safety factor will need to take account of the particular circumstances but could typically be of the order of 1.1.

6.2 Worked example

A square cofferdam with side length of 10m is going to be built around a bridge pier to allow for repair work to be carried out. The flow conditions at the site are such that, at mean tide level, the water depth is 4m and the corresponding flow velocity is estimated to be 1.1m/s. The bed material is a gravel with a d_{50} size of 7mm.

In order to determine a suitable depth to which the sheet piles of the cofferdam should be driven for structural stability, estimate the depth of scour that is likely to be produced around the cofferdam.

It is first necessary to estimate the critical flow velocity, U_c, of the bed sediment. Using Equation (11) and assuming that the relative density of the bed is 2.65:

$$U_c = a\,[g\,(s\text{-}1)\,d]^{0.5}\left(\frac{y_o}{d}\right)^{0.2}$$

For d_{50} = 7mm, a =1.0

$U_c = [9.81 \times (2.65 - 1) \times 0.007]^{0.5}\,(4/0.007)^{0.2} = 1.198$m/s.

Calculate the time factor (Equation 21):

$$T_{50} = \frac{5500B}{(\beta U - U_c)}$$

For square structures β=2.67

$$T_{50} = \frac{(5500 \times 10)}{(2.67 \times 1.1 - 1.198)} = 31\,630 \text{ seconds}$$

Calculate the scour depth in equivalent unidirectional flow conditions, S_∞ (Equation 26):

$$S_\infty = 1.76\,B\left(\frac{y_o}{B}\right)^{0.6}\left(\frac{1.6U}{U_c} - 0.6\right)$$

$$= 1.76 \times 10 \times \left(\frac{4}{10}\right)^{0.6}\left[\left(\frac{1.6 \times 1.1}{1.198}\right) - 0.6\right] = 8.83\text{m}$$

For a half-cycle tidal duration of 6 hours, calculate the duration of the equivalent tide at constant critical velocity (Equation 28):

$$D_T = \left(\frac{2}{\pi}\right) \times 6 = 3.82 \text{ hours}$$

Calculate the time ratio $\frac{D_T}{T_{50}}$, where D_T is the half-cycle tidal duration:

$$\frac{D_T}{T_{50}} = \frac{(3.82x3600)}{31630} = 0.435$$

Calculate $S_{50} = \frac{1}{2} S_\infty$

$S_{50} = 0.5 \times 8.83m = 4.415m$

Calculate the scour depth after one half tidal cycle (Equation 22):

$$S_{DT} = S_{50} \left(\frac{D_T}{T_{50}} \right)^\alpha$$

For square structures $\alpha = 0.165$,

$S_{ST} = 4.415 \times 0.435^{0.165} = 3.85m$

Calculate the equilibrium scour depth in tidal conditions (Equation 24a):

$$S_{eq} = \left[1.80 - \frac{0.24 D_T}{T_{50}} \right] S_{DT}$$

$= (1.80 - 0.24 \times 0.435) \times 3.85 = 6.53m$

Apply reduction factor to calculate scour depth under sinusoidal variation of flow velocity during tidal flows:

$S_{eq} = 0.9 \times 6.53 = 5.9m$

It is recommended to apply a safety factor to the above value. Assuming a typical safety factor of 1.1 produces a scour depth of 6.49m.

The length of sheet piles for the cofferdam should be determined on the basis that tidal flows could cause local scour to a depth of about 6.5m below mean bed level if no protection is placed around the structure.

If it is decided to protect the cofferdam with riprap or another suitable type of scour protection, this should be placed with its top surface level with or slightly below the existing bed level; the minimum extent of protection should be 10m around the perimeter of the cofferdam.

7. TESTS AND ANALYSIS OF PROTOTYPE STRUCTURES

An investigation of the scour produced by tidal flows around complex pier shapes was also carried out during the current study. Data was available on prototype piers that were designed to support the deck of a new estuary crossing. The data on the geometric characteristics of the piers was complemented by very recent surveys of the estuary, which had co-ordinated field measurements of both the flow velocity and the scour depth around the piers. In general terms the piers were formed by eight vertical cylindrical piles linked by a pier cap above which extended the bridge pier structure.

It was decided to conduct tests on two piers, P1 and P2, which had the above overall shape (i.e. they were essentially capped pile structures) but were of different dimensions. A generic schematic of the piers is shown in Figure 23 and the geometric characteristics of these piers are summarised in the following table (prototype values):

PIER	B (m)	L (m)	D_p (m)	Z (m)	P/D_p
P1	8.5	25.7	1.7	10.3	3.06
P2	10.6	28.1	2.2	1.1	3.00

In this table B is the transverse width of the pile cap, L is the longitudinal length of the pile cap, D_p is the diameter of each of the eight piles forming the pier, Z is the level of the undersize of the pile cap above the level of the upstream undisturbed bed and P is the spacing between the centrelines of the piles. The main differences between the geometries of the two piers resided in the underside level of the pier cap in relation to the bed level: pier P2's cap was considerably closer to the bed than pier P1's cap.

Pier P1 was modelled at a geometric scale of 1:100 and pier P2 at a scale of 1:125 (see Plates 14 and 15). As mentioned in previous sections (and particularly in Section 4.5), it has been established that for models using non-cohesive sediment, the relative scour depth does not depend significantly on the relative size of the sediment particles. It was therefore not necessary to scale the sediment size geometrically from prototype to model, and the sand used in the tests had a mean size of 0.75mm and a specific gravity of $2.62 kg/m^3$.

Each model pier was first tested in unidirectional flow with constant water levels that corresponded to the mean tide level at the site: water depths of 0.122m for pier P1 and 0.050m for pier P2. These levels were such that the water surface was above the underside level of the pier caps (but below their top level). In order to obtain maximum equilibrium scour depths for these pier shapes, the flow velocity in the tests was the critical velocity for the sediment, which was calculated using Hanco's equation (see Section 3.3). The tests were continued for a model duration of 24 hours in the case of pier P1 and 31 hours in the case of pier P2 (see Plates 16 and 15, respectively).

Tests were then carried out to study the maximum scour depths achieved with tidal flow conditions. As in previous tidal tests (see Section 4.2), the tides were simulated by a constant water depth and a constant flow velocity, which was reversed in direction every half-cycle. Pier P1 was tested with critical velocity and, since the available survey data had been obtained under a lower flow velocity, which corresponded to 0.66 of the critical velocity, this was also simulated in the laboratory. The tests were continued for about six complete cycles to allow the bed to reach equilibrium conditions, but it was found that after only two or three cycles the maximum scour depths did not alter appreciably.

The value of the half-cycle duration was determined according to Froudian similarity from an assumed six hour prototype half-cycle duration. A reduction factor was applied to this value to allow for the difference between the approximately sinusoidal variation of velocity in the prototype and the constant velocity used in the model. If D_T is the half-cycle duration (with subscripts m and p representing model and prototype, respectively) and λ is the geometric scale of the model, the relation between D_{Tm} and D_{Tp} was:

$$D_{Tm} = \lambda^{0.5} [(2 / \pi) D_{Tp}] \quad (30)$$

Table 8 summarises the flow conditions during the tests. As for the simple geometric shapes tested, measurements of scour depth were carried out regularly during the tests with prototype shapes and the mobile bed was carefully surveyed at the end of each test. The scour pattern described in Section 2.2, where the maximum depths are concentrated around the individual piles, was also observed in the present study. For all the tests performed at critical flow velocity, a large scour hole with a shallow bowl shape that surrounded the whole structure was observed to form, and deeper, localised holes were observed very close to the piles (see, Plate 16 showing test P1U). Test P1B at $U<U_c$, produced considerably smaller scour depths and a scour pattern which differed significantly from that obtained for critical flow velocity. The maximum scour depths were also concentrated around the piles but the individual scour holes did not coalesce to form a larger hole, and a relatively large accumulation of sediment was observed between the four innermost piles (Plate 17).

The results of the tests are presented in Table 9, where it can be seen that the maximum scour depths tended to occur at piles positioned at the ends of the pier, which reflects the finding that build-up of sediment was usually observed in the mid section of the pier. Table 9 also includes the maximum equilibrium values of scour depth measured in each test and the results of a field survey carried out on 6 May 1997 to measure the scour depth around pier P1. The flow conditions during this survey were reproduced in test P1B (at a Froudian scale of 1:100). It can be seen from the table that the model values converted to prototype values do not differ greatly from the survey data, bearing in mind the simplified scaling law used in the model (Froudian scale) and the inherent difficulties in achieving high accuracy in the prototype measurements under water. The model data shows a maximum equilibrium scour depth of 2.1m (prototype value), compared with a value of 1.7m obtained from the survey. The value of 2.1m was obtained directly from application of Froudian scaling laws, without consideration of the characteristic time for the scouring process in tidal flows (see discussion in Chapter 5). Application of the prediction method described in Chapter 5, which takes into account the characteristic time for the flow conditions of the survey led to a value of 2.07m, i.e. to a slight overestimation of the measured survey value. This indicates that the prediction method, which incorporates a safety factor and therefore will give somewhat higher estimates of the scour depth, is a suitable tool for estimating scour depths around structures including those of complex geometry such as pier P1.

8. CONCLUSIONS

- An extensive laboratory study was carried out to investigate scour development around large obstructions (such as cofferdams and caissons) under tidal conditions. The study involved investigating the effect on the equilibrium scour depths of the following parameters: water depth, shape of the obstruction, reversal of the flow direction, tidal cycle duration and sediment size.

- The tests were conducted in a 24m long flume by 0.6m width, which was fitted with an axial pump that allowed the reversal of the flow direction and variations in the flow velocity and water depth. The test section was formed by a 4m long granular bed where typical structure shapes were placed. The shapes studied were: square, circular, rectangular and square with a transverse sill (as illustrated in Figure 3). Tests were also carried out with scale models of two complex bridge piers formed by eight capped piles.

- The results of all the tests with regular shapes were analysed, and allowed some general conclusions to be drawn. With regard to the shape effect, it was found that square structures produced the largest scour depths and that the square shape with transverse sill produced the smallest. With regard to the influence of the water depth, the tests showed a marked decrease in scour depth with a decrease in water depth (for ratios of water depth to structure width in the range 0.5 to 1.0).

- Using data obtained in an earlier study of unidirectional flow conditions as well as the present results, a general design procedure was developed that allows the estimation of equilibrium scour depths

around large structures under tidal flow conditions. The method first determines the equilibrium scour depth produced in unidirectional flow and is then "corrected" to take into account tidal effects. The prediction method is applicable to cases where the peak tidal velocity does not exceed the critical velocity for the bed material. Application of the prediction method to the conditions of a recent field survey of scour around complex bridge piers showed good agreement between predicted and surveyed scour depths, which supports the validity of the proposed method.

- For the flow conditions and sediments tested, it was found that the extent of scour in plan around a large obstruction in tidal waters can be estimated by Equations (13) and (15).

- The study has shown that the extent of protection needed to prevent scour around a structure can be significantly smaller than the size of the scour hole that would develop if protection were not provided.

- When bed protection is placed to minimise the risk of scour developing close to a structure and eventually jeopardising its stability, it is recommended that the protection should extend outwards from the sides of the structure by a distance equal to or greater than the width, B, of the structure measured transverse to the flow. This recommendation is illustrated in Figure 19 and is valid for cases where the water depth, y_o, does not exceed the width, B, of the structure. The recommended extent is based on tests carried out with a stable stone mattress, with a thickness of about three times the d_{50} size of the stone; it is also applicable to other suitable bed protection systems, such as open stone asphalt mats or cabled concrete block mattresses.

- It is recommended that further research be carried out to extend the range of applicability of the design method to tidal conditions where the peak velocity significantly exceeds the critical velocity for the bed material.

9. ACKNOWLEDGEMENTS

The authors would like to acknowledge the work of Ms Ruth Cano, who carried out the great majority of the experimental tests during her training period at HR Wallingford. The contribution of Mr Andrea Bertagni to the analysis of some of the data is also gratefully acknowledged.

Data on the geometry of prototype capped piers and records of bathymetric and velocity surveys were kindly provided by Novaponte.

10. REFERENCES

Ahmed F & Rajaratnam N (1998). Flow around bridge piers. Jnl Hyd Eng, ASCE, Vol. 124, No. 3, March 1998.

Breusers H N C, Nicollet G & Shen H W (1977). Local scour around cylindrical piers. Jnl Hydr Res, Vol 15, No3, pp 211-252.

Breusers H N C & Raudkivi A J (1991). Scouring. International Association for Hydraulic Research. A.A. Balkema/Rotterdam/Brookfield, The Netherlands. ISBN 90 6191 983 5.

Graham D S & Mehta A J (1981). Burial design criteria for tidal flow crossings. Transp. Eng. Jnl., Proc. ASCE, Vol 107, No. TE2, March 1981.

Hanco S (1971). Sur le calcul des affouillements locaux dans la zone des piles de ponts. Proc. 14th IAHR Congress, Paris, Vol 3, pp 299-313.

May R W P & Willoughby I R (1990). Local scour around large obstructions. HR Wallingford, Report SR240.

Melville B W and Sutherland A J (1988). Design method for local scour at bridge piers. Jnl Hydr Eng., ASCE, Vol 109, No.3, pp 338-350.

Mitchener H J, Torfs H and Whitehouse R J S (1996). Erosion of mud/sand mixtures. Coastal Engineering, 29, pp 1-25.

Whitehouse R J S (1997). Scour at marine structures. A manual for practical applications. HR Report SR 417. August 1997.

Tables

Table 1 Results of tests with square structure and sand 0.75 mm (laboratory values)

Structure: SQUARE 75 mm × 75 mm (laboratory values)
Sediment: SAND d_{50} = 0.75 mm (laboratory value)

Test	Type of flow Tidal cycle duration	Water depth y_o (m)	Velocity U (m/s)	Max scour depth S_{max} (m)	Eq. scour depth S_{eq} (m)
Unidirectional test					
UD	Unidirectional $U = U_c$	0.075	0.274	_	0.116
Tidal tests					
			$U = U_c = 0.274$		
C0	Constant velocity 30 min	0.075	0.274	0.057	0.057
C1	Constant velocity 1 hour	0.075	0.274	0.067	0.064
C2	Constant velocity 2 hours	0.075	0.275	0.070	0.066
C3	Constant velocity 4 hours	0.075	0.275	0.088	0.079
V0A	Sinusoidal 30 min	0.075	Variable between 0 and U_{max} ($U_{max} > U_c$)	0.102	0.100
V1A	Sinusoidal 1 hour	0.075		0.109	0.105
V2A	Sinusoidal 2 hours	0.075		0.120	0.118
V0B	Sinusoidal 46 min	0.075	Variable between 0 and U_{max} ($U_{max} = U_c$)	0.052	0.049
V1B	Sinusoidal 1 h 34 min	0.075		0.057	0.057
V2B	Sinusoidal 3 h 08 min	0.075		0.059	0.059
V3B	Sinusoidal 6 h 16 min	0.075		0.070	0.068
C0M	Constant velocity 30 min	0.075	0.430	0.111	0.110
C1M	Constant velocity 1 hour	0.075	0.430	0.122	0.120
			$U = U_c = 0.259$		
C0A	Constant velocity 30 min	0.056	0.259	0.049	0.049
C1A	Constant velocity 1 hour	0.056	0.259	0.053	0.050
C3A	Constant velocity 4 hours	0.056	0.259	0.071	0.068
			$U = U_c = 0.239$		
C0B	Constant velocity 30 min	0.0375	0.239	0.041	0.032
C1B	Constant velocity 1 hour	0.0375	0.239	0.039	0.035
C3B	Constant velocity 4 hours	0.0375	0.239	0.044	0.042

Table 2 Results of tests with circular structure (laboratory values)

Structure: CIRCULAR ϕ = 75 mm (laboratory value)
Sediment: SAND d_{50} = 0.75 mm (laboratory value)

Test	Type of flow Tidal cycle duration	Water depth y_o (m)	Velocity U (m/s)	Max scour depth S_{max} (m)	Eq. scour depth S_{eq} (m)
Tidal tests					
CC0	Constant velocity 30 min	0.075	$U = U_c = 0.274$ 0.274	0.060	0.057
CC1	Constant velocity 1 hour	0.075	0.274	0.065	0.064
CC2	Constant velocity 2 hours	0.075	0.274	0.070	0.068
CC3	Constant velocity 4 hours	0.075	0.274	0.073	0.072

Table 3 Results of tests with rectangular structure (laboratory values)

Structure: RECTANGULAR 75 mm width × 150 mm length (laboratory values)
Sediments: SAND d_{50} = 0.75 mm (laboratory value)

Test	Type of flow Tidal cycle duration	Water depth y_o (m)	Velocity U (m/s)	Max scour depth S_{max} (m)	Eq. scour depth S_{eq} (m)
Tidal tests					
RC0	Constant velocity 30 min	0.075	$U = U_c = 0.274$ 0.274	0.056	0.050
RC2	Constant velocity 2 hours	0.075	0.274	0.070	0.060
RC3	Constant velocity 4 hours	0.075	0.274	0.075	0.070

Table 4 Results of tests with square structure and sill (laboratory values)

Structure: SQUARE 75 mm × 75 mm WITH SILL (laboratory values)
Sediment: SAND d50 = 0.75 mm (laboratory value)

Test	Type of flow Tidal cycle duration	Water depth y_o (m)	Velocity U (m/s)	Max scour depth S_{max} (m)	Eq. scour depth S_{eq} (m)
		Tidal tests			
SC1	Constant velocity 1 hour	0.075	$U = U_c = 0.274$ 0.273	0.055	0.055
SC3	Constant velocity 4 hours	0.075	0.274	0.065	0.054

Table 5 Results of tests with square structure and sand 0.44 mm (laboratory values)

Structure: SQUARE 75 mm × 75 mm (laboratory values)
Sediment: SAND d_{50} = 0.44 mm (laboratory value)

Test	Type of flow Tidal cycle duration	Water depth y_o (m)	Velocity U (m/s)	Max scour depth S_{max} (m)	Eq. scour depth S_{eq} (m)
Unidirectional test					
FUD	Unidirectional $U = U_c$	0.075	$U = U_c = 0.253$ 0.253	–	0.112
Tidal tests					
FC0	Constant velocity 30 min	0.075	$U = U_c = 0.253$ 0.253	0.056	0.051
FC2	Constant velocity 2 hours	0.075	0.253	0.075	0.072
FC3	Constant velocity 4 hours	0.075	0.253	0.087	0.081

Table 6 Extent of scour in plan

Test	B (m)	y_o (m)	y_o/B	S_{eq} (m)	S_{max} (m)	Max extent of scour E_x (m)	E_x/S_{eq}	E_x/S_{max}	E_x/y_o
Tidal tests									
Square structure									
C0	0.075	0.075	1	0.057	0.057	0.135	2.37	2.37	1.80
C1	0.075	0.075	1	0.064	0.067	0.140	2.19	2.09	1.87
C2	0.075	0.075	1	0.066	0.070	0.175	2.65	2.50	2.33
C3	0.075	0.075	1	0.079	0.088	0.200	2.53	2.27	2.67
C0A	0.075	0.056	0.75	0.049	0.049	0.140	2.86	2.86	2.50
C1A	0.075	0.056	0.75	0.050	0.053	0.155	3.10	2.92	2.77
C3A	0.075	0.056	0.75	0.068	0.071	0.50*	7.35*	7.04*	8.93*
C0B	0.075	0.0375	0.5	0.032	0.041	0.090	2.81	2.20	2.40
C1B	0.075	0.0375	0.5	0.035	0.039	0.075	2.14	1.92	2.00
C3B	0.075	0.0375	0.5	0.040	0.044	0.140	3.50	3.18	3.73
Circular structure	Diameter (m)								
CC0	0.075	0.075	1	0.057	0.060	0.175	3.07	2.92	2.33
CC1	0.075	0.075	1	0.064	0.065	0.150	2.34	2.31	2.00
CC2	0.075	0.075	1	0.068	0.070	0.170	2.50	2.43	2.27
CC3	0.075	0.075	1	0.072	0.073	0.195	2.71	2.67	2.60
Rectangular structure	B (m) L (m)								
RC0	0.075 0.150	0.075	1	0.050	0.056	0.140	2.80	2.50	1.87
RC2	0.075 0.150	0.075	1	0.060	0.070	0.095	1.58	1.36	1.27
RC3	0.075 0.150	0.075	1	0.070	0.075	0.200	2.86	2.67	2.67
Square with sill	B (m)								
SC1	0.075	0.075	1	0.055	0.055	0.225	4.10	4.10	3.00
SC3	0.075	0.075	1	0.054	0.065	0.275	5.10	4.20	3.67

*Uncertainties in measurements due to disturbed bed.

Table 7 Results of tests with scour protection (laboratory values)

Tidal cycle duration = 1 hour
$U = U_c = 0.274$m/s
Water depth = 0.075m
Scour protection: uniform gravel $d_{50} = 8$mm
Bed sediment: sand $d_{50} = 0.75$ mm

Structure	Extent of protection (m)	Observations
Square (B=0.075m)	0.150	No signs of scour
	0.100	No signs of scour
	0.050	Scour hole formed at the perimeter of the bed protection
Circular (ϕ = 0.075m)	0.050	As above
Square with sill (B = 0.075m)	0.075	No signs of scour

Table 8 Model tests with prototype structures (model values)

Pier	Test	Type of flow	Water depth y_o (m)	Velocity U (m/s)
P1	P1U	Unidirectional $U = U_c$	0.122	0.302
	P1A	Constant velocity $U = U_c$	0.122	0.302
	P1B	Constant velocity $U < U_c$	0.122	0.200
P2	P2U	Unidirectional $U = U_c$	0.050	0.253
	P2A	Constant velocity $U = U_c$	0.050	0.253

Table 9 Results of tests of prototype structures (model and prototype values)

Test	Equilibrium scour depth Model values in mm Values measured in the model converted to prototype in m Prototype survey values in m								
	Pile 1*	Pile 2*	Pile 3*	Pile 4*	Pile 5*	Pile 6*	Pile 7*	Pile 8*	Maximum equilibrium values
P1U	69 6.9	69 6.9	- -	- -	- -	- -	- -	- -	69 6.9
P1A	10 1.0	7 0.7	28 2.8	20 2.0	32 3.2	25 2.5	40 4.0	32 3.2	40 4.0
P1B	12 1.2 1.2-1.7	9 0.9 1.1-1.6	- -	- -	- -	- -	21 2.1 1.1-1.3	13 1.3 0.7-0.8	21 2.1
P2U	68 8.5	71 8.9	58 7.25	59 7.4	30 3.8	35 4.4	14 1.8	21 2.6	71 8.9
P2A	32 4.0	33 4.125	0 0	3 0.375	5 0.625	10 1.25	34 4.25	34 4.25	34 4.3

*Refer to Figure 23

Figures

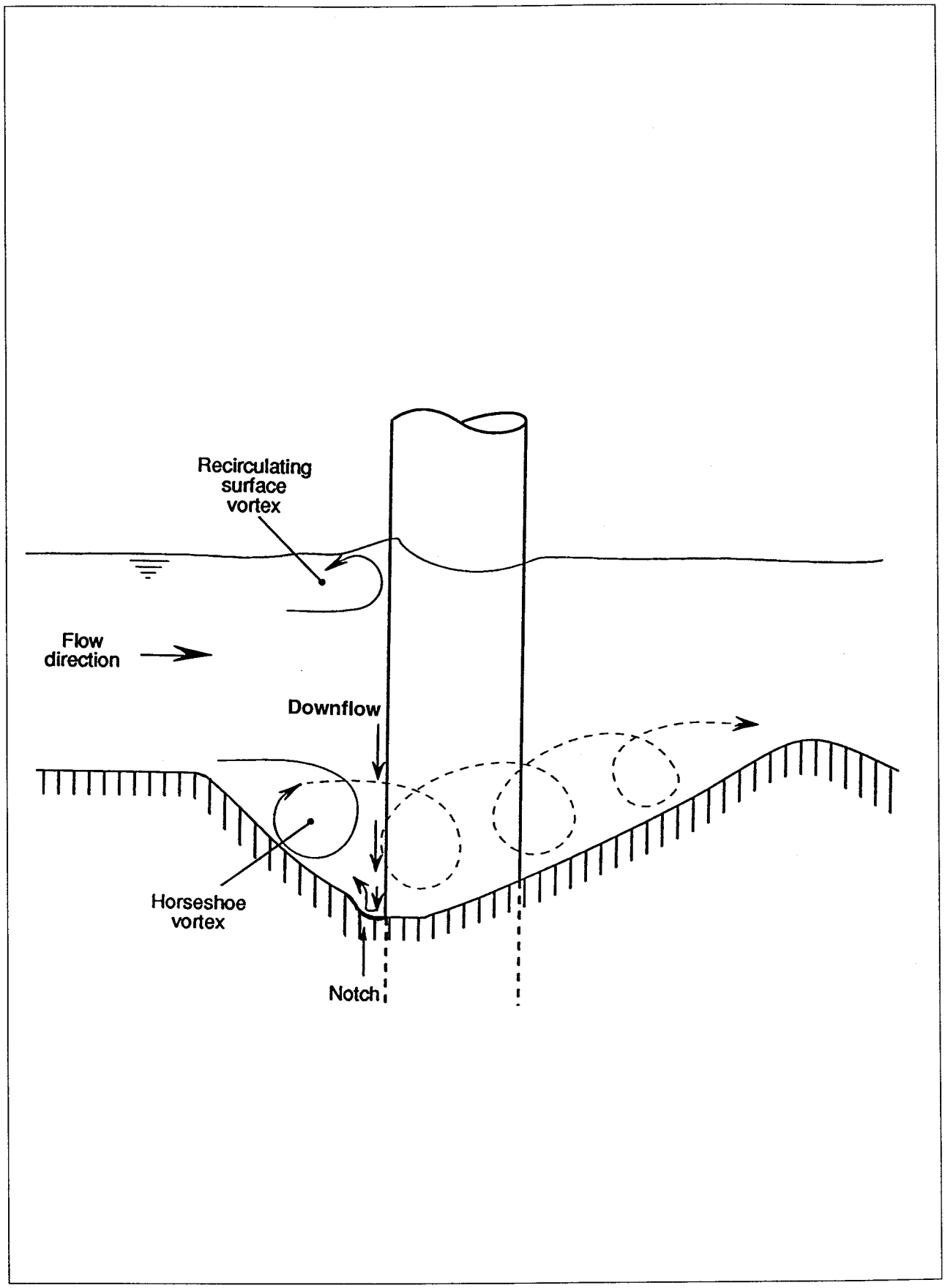

Figure 1 General flow patterns around a circular pier (adapted from May & Willoughby, 1990)

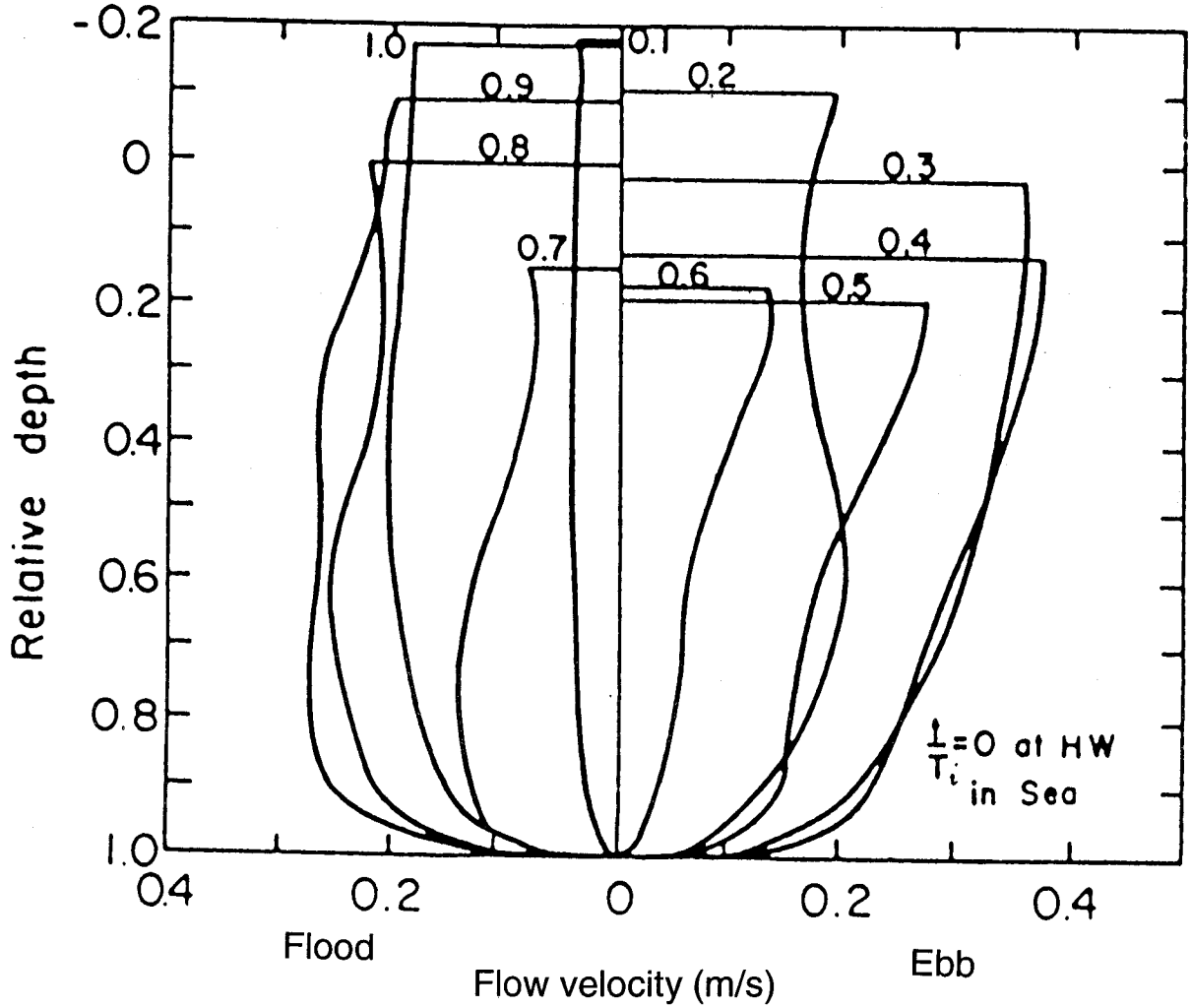

Figure 2 **Variation in velocity profile at different phases of the tidal cycle represented by t/T_i with respect to high water in sea (from Graham & Mehta, 1981)**

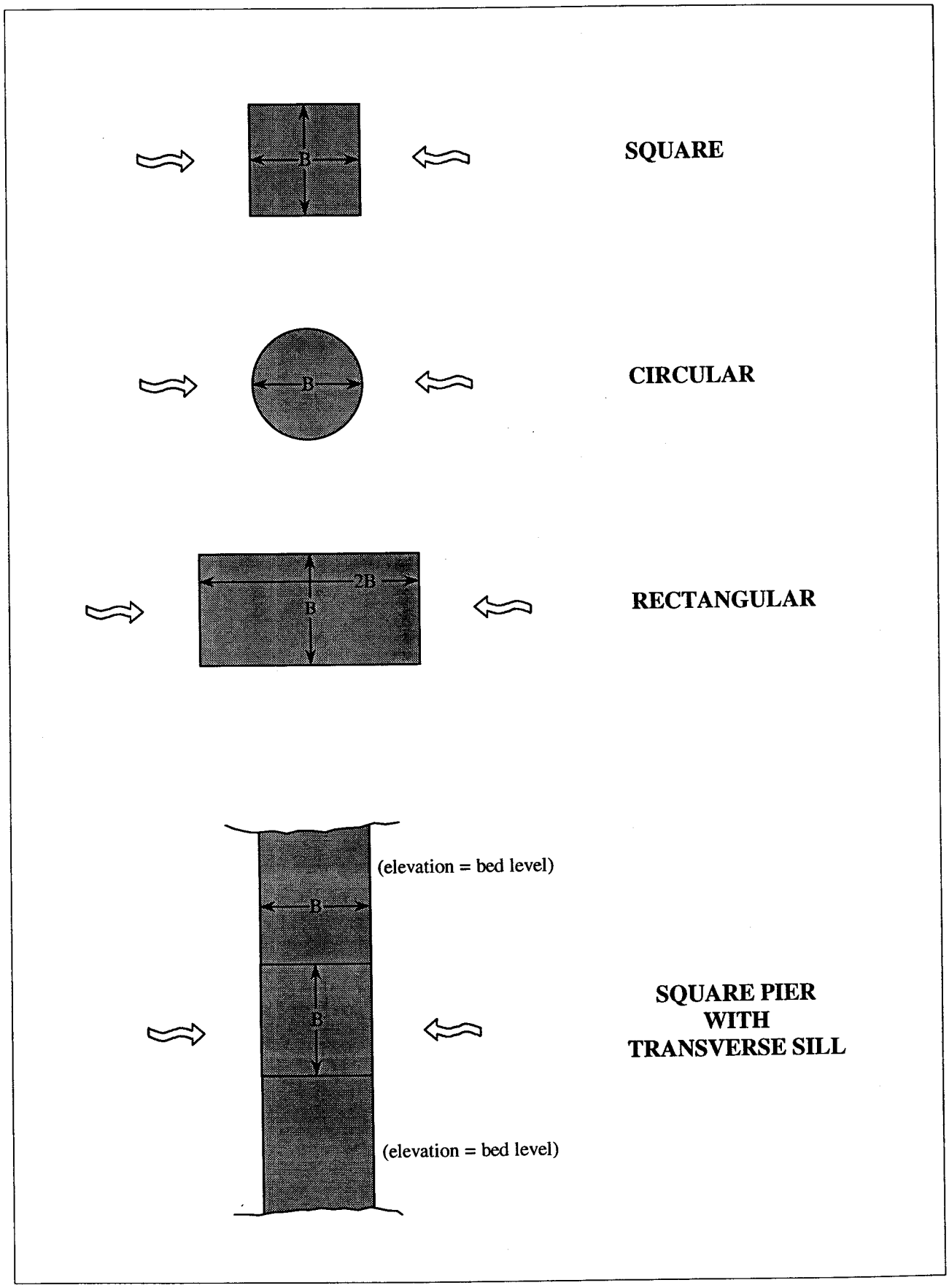

Figure 3 Plan shapes of the structures tested

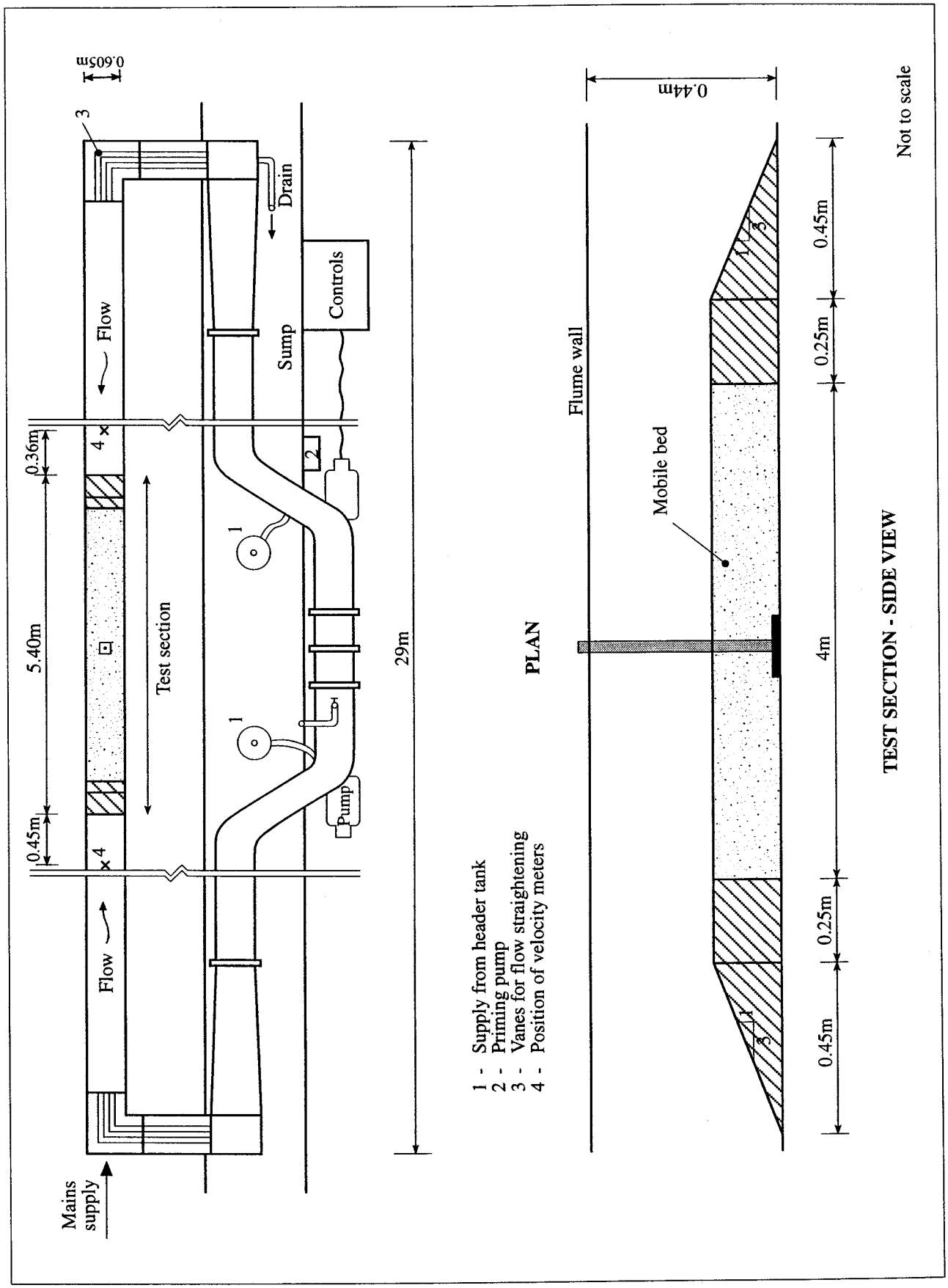

Figure 4 **General plan layout of test rig and close-up of test section**

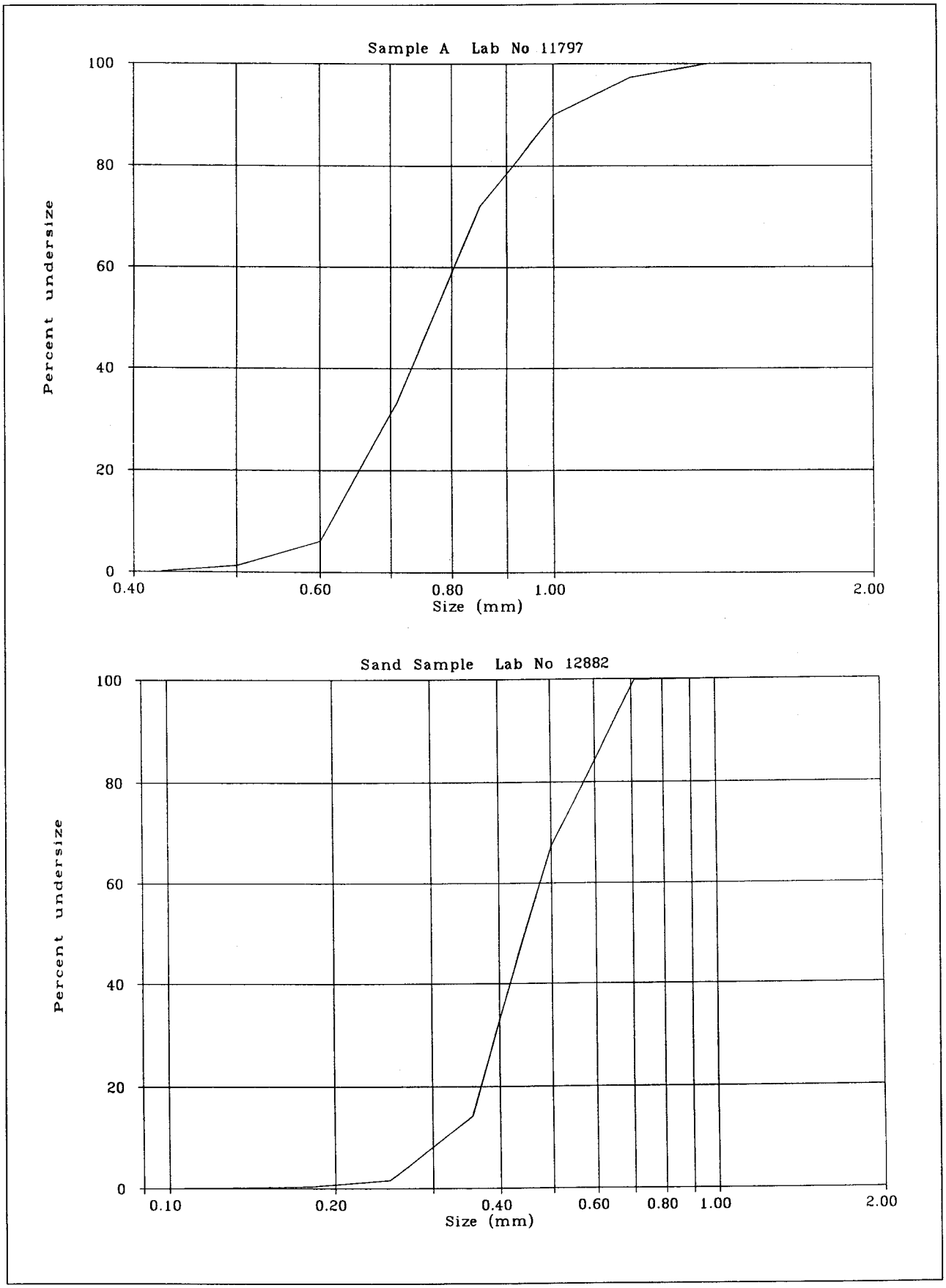

Figure 5 **Grading curves of bed sediment**
0.75mm (top)
0.44mm (bottom)

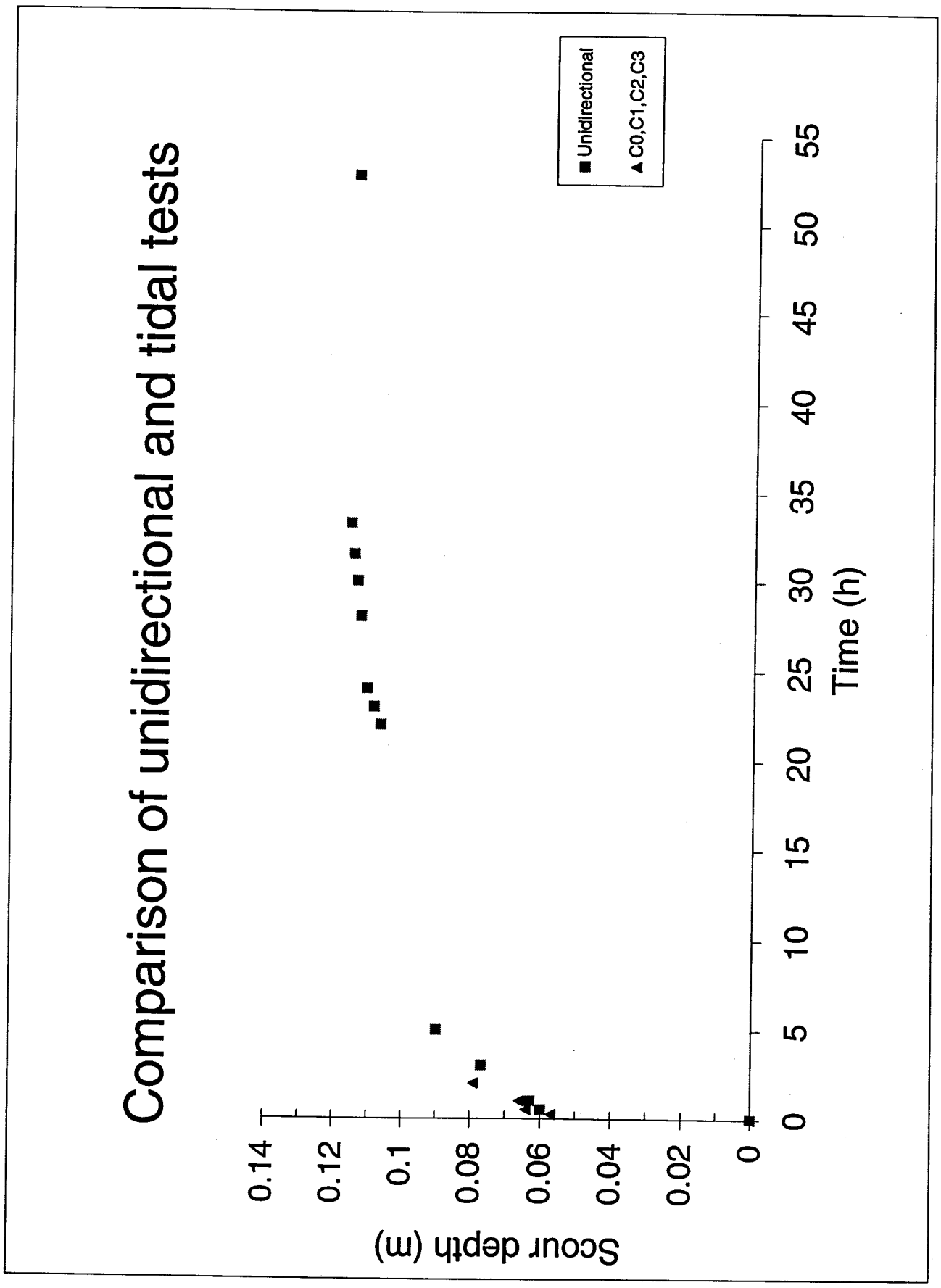

Figure 6 **Effect of flow direction on scour depth (laboratory values)**

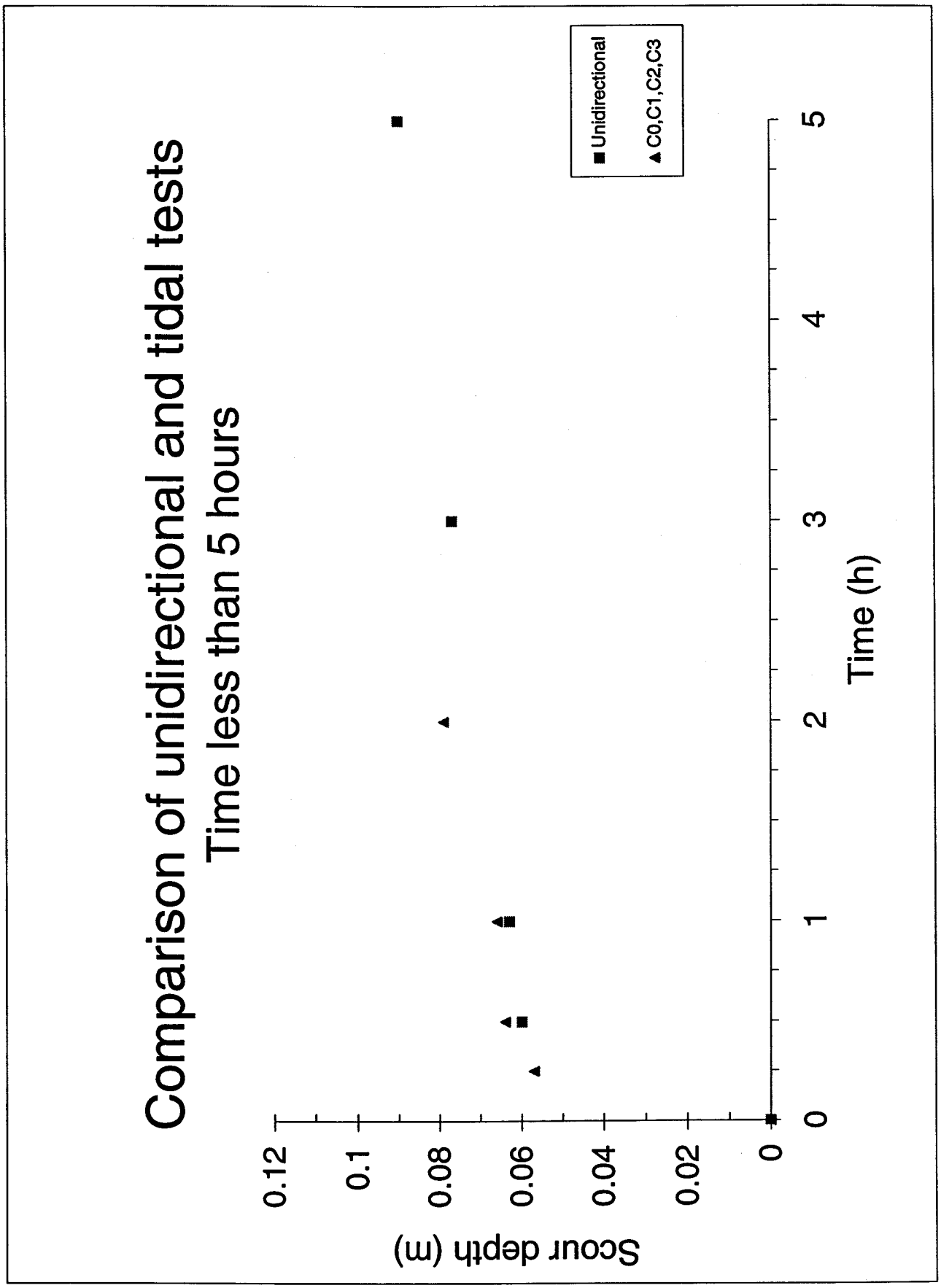

Figure 7 **Effect of flow direction on scour depth (time less than 5 hours) - laboratory values**

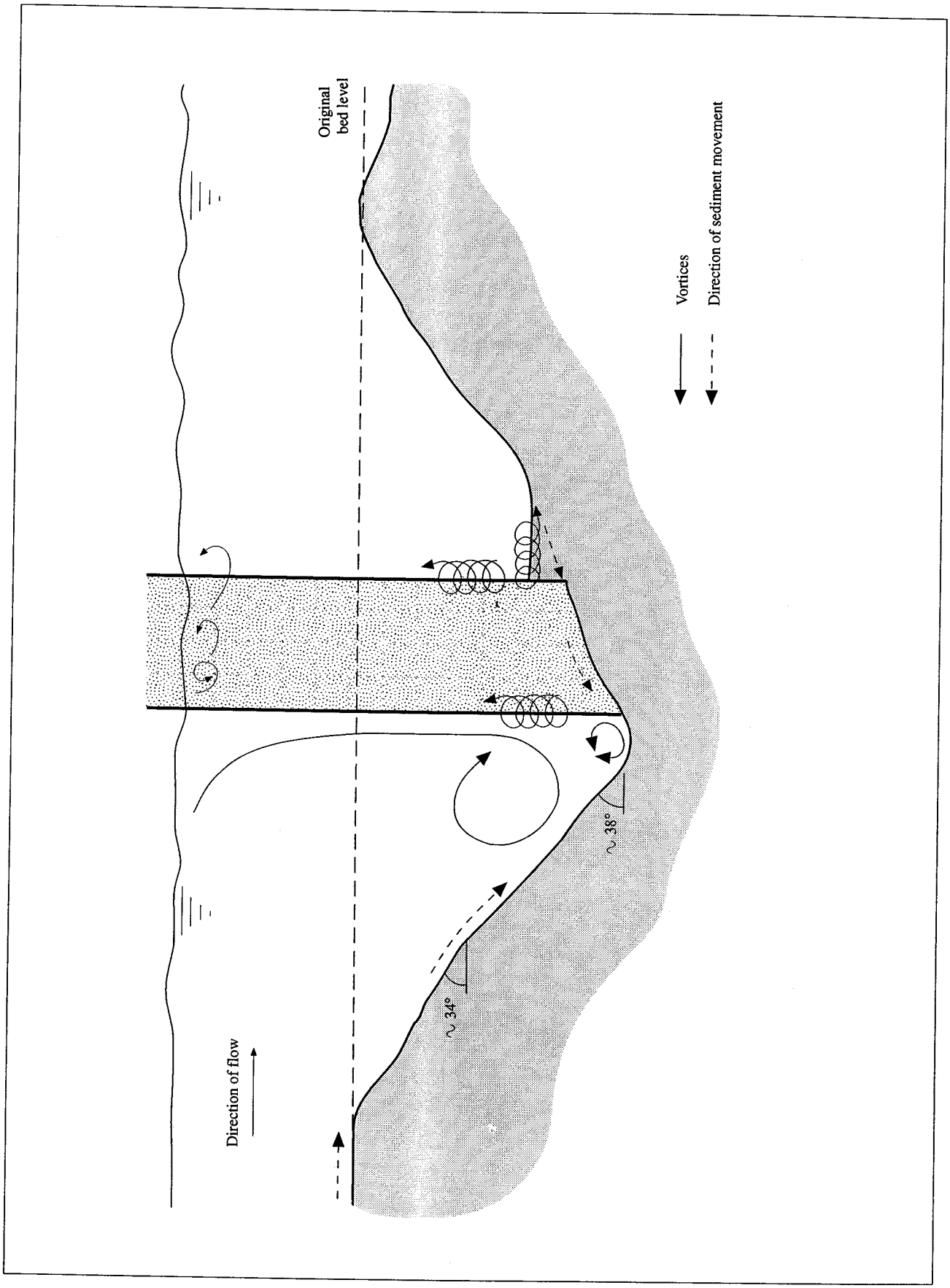

Figure 8 **Flow patterns observed in the scour hole during tidal tests**

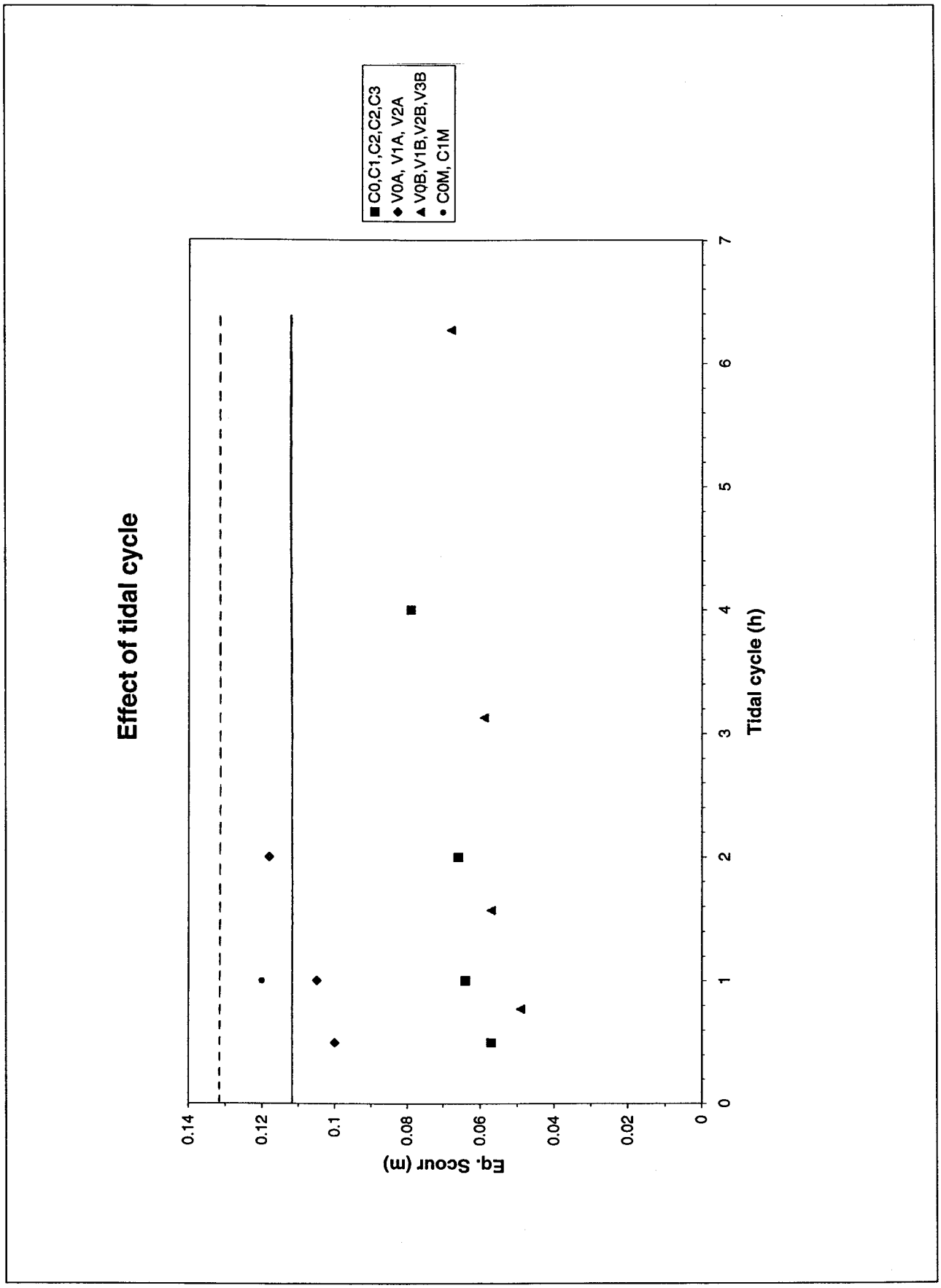

Figure 9 **Effect of tidal cycle on equilibrium scour (laboratory values)**

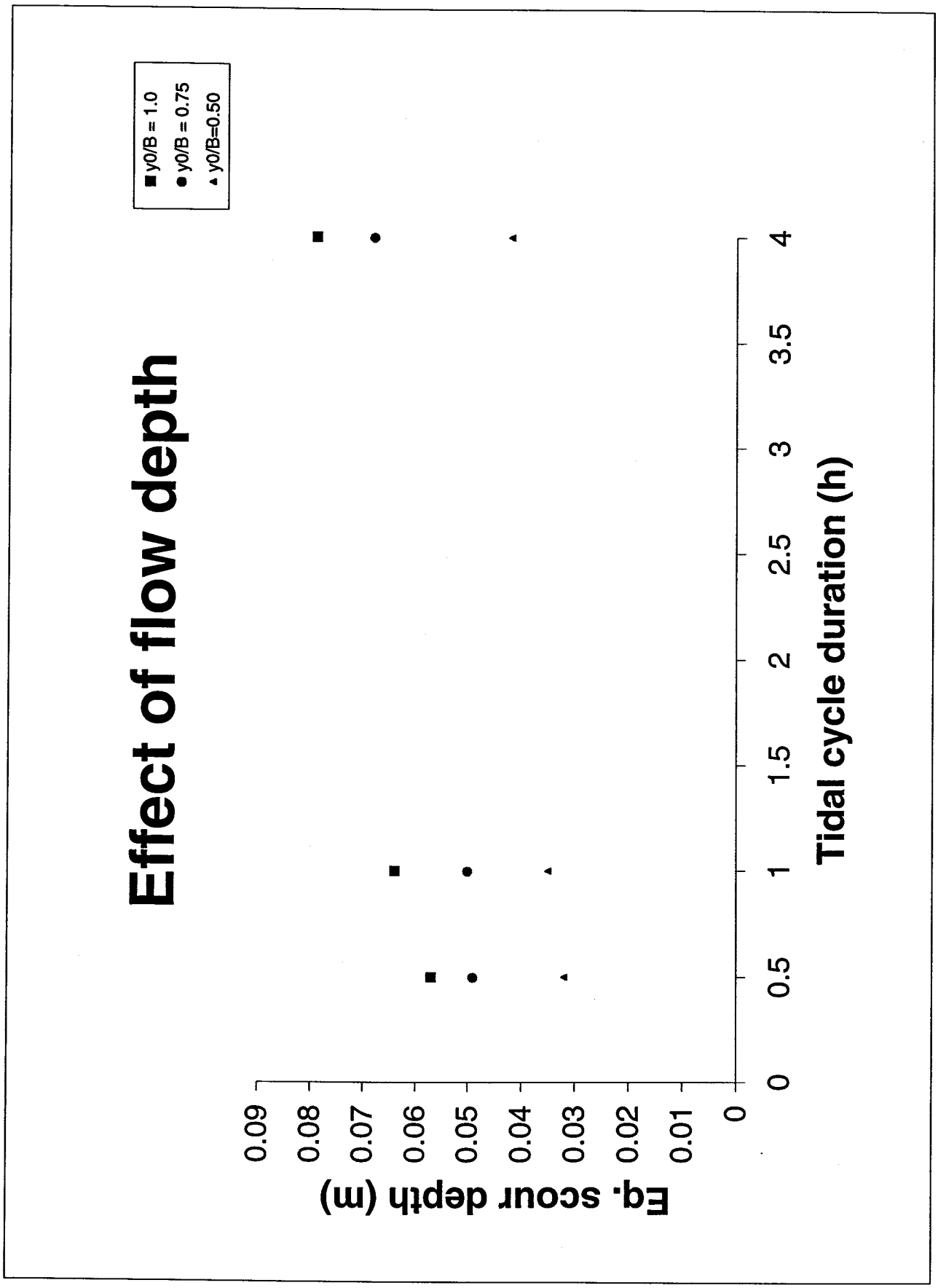

Figure 10 **Effect of flow depth on equilibrium scour depth (laboratory values)**

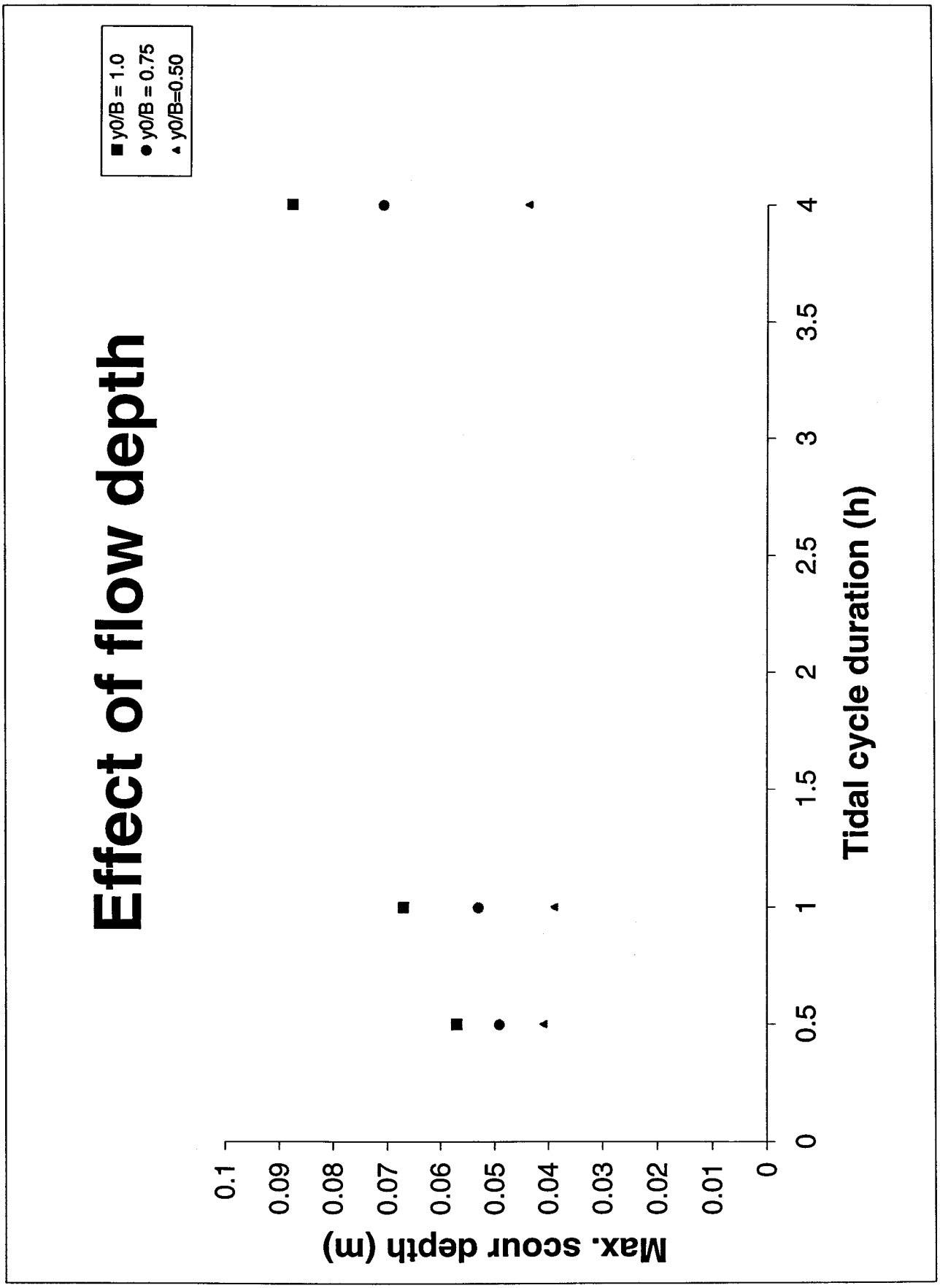

Figure 11 **Effect of flow depth on maximum scour depth (laboratory values)**

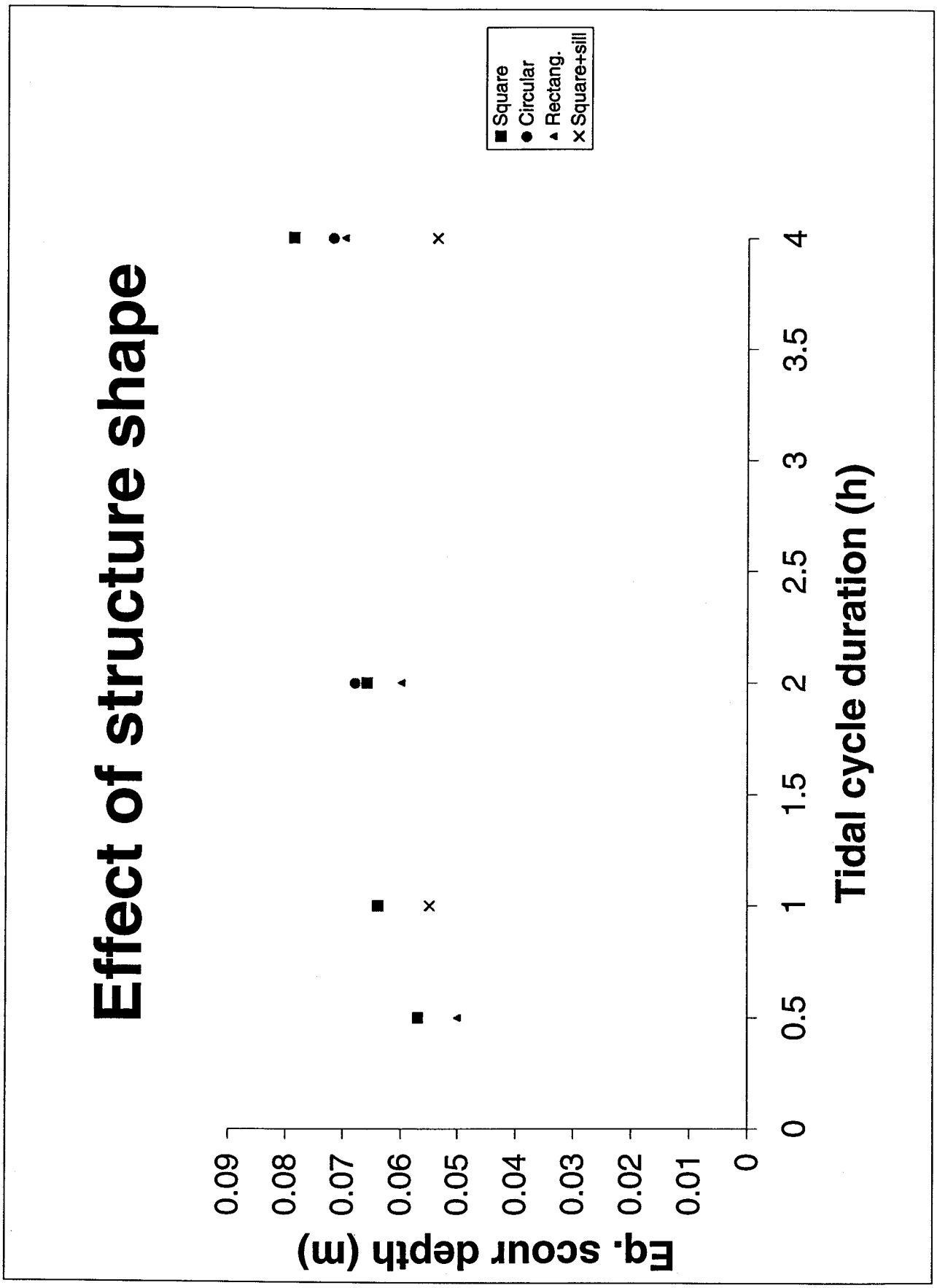

Figure 12 **Effect of structure shape on equilibrium scour depth (laboratory values)**

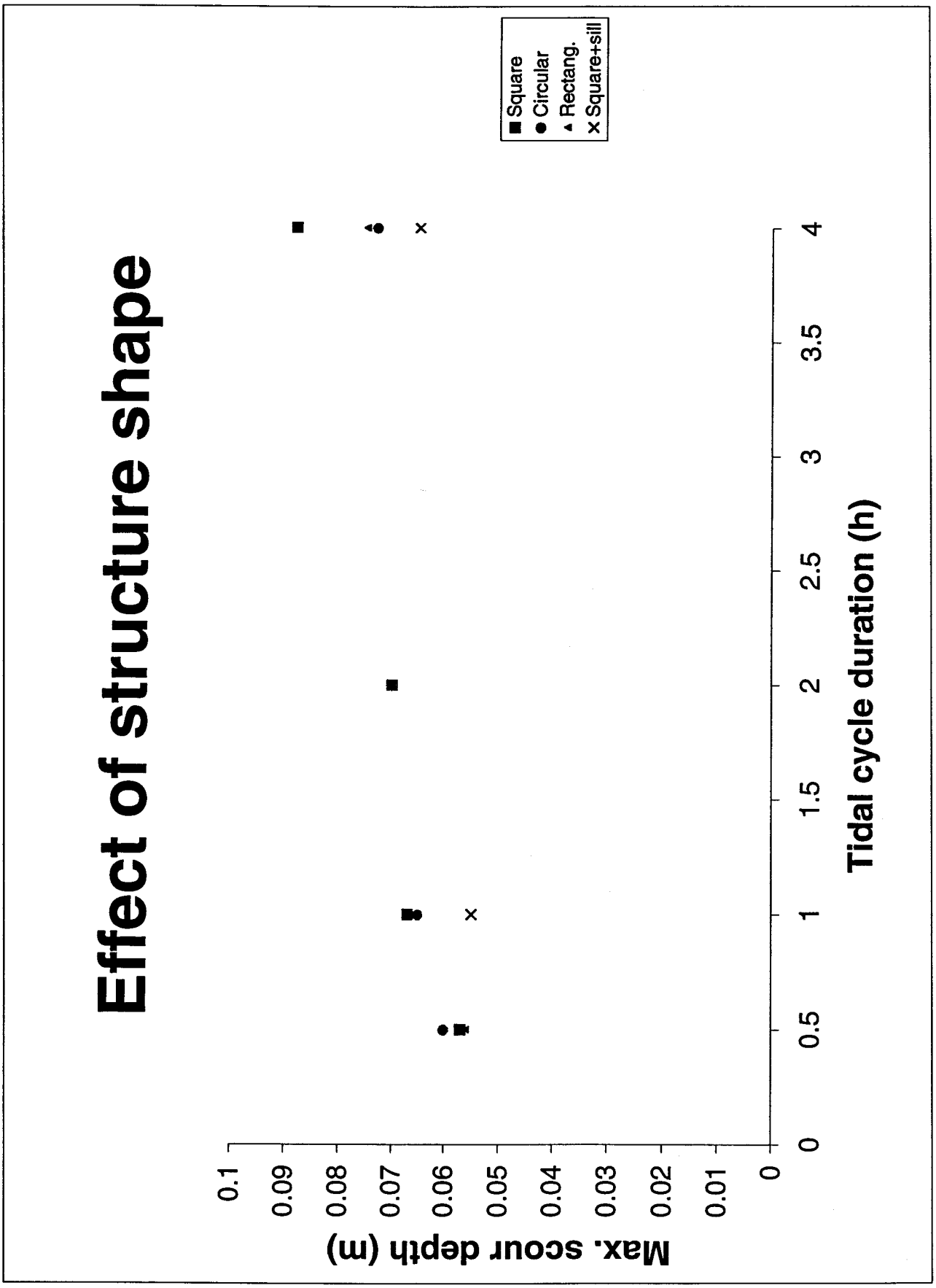

Figure 13 **Effect of structure shape on maximum scour depth (laboratory values)**

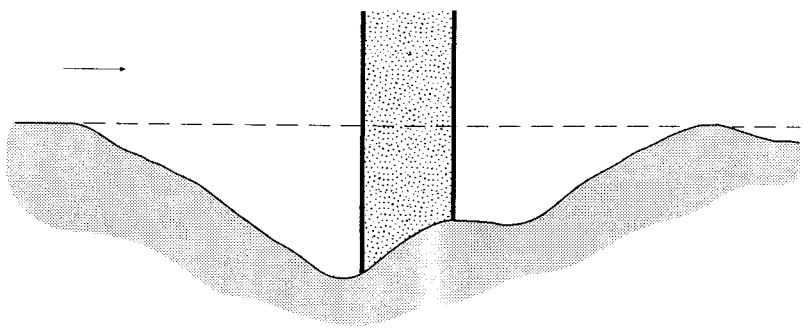

a) Longitudinal profile along the centreline of the flume

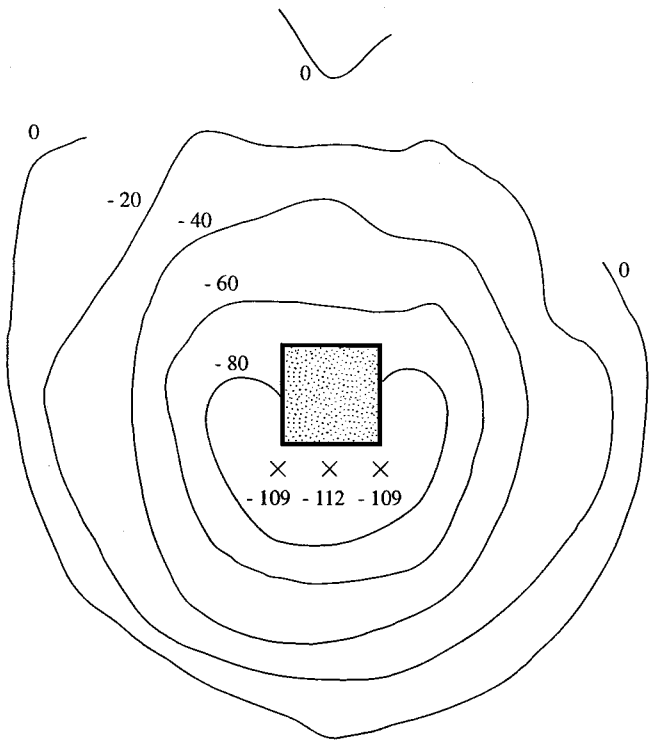

(Bed levels in mm)

a) Plan view

Figure 14 Scour depth after unidirectional test, FUD, with sediment size d_{50}=0.44mm

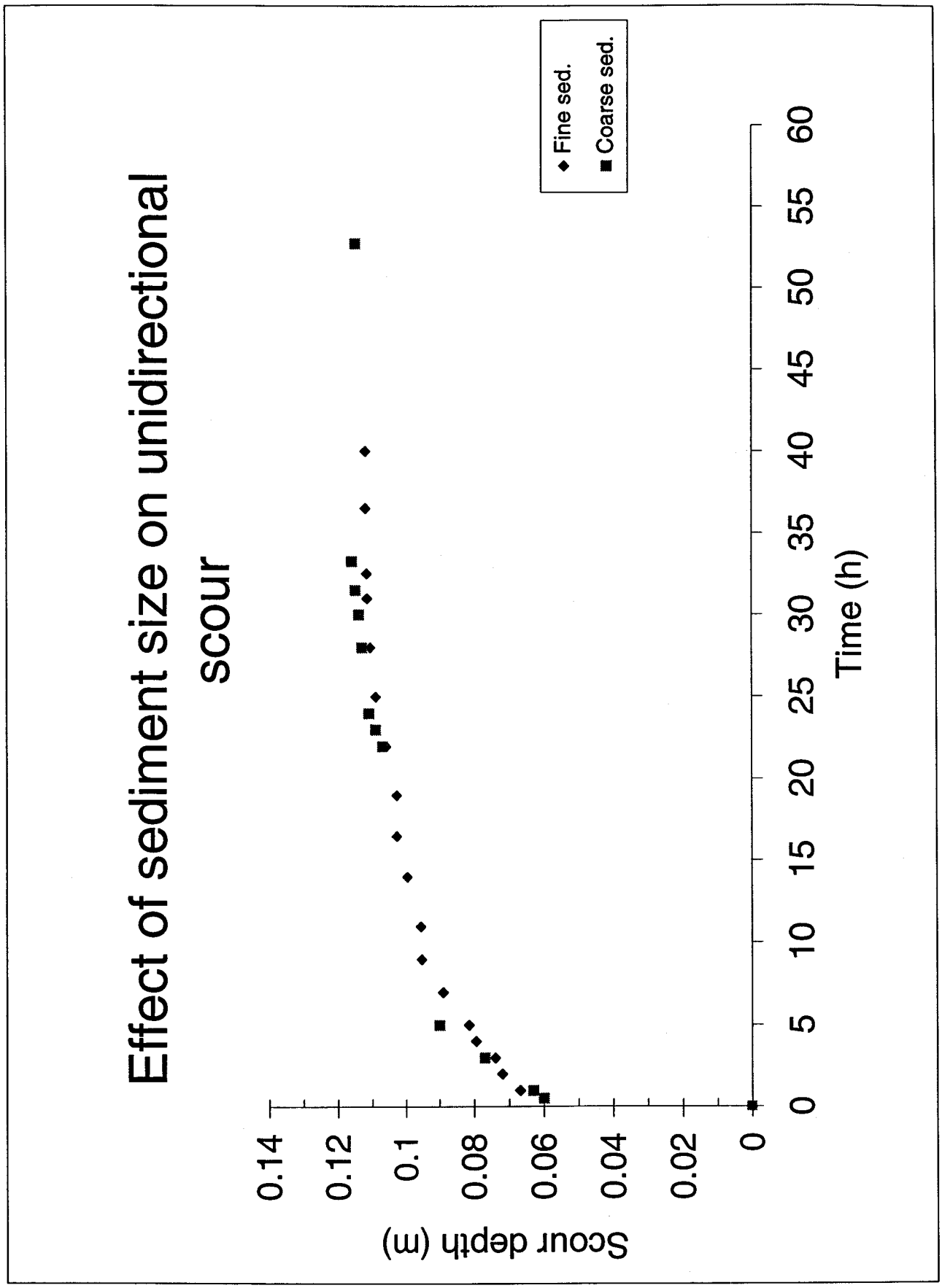

Figure 15 **Effect of sediment size on unidirectional scour depth (laboratory values)**

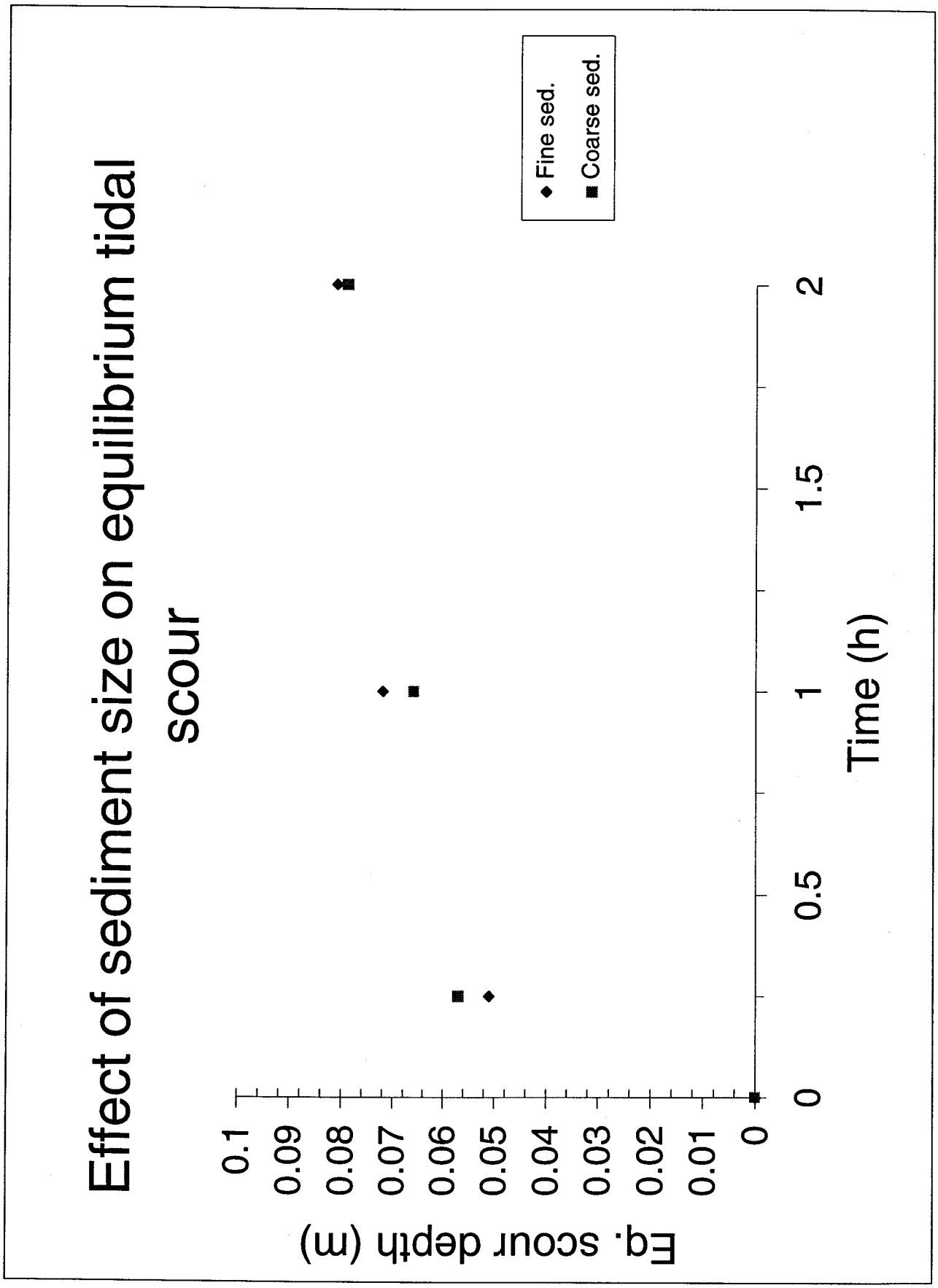

Figure 16 **Effect of sediment size on equilibrium tidal scour (laboratory values)**

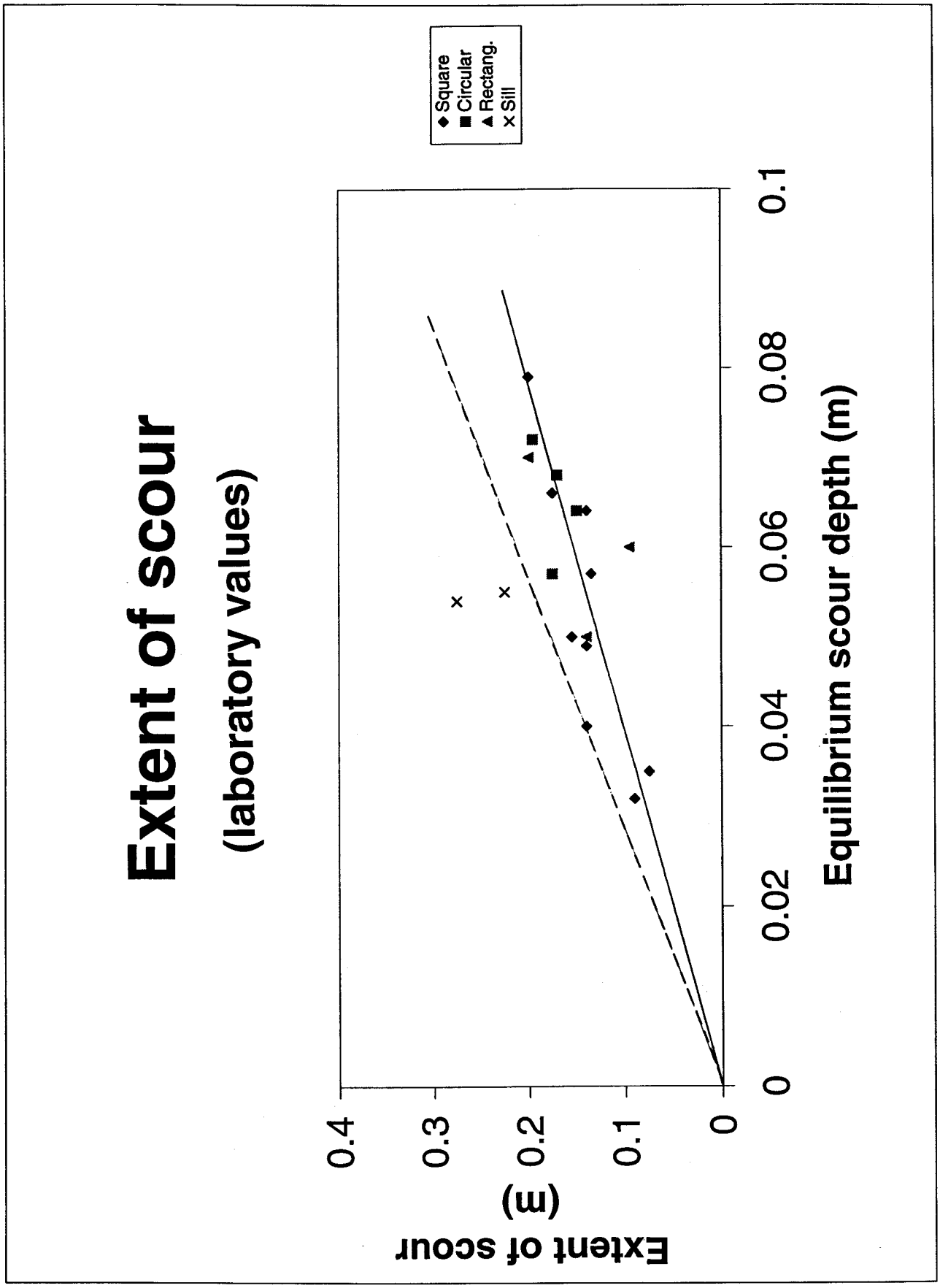

Figure 17 **Relationship between extent of scour and equilibrium scour depth (laboratory values)**

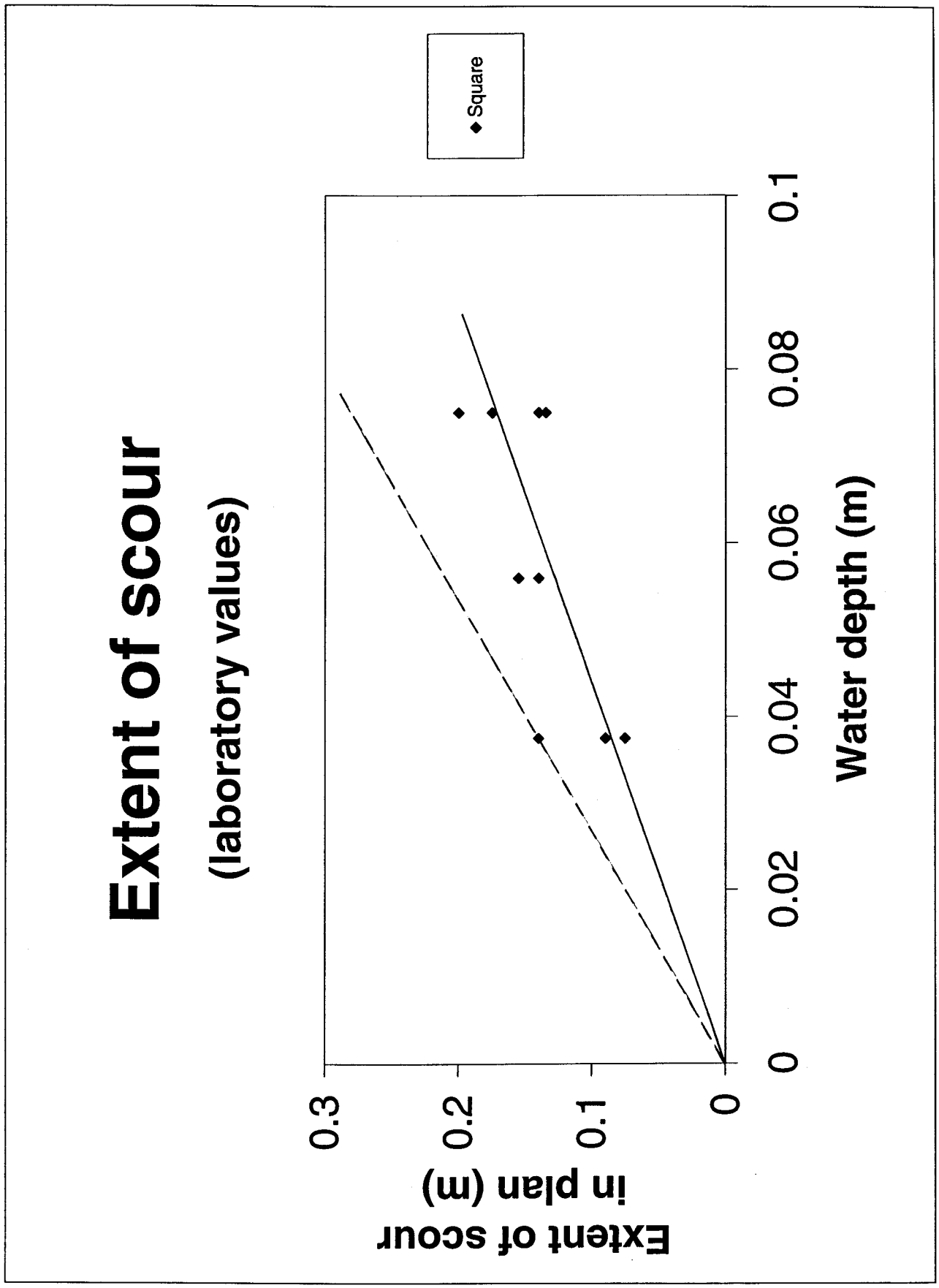

Figure 18 **Relationship between extent of scour and water depth (laboratory values)**

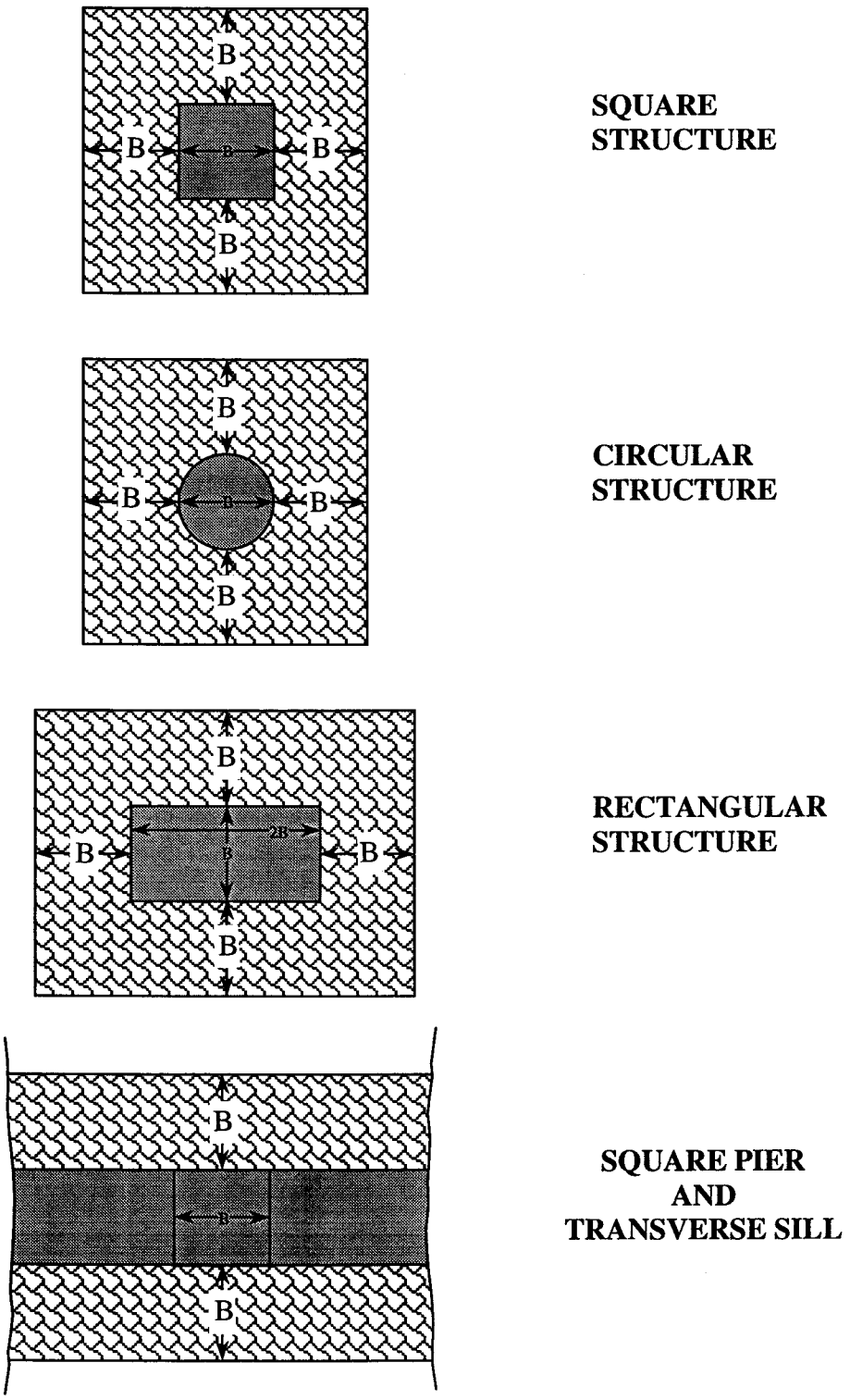

Figure 19 **Recommended minimum extent in plan of bed protection around large obstructions in tidal flows ($y_o/B \leq 1$)**

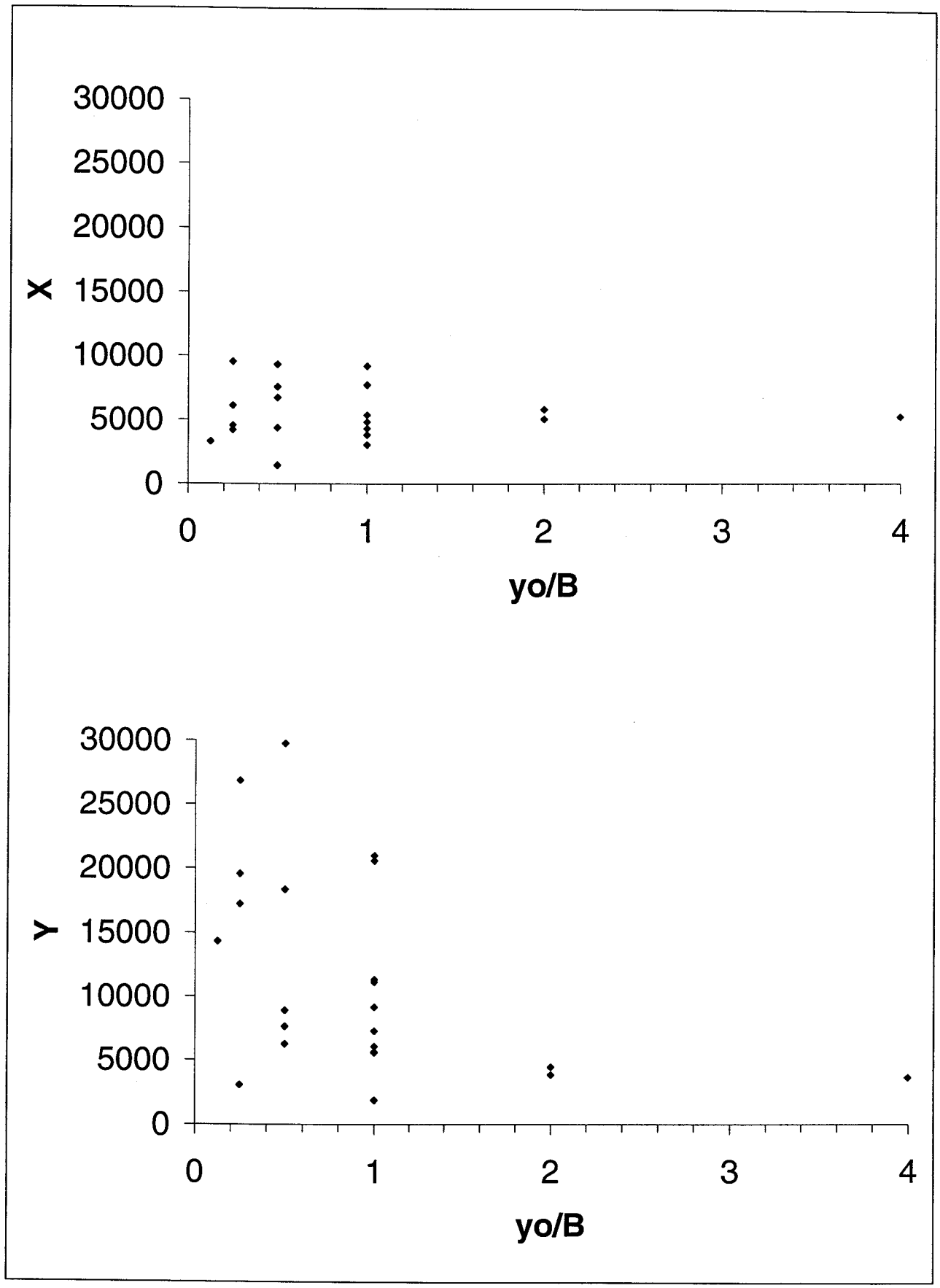

Figure 20 **Determination of constant in the definition of time factor T_{50}**

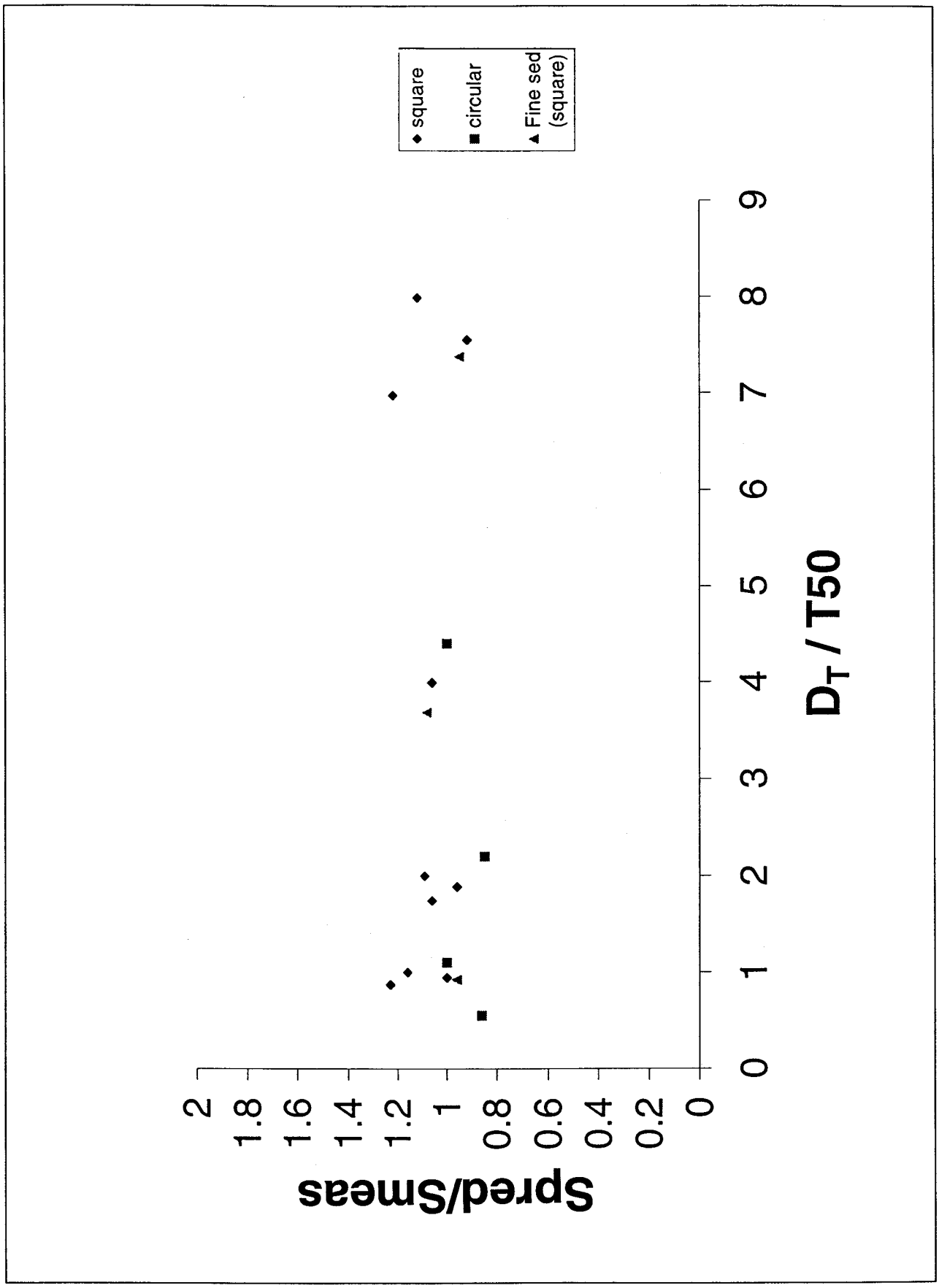

Figure 21 **Relationship between calculated and measured scour after half tidal cycle**

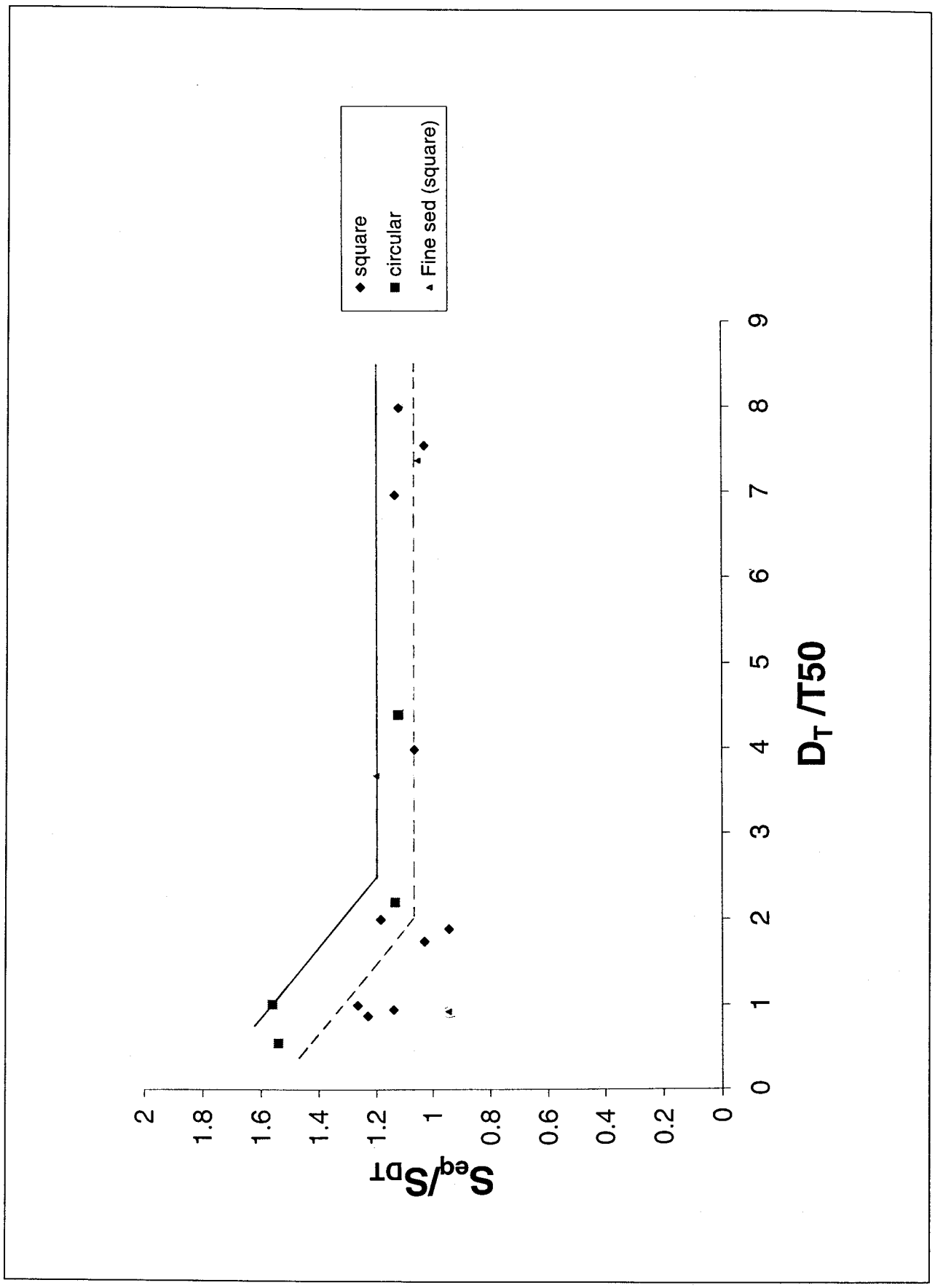

Figure 22 **Relationship between equilibrium scour depth in tidal conditions and scour depth after half tidal cycle**

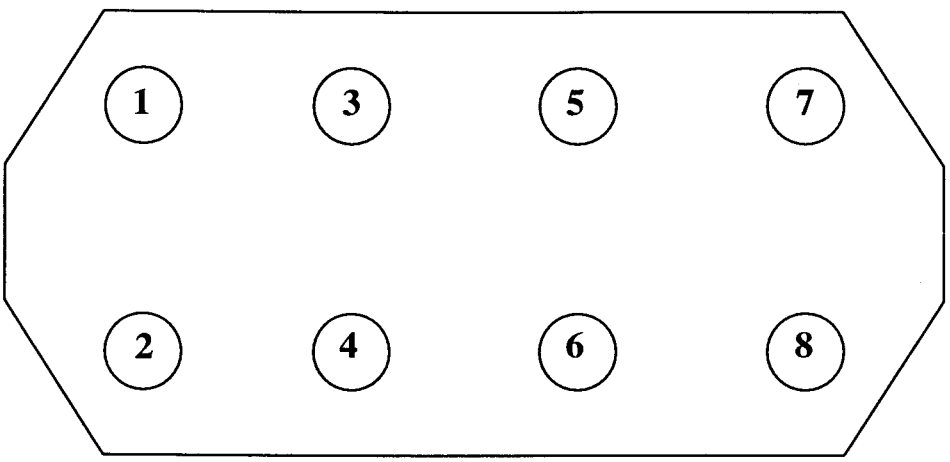

PLAN

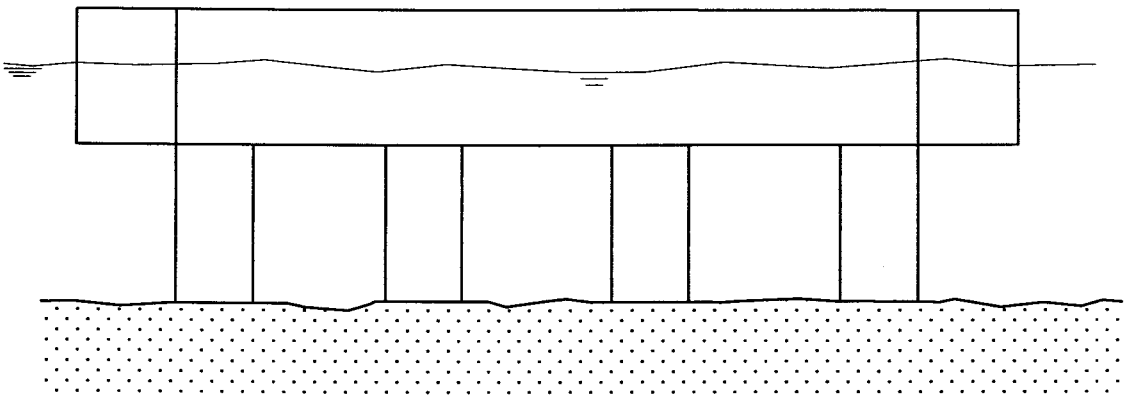

SIDE VIEW

Figure 23 **Generic shape of prototype piers tested**

Plates

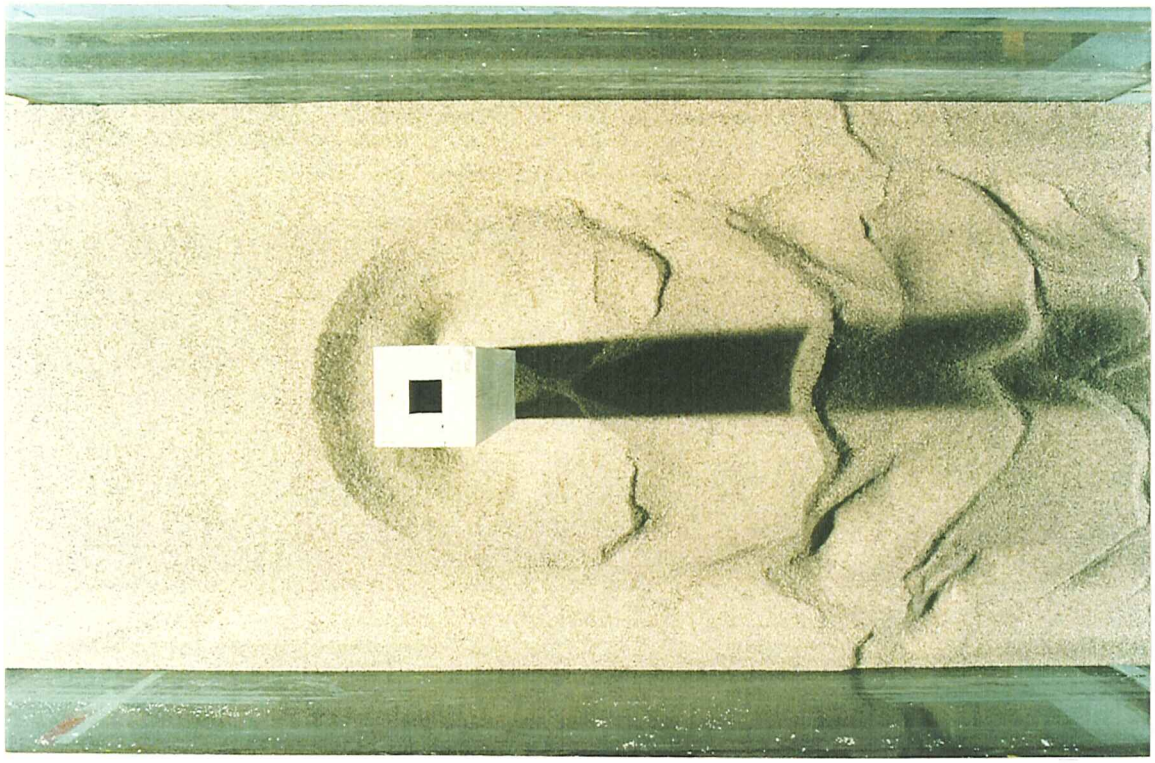

Plate 1 Square structure. Scour at end of test UD

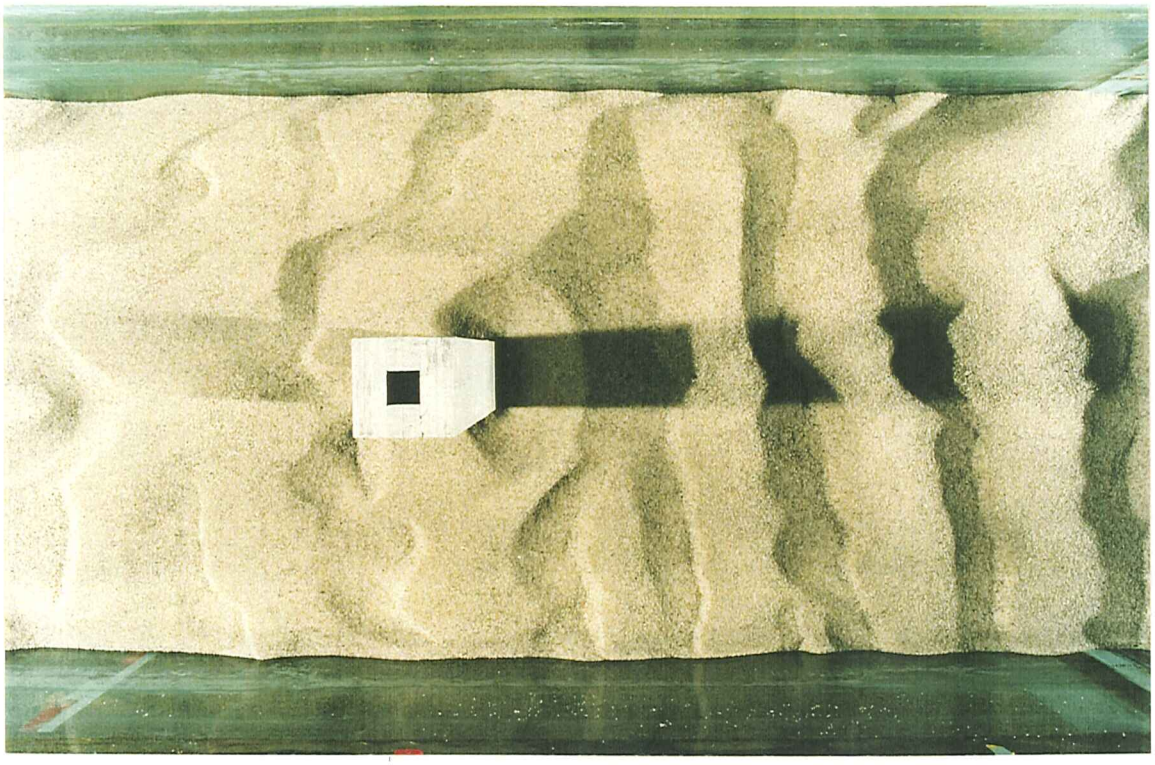

Plate 2 Square structure. Scour at end of test C2

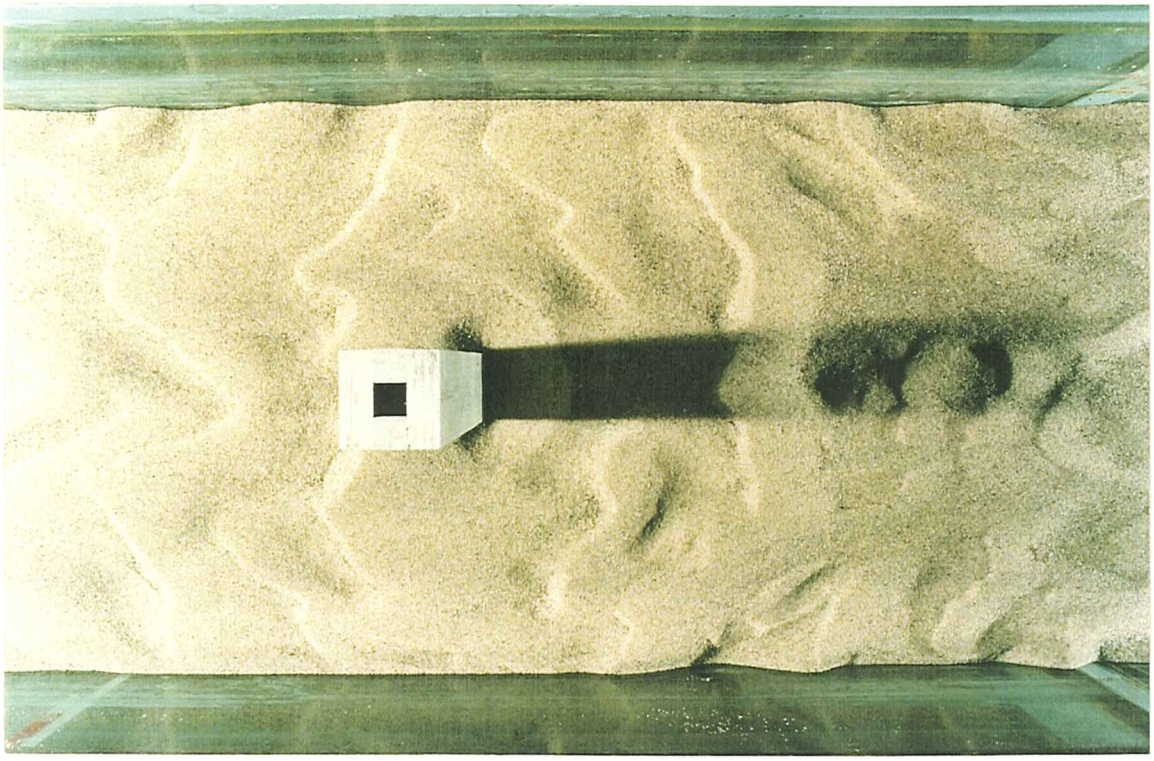

Plate 3 Scour around square pier at end of test C1

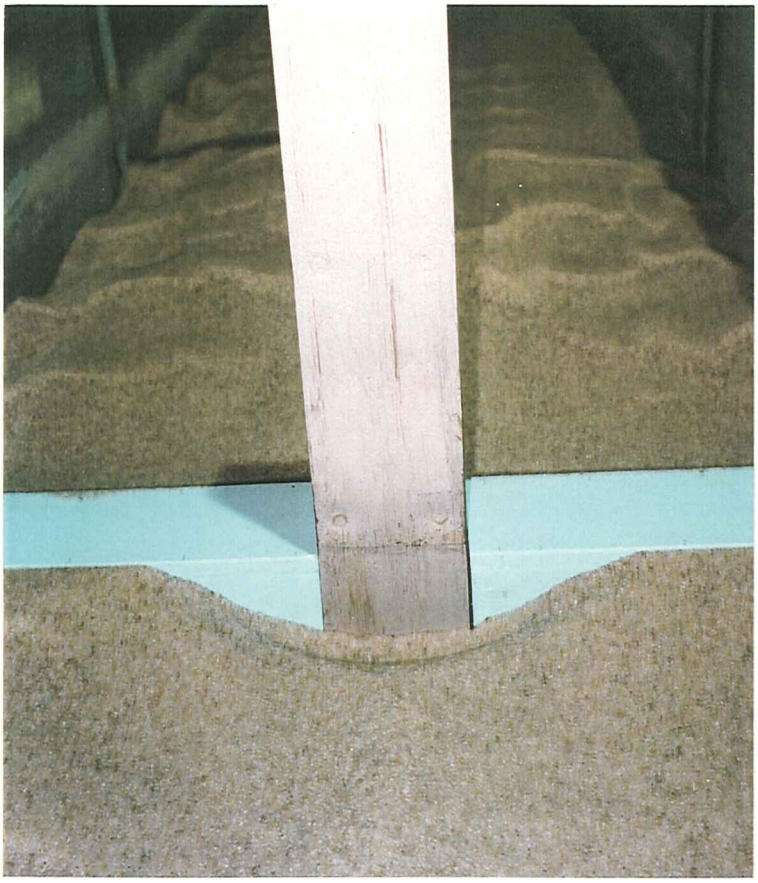

Plate 4 Square structure with sill. Scour at end of test SC1. View from upstream

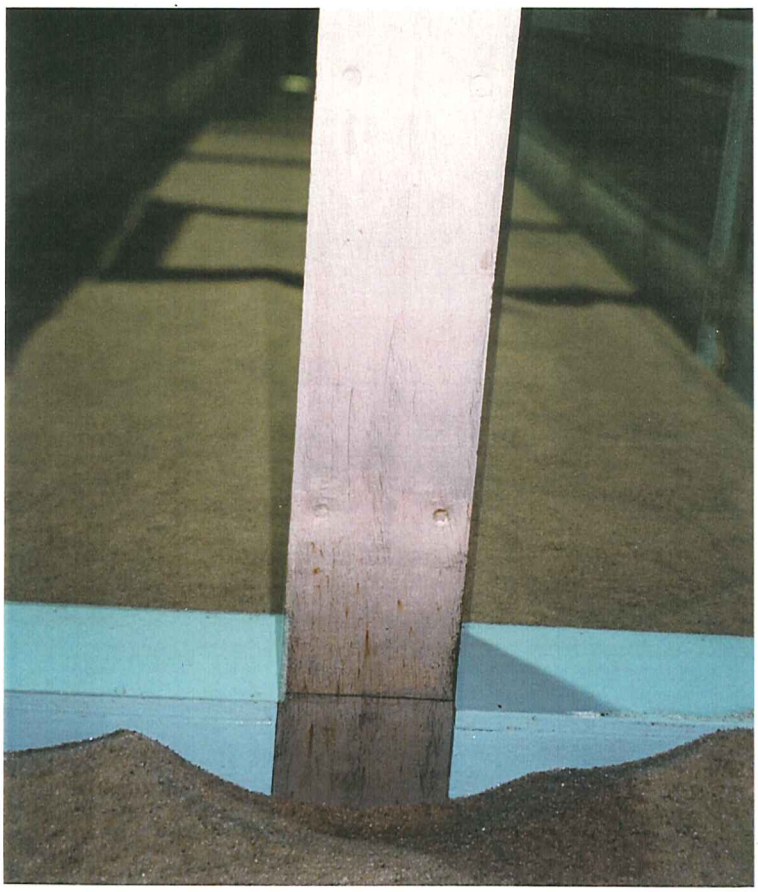

Plate 5 Square structure with sill. Scour at end of test SC1. View from downstream

Plate 6 **Rectangular structure. Scour pattern (in plan) at end of test RC2**

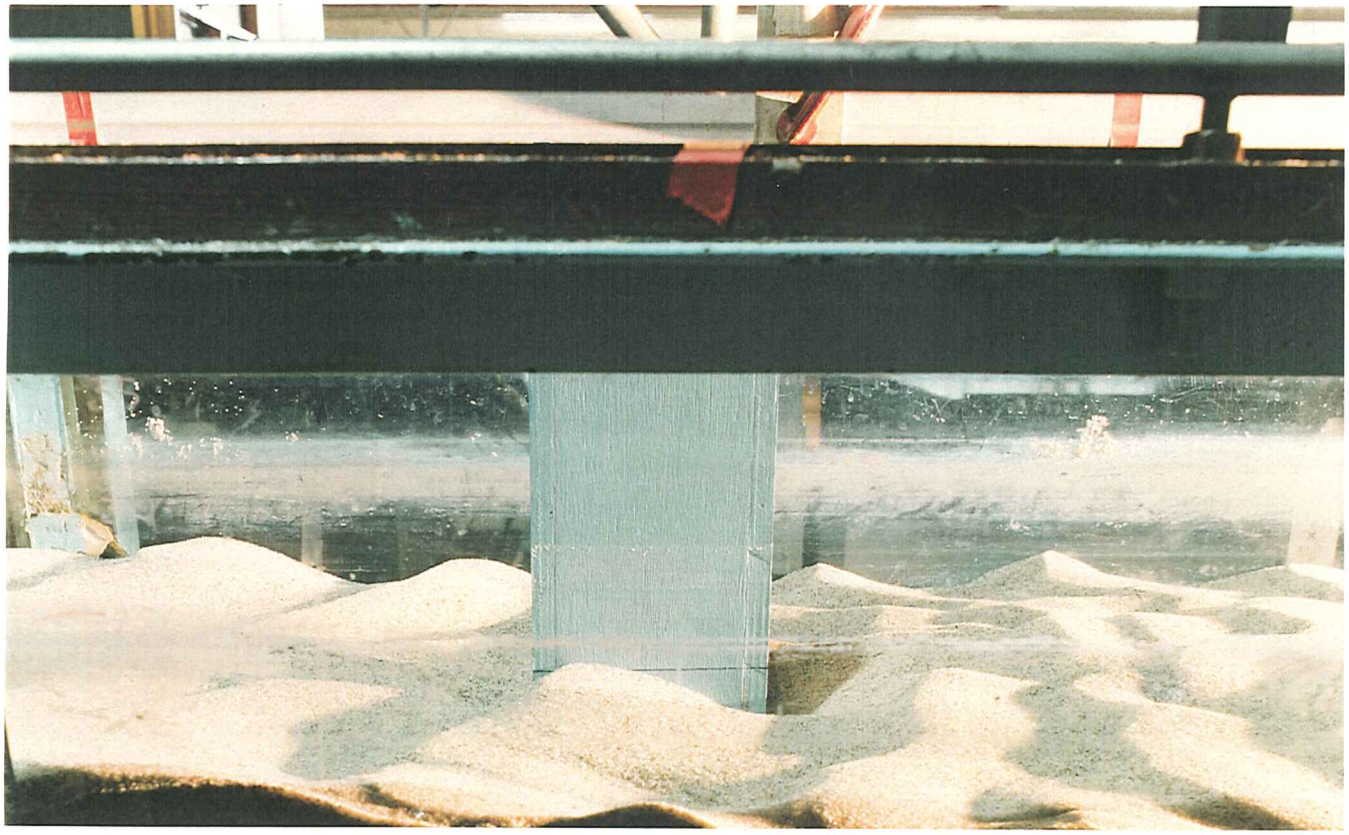

Plate 7 **Rectangular structure. Scour pattern (side view) at end of test RC2**

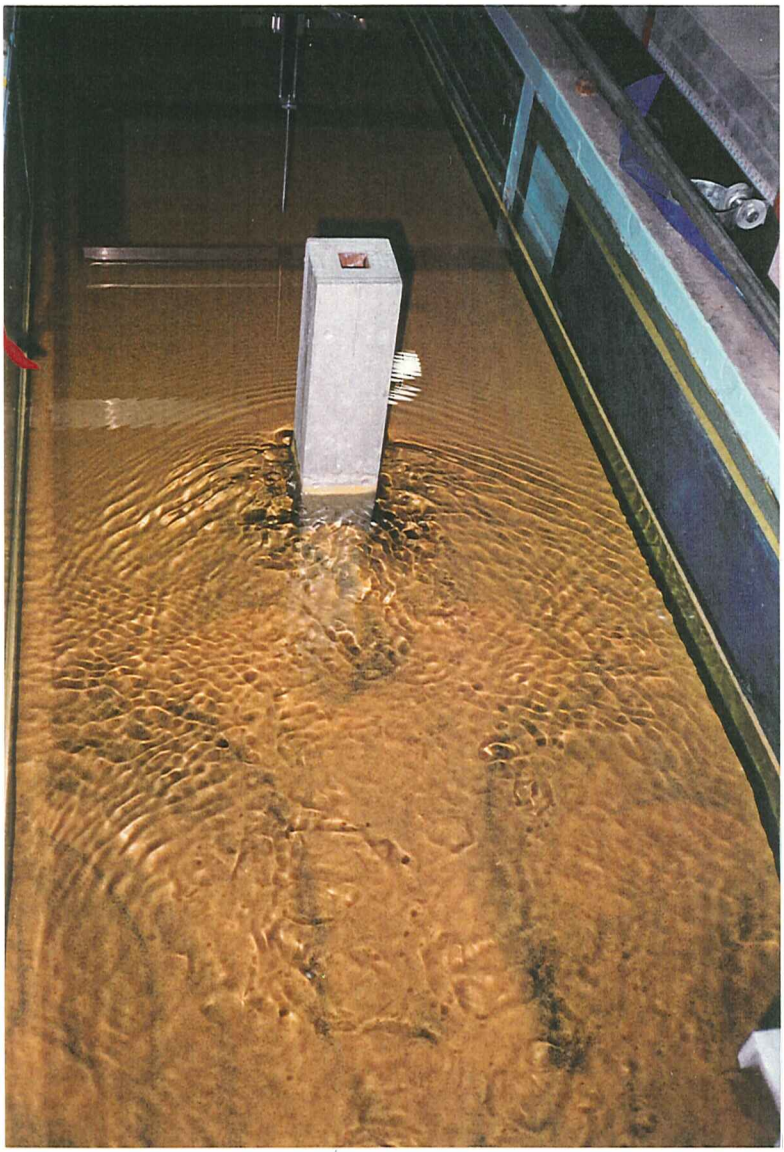

Plate 8 **Unidirectional test with sediment size d_{50}=0.44mm**

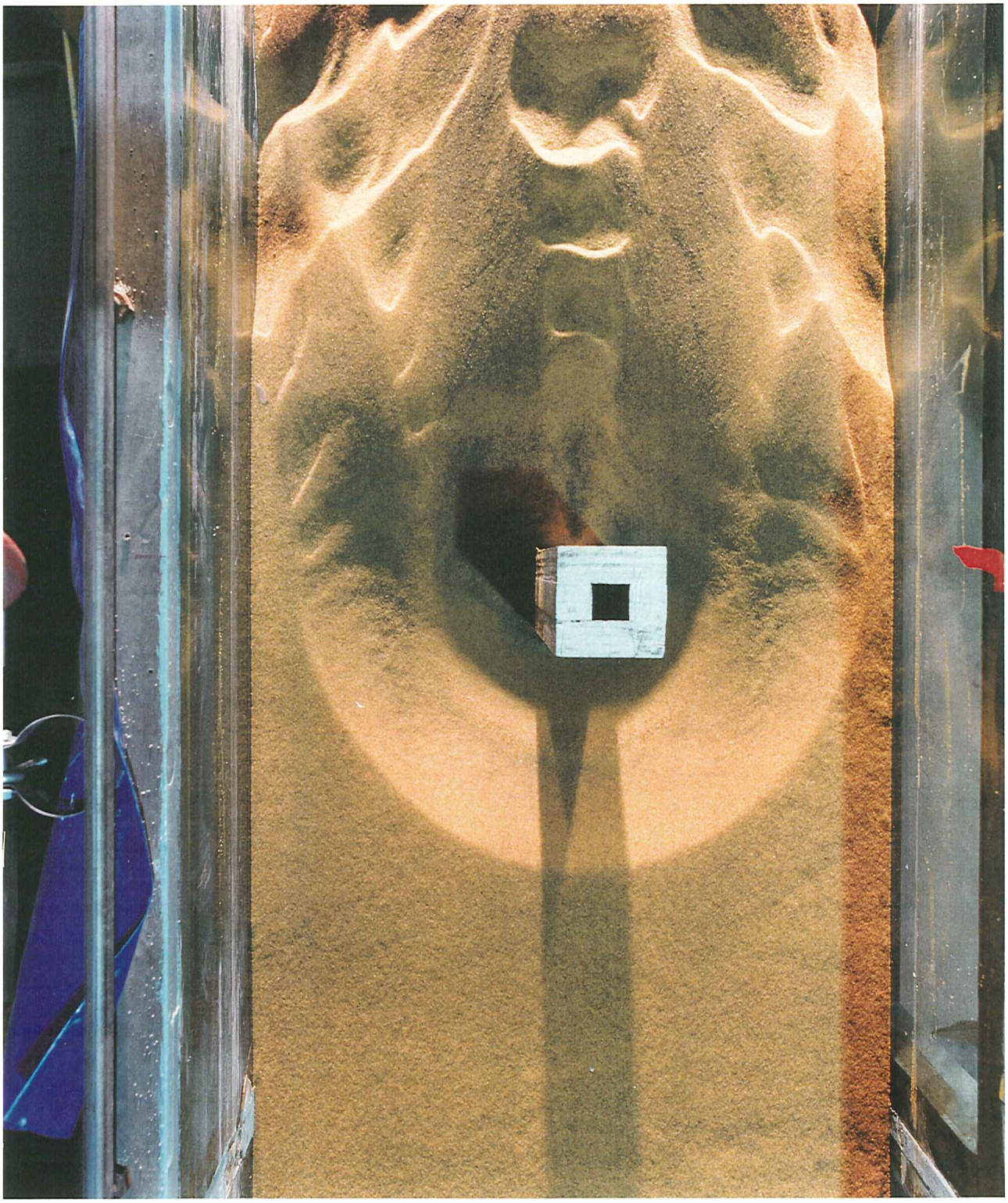

Plate 9 **Fine sediment. Scour pattern (plan view) at end of unidirectional test FUD**

Plate 10 Fine sediment. Scour pattern (side view) at end of unidirectional test FUD

Plate 11 **Stone mattress 150mm wide at end of tidal test**

Plate 12 **Stone mattress 50mm wide at end of tidal test**

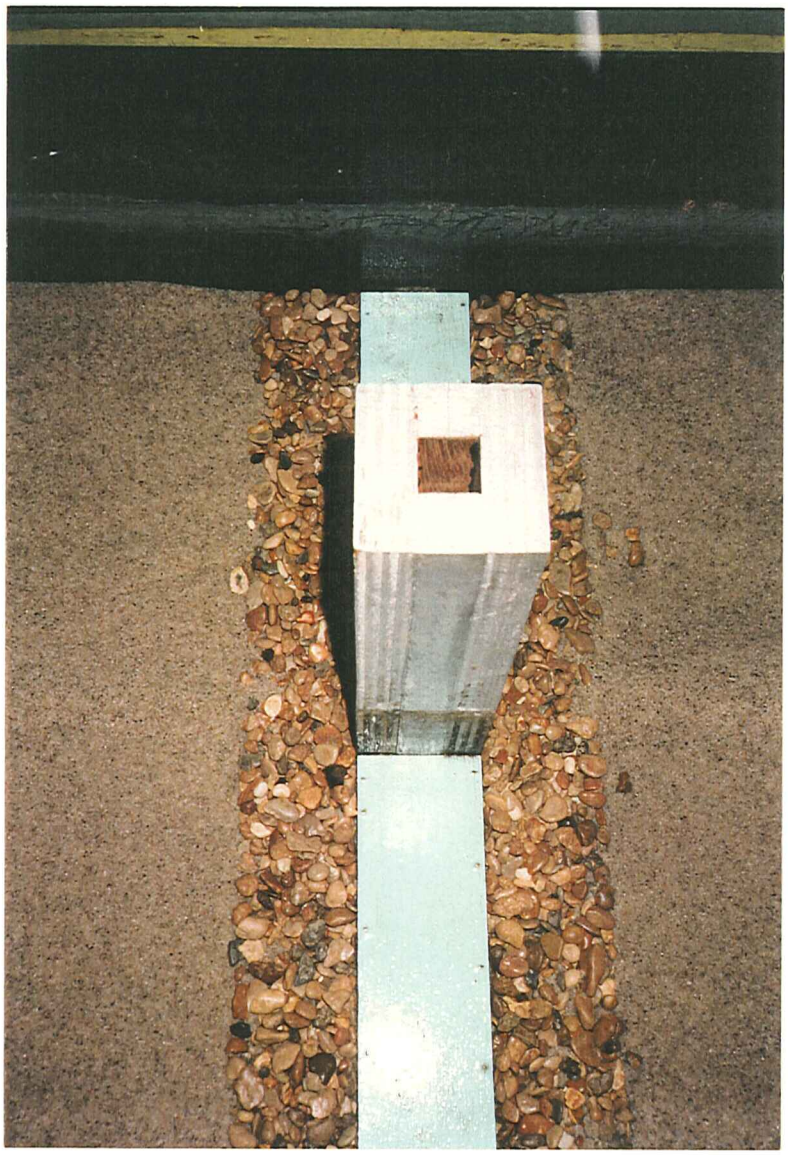

Plate 13 Stone mattress 75mm wide at end of tidal test

Plate 14 Pier P1 at end of test P1A

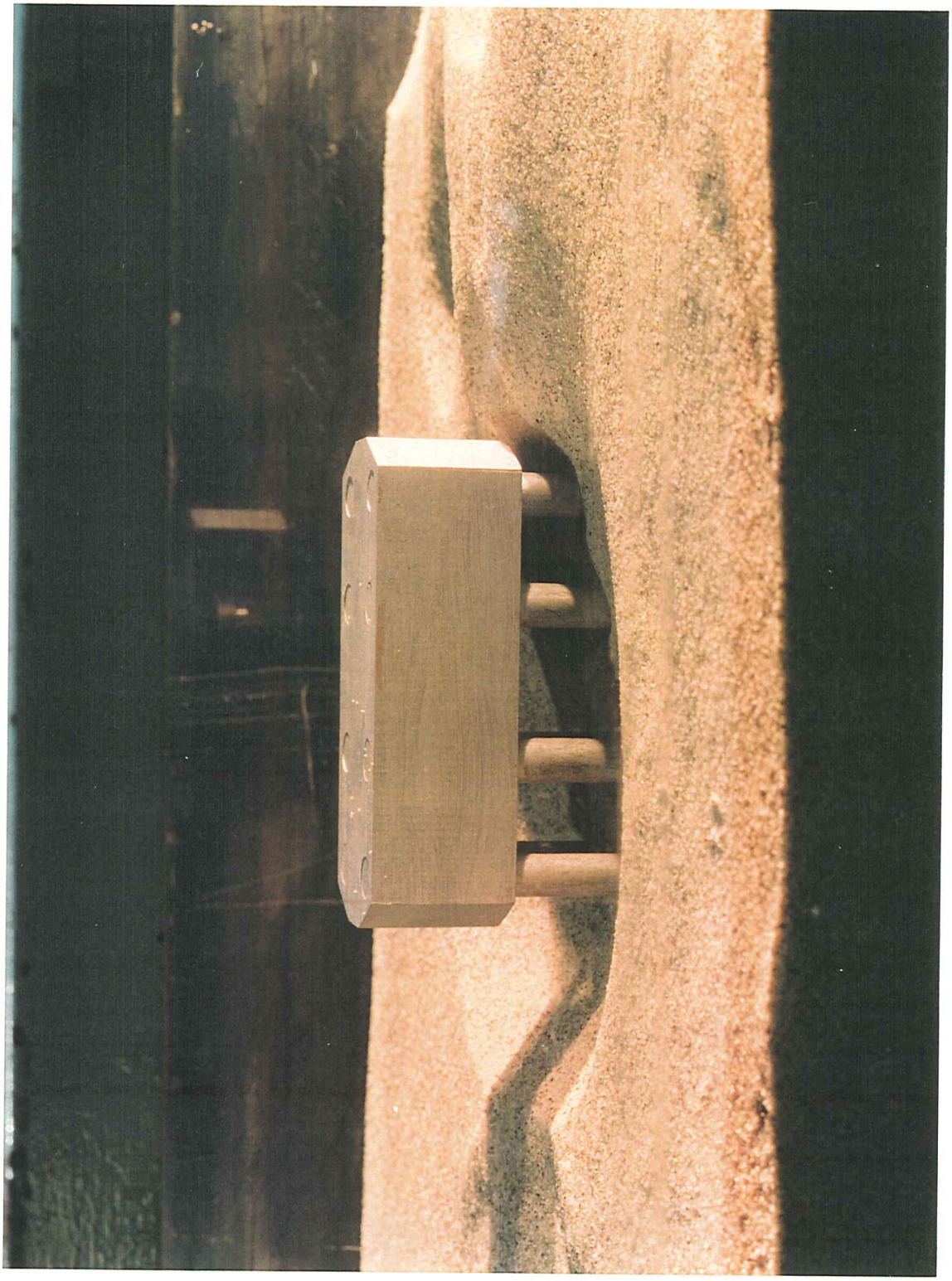

Plate 15 Pier P2 at end of unidirectional test P2U

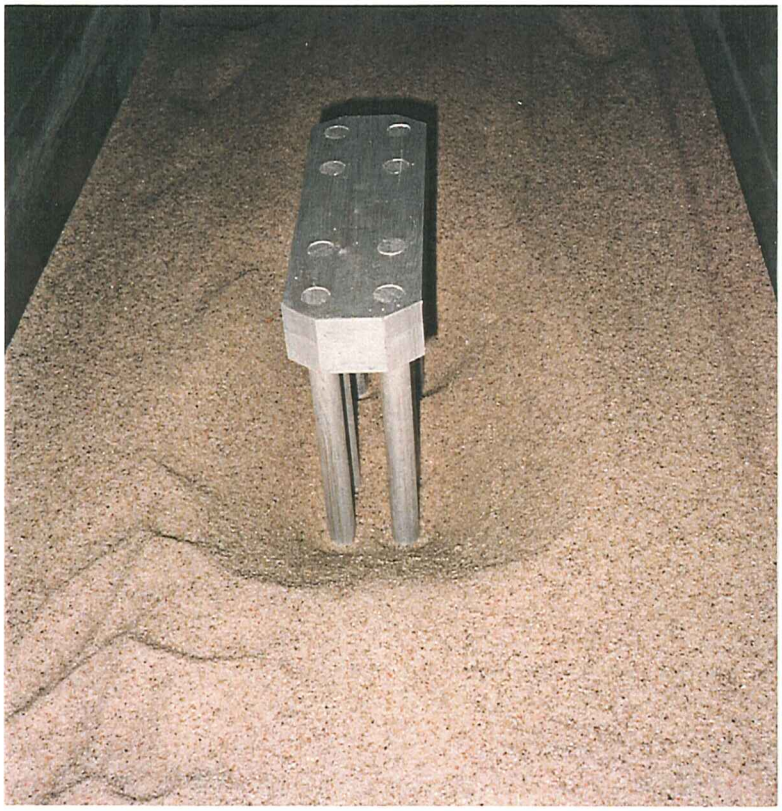

Plate 16 **Pier P1 at end of unidirectional test P1U**

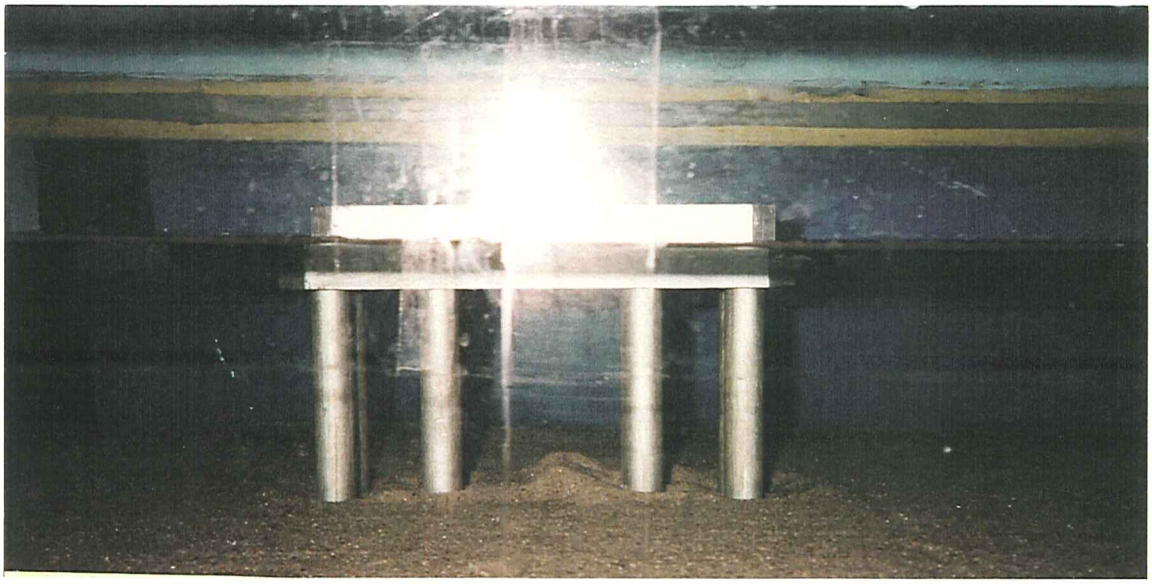

Plate 17 **Pier P1 at end of test P1B ($U<U_c$)**